RATE-DISTORTION BASED DEPENDENT CODING FOR STEREO IMAGES AND VIDEO: DISPARITY ESTIMATION AND DEPENDENT BIT ALLOCATION

by

Woontack Woo

A Dissertation Presented to the
FACULTY OF THE GRADUATE SCHOOL
UNIVERSITY OF SOUTHERN CALIFORNIA
In Partial Fulfillment of the
Requirements for the Degree
DOCTOR OF PHILOSOPHY
(Electrical Engineering)

December 1998

Dedication

For the 3D paranoid...

Keep moving forward!
3D will be as ubiquitous in our life
as color is today,
by the next millennium...

Acknowledgements

First of all, I would like to take this opportunity to thank my advisor and committee chair, Prof. Antonio Ortega, for his support, guidance and encouragement during my years at University of Southern California. I have greatly benefited not only from his academic excellence but also from his reliability, integrity and sincerity.

I would like to extend my deepest gratitude to Prof. C.C.-Jay Kuo and Prof. Ulrich Neumann for their constructive feedback as committee members. I also would like to thank Prof. Christos Kyriakakis and Prof. Zhen Zhang, who have kindly served on my qualifying examination committee. I would like to express my special appreciation to Prof. Hong Jeong who was my advisor in the MS program at Pohang University of Science and Technology, Korea. His careful guidance shaped my understanding on research life as well as on my chosen field. I also would like to acknowledge to Prof. Youngho Ha who ceaselessly encouraged me to study abroad. I was very fortunate to have met him in my early years at Kyungpook National University, Korea. My special thanks go to Prof. Jongwon Kim, Prof. Mel Siegel at Carnegie Mellon University and Dr. Belle Tseng at IBM Watson Research Center for all the fruitful discussions on stereo image/video coding and segmentation issues.

I would like to thank all faculty and colleagues at Signal and Image Processing Institute, EE-Systems, USC. Especially, I am highly indebted to my officemates Wenqing Jiang, Sangyoung Lee and Raghavendra Singh. The long hours in the office could not have been enjoyable without their help. I am grateful of all members at Video Communication Group, who shared the weekly Pizza-meeting in a pleasant atmosphere. Especially, my thanks go to Nazeeh Aranki, Baltasar Beferull-Lozano, Paul

Fernandez, Hyunsuk Kim, Yonggap Kwon, Krisda Lengwehasatit and Zhourong Miao. I cannot neglect former members: Christos Chrysafis at HP Labs, Dr. Chi-Yuan Hsu at SONY Semiconductor Systems and Dr. Yongjun Yoo at Texas Instruments. I thank Yonjun Chung, Jitae Sin and Hwangjun Song. Exchanging ideas and sharing experiences with them has greatly influenced my research. I also cannot overestimate the energetic support from the staffs of SIPI and EE-Systems. I especially thank Ms. Regina Morton, Ms. Linda Vanilla, Dr. Allan Weber and Mr. Tim Boston. It was a great pleasure to work and study with all of them.

I cannot forget the days I spent with all my friends during my years in Southern California. My special thanks go to Dr. Sungook Kim, Prof. Daniel C. Lee, Dongjun Lee, Dr. Jeonghyun Oh, Dr. Chankyung Park, Dr Dongjun Shin and many other KEGS members. I appreciate their productive cooperation and insightful discussion. I have to mention Sangyoub Lee, Byounggi Park and Kyueun Yi with whom I have greatly enjoyed establishing KNUAAA. I also thank my fabulous neighbor, Dr. Jinwoo Suh, who have shared so many wonderful moments with me. My sincere thanks go to Woohyun Park, Jongsoon Lim and many other friends for their encouragement and emotional support.

Finally, I owe my family all my thanks for their support in the pursuit of my aspirations through all of the years of my study. Most of all, I greatly acknowledge my parents, Jongchul Woo and Kiha Lee, and my parents-in-law, Chungkil Cho and Kyungja Song, for their love and support. I cannot thank my late grandparents, Sooki Woo and Jaeyoon Choi, enough for their greatest love for me. A very sincere thanks goes to my lovely kids, Sanghyun and Sangmin, and my wonderful wife, Sungjum, for their deepest love, endless patience, tremendous sacrifices and continued support during the many ups-and-downs in my USC life.

Again, it is the time to depart on a new journey that might be lengthy and difficult. I feel thrilled rather than fearful because I believe that this is the way our lives unfold. Good luck to all of you who remember me!

Contents

List Of Figures

List Of Tables

Abstract

In this dissertation, novel coding schemes for stereo images/video are proposed. Recently, the demand for 3D imaging has been increasing because the stereoscopic method provides realism to 2D images. The price for this added realism is the doubling of data and thus, as in the single-channel case, the limited bandwidth of existing channels becomes the main bottleneck. To achieve an optimal coding gain for a pair of stereo images, we have proposed various efficient encoding schemes, which can be mainly grouped into two classes *blockwise dependent bit allocation* and *disparity estimation/compensation*.

In the proposed optimal blockwise dependent bit allocation scheme, the quantization parameters are selected simultaneously for blocks in both the reference image and the disparity compensated difference frame. In this manner, an average distortion measure can be minimized, while meeting any applicable bit budget constraints. In general, the bit allocation problem is complicated by the dependencies arising from using predictions based on the quantized reference image. Therefore, only approximate solutions are feasible in the case of motion compensated video. However, in the case of stereo images, an optimal solution can be estimated with reasonable complexity given the special characteristics of the "binocular dependency." A fast algorithm is also proposed, which provides most of the gain at a fraction of the complexity.

The proposed two hybrid estimation/compensation schemes are based on fixed and variable size blocks, respectively. The first scheme, *modified overlapped block disparity compensation*, can overcome drawbacks of conventional block-based schemes that use the smoothness constraints arising in causal neighborhoods by estimating

a relatively smoother disparity field. Simultaneously, selective overlapped block disparity compensation for the blocks with higher prediction errors reduces blocking artifacts, while reducing computational complexity over the conventional overlapped matching scheme. The other scheme, *quadtree-base hybrid block segmentation*, can further improve the encoding efficiency along object boundaries. Similarly, a Markov Random Field model-based hierarchical approach allows the estimation of a consistent disparity field, even for small blocks. Furthermore, RD-based block segmentation and selective overlapped disparity compensation improve the encoding performance.

Chapter 1

Introduction

In this Chapter, we first provide motivation for stereo images/video compression and then briefly describe the main contributions of our research. Afterwards, we formulate the coding problem for stereo images within the framework of predictive (or dependent) coding. Usually, a predictive coding system includes displacement (disparity or motion) estimation/compensation, transform/quantization and entropy coding. Therefore, the overall encoding performance can be controlled by various factors. Especially, for the stereo image coding case, an efficient prediction reduces the "binocular redundancy" between two images in a stereo pair. In addition, optimal quantization that takes into account the "binocular dependency" can further improve the overall encoding performance. Therefore, the proposed novel coding schemes consist of two central parts: (i) efficient disparity estimation/compensation and (ii) optimal bit allocation. The dissertation overview is provided at the end of this Chapter.

1.1 Motivation of Stereo Image Coding

Over the past few decades, efficient representation schemes for visual data, such as image and video, have been actively developed. Communication technologies have matured so fast that various commercial systems are already available for real-time

2D visual communications based on standards such as JPEG, MPEG-1, MPEG-2, or H.26x. As a result, face-to-face meetings are possible through teleconferencing or telepresence, without the high cost of travel. In addition, technologies in various related areas (*e.g.* telecommunication, computer, TV and film) are converging rapidly and enabling more natural multimedia communication. New standards such as MPEG-4 and MPEG-7 are recently being developed to meet those new demands on interactive multimedia communications.

What is next? The main development trend in image/video-related technologies has been the addition of (perceptual) sensations. For example, monochrome video added realism to still photographs. Later, the addition of color improved the limited quality of the monochrome video. Recently, this realism has been further enhanced by increasing the resolution of the video signals with a bigger and wider screen, *e.g.*, High-Definition Television (HDTV)[1]. The HDTV provides more realism than conventional color TV. However, the current imaging systems still have their limitations in representing natural and real scenes.

A promising way of providing visual realism to images/video is to add depth information. This is because the human visual system (HVS) reacts more strongly to 3D than to 2D images [1,2]. In general, humans perceive 3D using various 3D cues such as perspective, occlusion and shading. However, those 3D cues alone are not enough to provide realistic 3D. Another efficient method of providing depth information for images/video is to use stereoscopic approaches, which display well-composed stereo pairs simultaneously for each eye, based on the fact that humans perceive a scene in 3D by simultaneously viewing a scene from slightly different positions. The selected pairs of stereo images are in Appendix B. Unfortunately, a wider deployment of stereo systems has been primarily limited by the requirement of inconvenient stereo glasses.

[1] The experimental broadcasting of HDTV, called Hi-Vision, has been ongoing in Japan since 1988. In USA, leveraging more than 10 years of research and development in digital television, the first High-Definition digital broadcast signals have been transmitted in 1998.

Therefore, newly introduced technologies for autostereoscopic displays are likely to contribute to a widespread usage of stereo techniques. For example, lenticular monitors are replacing the need for those annoying stereo glasses, which have prevented widespread usage of stereo methods for a long time[2]. As a result, the usage of stereoscopic images/video will become increasingly popular as demand grows for more realistic 3D imaging. 3D imaging systems have a variety of potential applications such as visualization (CAD/CAM/medical data), telecommunication (telemedicine, telepresence) [3–5], telerobotics (remote control, autonomous navigation, surveillance) [6, 7], entertainment (interactive HDTV and cinema) [2, 8] and Virtual Reality [9].

The obvious price for this increased realism is the doubling of data size, as compared to mono channel cases. In general, the problem of increased data can be solved by: (i) increasing channel bandwidth, (ii) improving channel utilization with efficient protocol or/and (iii) reducing the source itself using efficient compression techniques. Up to now, as shown in Figure 1.1, the main bottleneck for 3D images, as well as monocular image/video case, has been the limited bandwidth of existing channel (or storage) [2, 10, 11]. As a means of alleviating the bottleneck, stereo image/video compression has been attracting considerable attention over last few years.

Analogous to other coding scenarios, compression for stereo images can be achieved by taking advantage of redundancies in the source data, *e.g.* spatial and temporal redundancies for monocular images and video. A simple solution for compression is using independent coding for each image/video with existing compression standard such as JPEG or MPEG. However, in the case of stereo images/video, an additional source of redundancy stems from the similarity, *i.e.* the strong "binocular redundancy" between two images in a stereo pair, due to stereo camera geometry. Exploiting this binocular dependency allows achieving higher compression ratios [12].

In this research, we will assume that "generic" transform coding and motion estimation are used to exploit the spatial and temporal redundancies, as shown in Figure

[2] For an overview of current display technologies, refer to Appendix A or the following web page at `http://escalus.usc.edu/~wwoo/Research/Stereo/display.html`

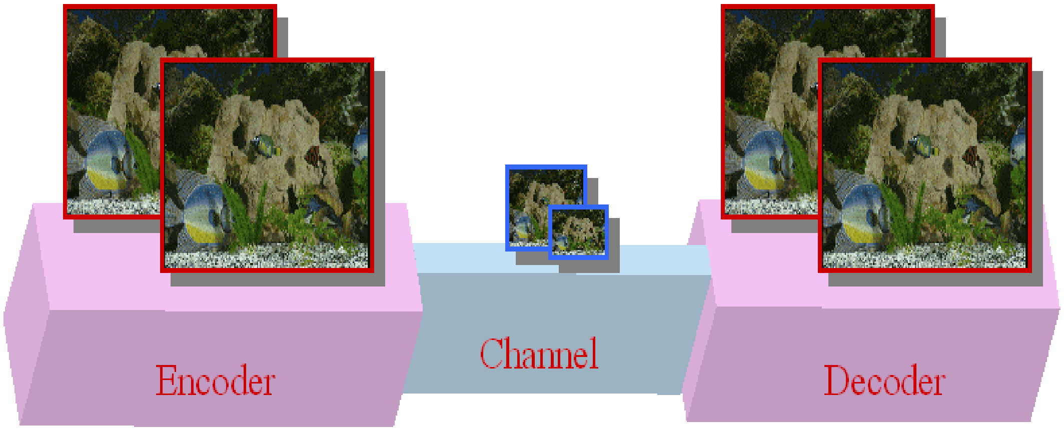

Figure 1.1: Motivation of stereo image/video coding. Up to now, the main bottleneck has been the limited bandwidth of existing channel. Therefore, stereo image/video compression has been attracting considerable amount of attention over the last few years. Note that the dependent image/sequence can further be compressed by exploiting the dependency between two images in a stereo pair.

1.2. We will then focus on the issues that are specific to disparity compensated coding.

1.2 Problem Formulation: Dependent Coding

Figure 1.3 shows a block diagram of a general predictive encoder for stereo images, where the encoder consists of disparity estimation/compensation, transform/quantization and entropy coding. Let F_1 and F_2, respectively, be the reference image and the target image in a stereo pair. In the predictive coding framework, an image is selected as a reference image (F_1) and then the dependent (or target) image (F_2) is estimated/compensated from the reference image. Similar to other predictive coding scenarios, displacement estimation/compensation reduces the redundancy between two images in a stereo pair. As explained, instead of encoding the original target image, the resulting disparity vector (DV) field and the disparity compensated difference (DCD) frame are encoded. The difference is computed between the original target image and the estimated target image ($\hat{F}_2$), *i.e.* $F_1(Q_1, V)$. Therefore,

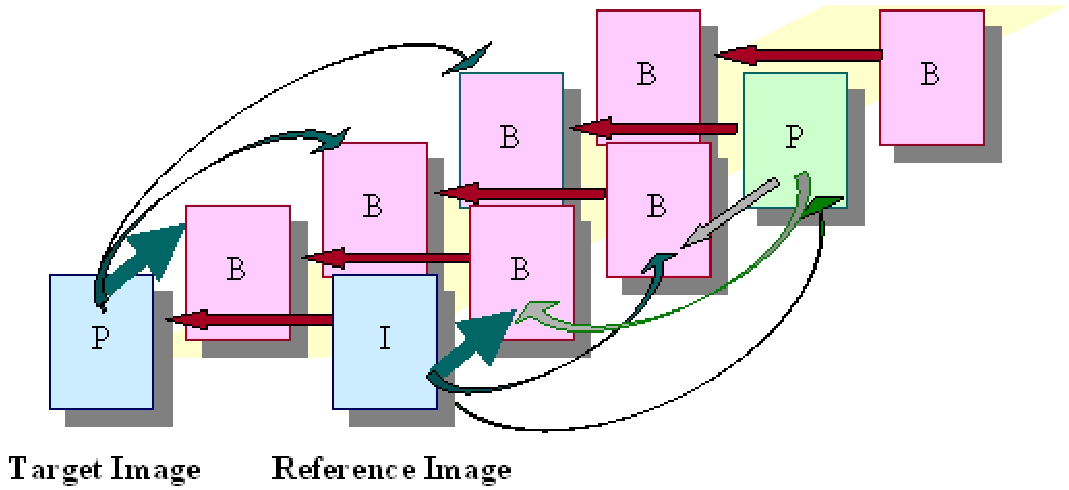

Figure 1.2: Stereo video coding using multiview profile in MPEG-2. In MPEG-2, the scalability syntax offers higher flexibility and thus various configurations can be supported.

as shown in Figure 1.3, the encoding performance mainly depends on the disparity estimation/compensation and quantizations, *i.e.* (V, Q_1, Q_2).

Let R and D be rate and distortion, respectively. In order to optimize the overall coding efficiency, the given bits have to be distributed between two images in a stereo pair, while minimizing the total distortion. Distributing bits by considering the two images together is called *dependent* bit allocation [13]. In disparity compensated coding, the target image in the stereo pair is replaced with the DV field and the DCD frame, and thus the given bits are distributed among the reference image, the DV field and the DCD frame. Then, given a bit budget, R_{budget}, the optimal (in terms of rate and distortion) bit allocation problem for stereo images can be formulated as follows

$$\begin{array}{ll} \text{Given} & F_1, F_2, R_{budget} \\ \text{find} & (V, Q_1, Q_2)^* \\ \text{such that} & (V, Q_1, Q_2)^* = \arg\min_{(V,Q_1,Q_2)} \{D_1(Q_1) + \alpha D_2(V, Q_2|Q_1(V))\} \\ \text{subject to} & R_1(Q_1) + R_2(V, Q_2|Q_1(V)) \le R_{budget} \end{array}$$

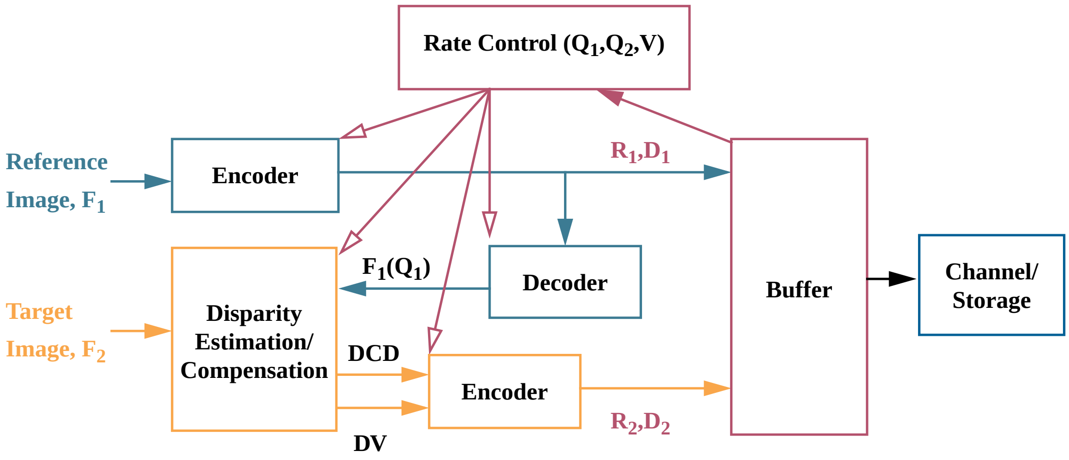

Figure 1.3: Block diagram of a general encoder for stereo images, where the encoder consists of disparity estimation/compensation, transform/quantization and entropy coding.

where V and Q refer to a DV field and a set of quantizers, respectively.

The relative importance of D_1 and D_2 can be controlled by the weighting constant α which allows us to support two different views of the depth perception process: *fusion theory* and *suppression theory* [14,15]. Fusion theory claims that both images in a stereo pair equally contribute in 3D perception, while suppression theory indicates that the highest quality image (or region) dominates the perception. Note that, according to suppression theory, the target image in a stereo pair can be highly compressed as long as the reference image retains the details of the scene. In our experiments, we set α equal to one.

At this stage, the dependency between the stereo pair seems too complicated to exploit, because the disparity estimation and the quantization are coupled with each other. In our research, this complicated joint optimization problem is decoupled into two independent optimization problems by using an open loop coding framework: (i) efficient disparity estimation is performed on the original (unquantized) data and (ii) optimal dependent quantization is performed after the DV field has been determined. As a result, distortion and rate can be represented as $D_1(Q_1) + D_2(Q_2|Q_1(V))$ and $R_1(Q_1) + R_2(Q_2|Q_1(V)) + R_2(V)$, respectively.

Figure 1.4 compares two types of stereo image codecs using the closed loop and the open loop framework. The disparity estimation based on the open-loop encoder is independent of the quantizer choices, so that any kind of estimation technique can be used as long as the scheme provides a good disparity field in terms of the rate and the estimation error. Note that the estimated disparity in the open-loop coder is suboptimal, because the estimation is performed between F_2 and F_1, whereas the compensation is performed between F_2 and $F_1(V, Q_1)$, which is available at the decoder. However, the open loop encoder generally tends to generate a relatively *accurate* and *consistent* DV field, as compared to the closed loop encoder.

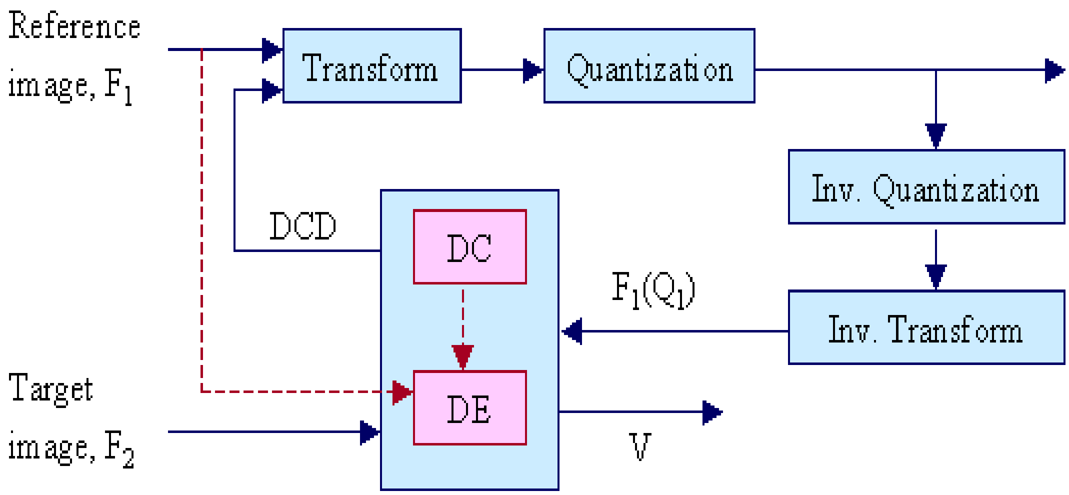

Figure 1.4: Comparison of codecs for stereo image coding: closed-loop encoder vs. open-loop encoder (dotted line). The same decoder is used in both cases.

The general procedure of the proposed optimal predictive (or dependent) coding for stereo images is as follows. Given two images in a stereo pair, a DV field is estimated based on blocks or meaningful objects to exploit binocular redundancy. The resulting DV field is first encoded. If object or shape-based estimation is adopted, the shape information also needs to be encoded as an additional side information. Based on the disparity field, the compensation is performed between the original target image and the estimated target image, where the target image is estimated from the quantized reference image. Then, the reference image and the DCD frame are transformed, quantized and encoded. At this stage, the bits have to be distributed properly between the transformed reference image and the difference frame. Note that, to optimize encoding efficiency, the reference image, F_1, can not be quantized independently because the distortion of the target image, D_2, depends on the quantization choices for the reference image along the DV field, *i.e.* $F_1(Q_1, V)$. The distribution can be controlled by adjusting the quantization steps (scales or factors) for both transformed F_1 and DCD frame. At the decoder, first the reference image is decoded and then the target image is reconstructed by adding the disparity compensated frame and the decoded difference frame.

1.3 Main Contribution

The primary aim of this research is to provide efficient encoding schemes for stereo images/video within the predictive coding framework, where the dependencies arising from using a prediction with a quantized reference image complicates an optimal dependent coding. In the proposed framework, using an open-loop encoding framework, we decouple this complicated joint optimization problem into two independent optimization problems: (i) "efficient" *disparity estimation* and (ii) "optimal" *dependent quantization*. In this dissertation, "efficient" means reducing the rate as much as possible, while maintaining a low distortion, which we assume will correlate with 3D perceptual visual quality. As a result, in the proposed framework, any efficient disparity estimation algorithm can be adopted as long as the estimation scheme provides a good DV field in terms of the rate of the DV and the energy of the estimation error. Note also that we interchangeably use the terms *coding* and *compression*. The proposed schemes are implemented with a JPEG-like codec but they can be easily modified to use an MPEG-like video codec to encode multiview images/video. A detailed list of the main contributions of this research follows.

- We have made a brief survey on conventional coding schemes for stereo images and addressed the main coding issues. We have proposed an optimal blockwise dependent quantization scheme. In the proposed framework, the quantization parameters are selected simultaneously for blocks in the reference image and the disparity compensated difference frame so as to minimize some averaged distortion measure, while meeting any applicable bit budget constraints. The encoding complexity and delay in the dependent quantization framework can be significantly reduced in the proposed structure by exploiting the predominant unidirectional property of the binocular dependency[3]. The experimental results show that the proposed scheme results in a higher rate being used for the reference frame (thus improving its MSE performance) that results in higher PSNR for the target frame as well (even though fewer bits are used). The proposed quantization scheme can be a benchmark for practical rate control schemes or aid in developing a fast and efficient bit allocation strategy. It also can be used in asymmetric applications such as CD-ROM, DVD and video-on-demand, which may involve offline encoding.

- We also have proposed a fast algorithm for the blockwise dependent quantization, based on the assumption of existence of a monotonicity property in the prediction between the two images in a stereo pair. The experimental results show that most of the gain can be obtained at a fraction of the complexity, as compared to the full search scheme.

- We have investigated various disparity estimation/compensation algorithms and proposed two schemes to overcome well-known limitations of block-based schemes such as inaccurate disparity estimation and blocking artifacts in the decoded image at low rate coding. The proposed schemes produce robust and

[3] In similar problems in motion compensated video only approximate solutions are feasible. Note that an optimal solution requires considering a whole image, due to 2D dependency between frames in a video sequences.

accurate DV fields, which in turn increase the encoding efficiency. The proposed disparity compensation schemes are based on: (i) fixed size block matching and (ii) variable size block matching.

- We have proposed a fixed size block-based scheme, *modified overlapped block disparity compensation*, that can overcome the drawbacks of conventional fixed sized block-based methods. The proposed hybrid scheme consists of (i) disparity estimation using a modified MRF model, *i.e.* using a smoothness constraint within a causal neighborhood and (ii) selective overlapped block disparity compensation. The disparity estimation with smoothness constraint results in a relatively smooth disparity field, while maintaining the energy level of the DCD frame. The selective overlapped block disparity compensation reduces blocking artifacts in the decoded target image and improves encoding efficiency, while reducing the computational complexity of overlapped block disparity compensation schemes. The incorporated half-pixel accuracy further improves the encoding efficiency.

- We have proposed a quadtree-based block segmentation scheme to overcome inherent limitations of fixed size block-based schemes. The proposed scheme achieves higher PSNR gain over fixed size block matching by relaxing the *one-vector-per-block* assumption. In addition, hierarchical disparity estimation with smoothness constraints in a causal neighborhood allows a consistent disparity field. The RD cost-based block segmentation improves encoding efficiency over conventional variable size block matching. The selective overlapped block disparity compensation for the segmented subblocks reduces blocking artifacts and thus further improves encoding efficiency for the DCD frame.

- Finally, we have presented and discussed various possible extensions of this research in the last Chapter of this dissertation. The extensions include

  - object-oriented hybrid segmentation using stereo images

- rate-distortion based contour coding
- blockwise dependent quantization for video coding
- joint estimation of disparity and motion for stereo video
- multiview image coding and intermediate view generation

1.4 Dissertation Overview

This dissertation is organized as shown in figure 1.5.

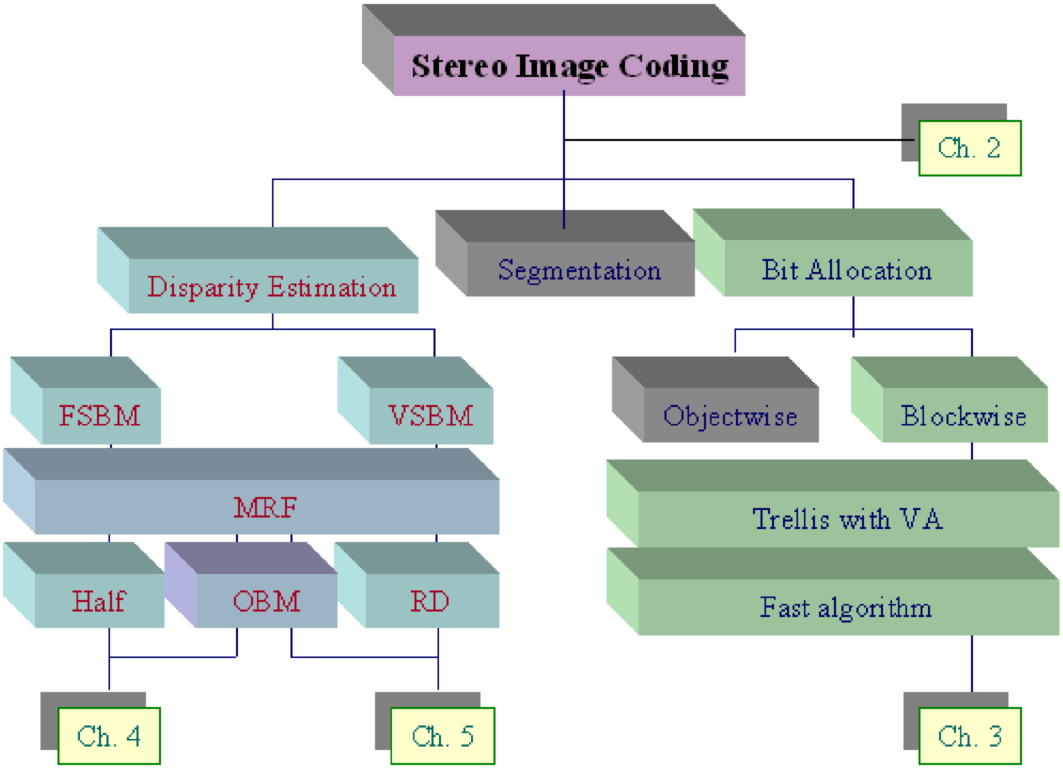

Figure 1.5: Overview of the dissertation.

In Chapter 2, we first formulate the stereo image coding problem using the predictive coding framework and explain that exploiting the “binocular” dependency is essential in optimizing the overall coding performance. We briefly review 3D and stereo vision as a background. We also survey various issues on stereo images and briefly review previous works on stereo image coding.

In Chapter 3, we propose a blockwise dependent quantization scheme and explain how to find optimal sets of quantizers for a pair of stereo images, *i.e.* the reference image and the disparity compensated difference frame. The proposed algorithm, based on dynamic programming, provides the optimal blockwise bit allocation. The RD-based cost function is defined using Lagrangian method. The predominant horizontal dependency helps construct a compact dependency tree, which is called a *trellis*, for each pair of "row of blocks (ROB)," one in the reference image and one in the target image. The finite set of admissible quantization scales and the corresponding Lagrangian cost are assigned to the nodes and the branches of the trellis, respectively. Then, optimal sets of quantizers are searched using the Viterbi algorithm. The same trellis structure is repeatedly applied for each pair of ROB. We also propose a fast algorithm that provides most of the gain at a fraction of the complexity.

In Chapter 4, we propose a block-based disparity estimation/compensation scheme, *modified overlapped block disparity compensation*, that overcomes the well-known limitations of conventional fixed size block matching schemes, such as blocking artifacts or inaccurate estimation. In the proposed scheme, smoothness constraints in causal neighborhood help us estimate a relatively smoother and more consistent disparity field, while maintaining encoding performance for the disparity compensated difference frame. Simultaneously, selective overlapped block disparity compensation reduces computational complexity of the conventional overlapped matching scheme, while reducing blocking artifacts. However, block-based methods have inherent limitations in removing the estimation errors, especially along the object boundaries. These kinds of errors can be reduced by using the variable size block matching and relaxing the uniform disparity assumption within the block, while keeping consistency of disparity vector field.

As a continuation of Chapter 4, in Chapter 5, we therefore introduce a variable size block-based scheme, *quadtree-based block segmentation*, to further improve encoding efficiency along object boundaries. In the proposed scheme, the MRF model-based disparity estimation allows consistent estimation even in small blocks and the RD cost-based block segmentation improves encoding efficiency. In addition, the selectively applied overlapped disparity compensation further improves encoding efficiency. In all the proposed schemes, the encoding efficiency is improved mainly by reducing the entropy of the disparity compensated difference along the object boundaries, while reducing the rate for the disparity field using hierarchical smooth constraint. The improved encoding performance also results from selective overlapped disparity compensation.

Finally, the summary and possible extension of this research are briefly addressed in Chapter 6.

Chapter 2

3D and Stereo Image Coding

A number of research results have been reported which demonstrate the advantages of stereoscopic images/video over conventional monoscopic image/video [2]. In general, objects are seen more sharply in 3D images than in 2D images because 3D images enable humans to perceive clear contours between objects and background using binocular depth information. However the cost for this increased realism is the doubling of the amount of data necessary to transmit or store. In general, efficient transmission can be achieved by exploiting spatial and temporal redundancy in each sequence. In the case of stereo images/video, the efficiency can be further improved by exploiting binocular dependencies in stereo pairs. Also note that, to allow compatibility with 2D displays, transmission of stereoscopic images/video over existing channels may require very low rate coding to accommodate the additional image/stream, while maintaining the quality of the reference image/sequence. In this chapter, we describe 3D and stereo vision as a background. We briefly review the main issues and the previous work on stereo image coding.

2.1 Brief History of 3D

In 300 B.C. Euclid recognized that depth perception is obtained when each eye receives simultaneously one of two *similar* images [16]. In the early 1830s, the Wheatstone Viewer[1] created the illusion of three dimensions using pairs of hand-drawn illustrations. The subsequent invention of photography in 1839 allowed for stereo photographs. Then, the stereo photographs became popular in the late 19th century after the creation of the refined and reduced version of Wheatstone Viewer[2]. The popularity of 3D peaked around the turn of the century. Ever since, 3D has been an important part of the history of photography and film[3].

The first 3D film showing scenes of New York and New Jersey premiered in New York City in 1915. Subsequently, 3D imaging was revitalized through the 30's and 40's. In 1933, the Tru-Vue Company introduced a stereoscope using a 35mm film. In 1939, Chrysler Motors paved the way for the projection of full-color 3D film by showing a 3D film using polarized material without color distortion. With the invention of the television in 1939 (London), electronic versions of 3D (based on anaglyph method) were prompted in 1942[4]. However, in the 1950s, due to the disadvantages of the anaglyphs methods, 3D survived mostly in the cinema, rather than TV. The 3D film was one of the great hopes for the movie industry to reverse the decline in the number of viewers lost to TV. However, 3D film also has not been widely accepted due to its drawback that viewers have to wear uncomfortable special glasses and thus can experience headaches.

In the early 1990s stereoscopic methods gained a renewed interest based on the recent developments of autostereoscopic display system[5]. For several decades, various

[1] The first stereoscope was invented by British scientist Sir Charles Wheatstone.

[2] The hand-held versions, the Brewster Stereoscope and the Holmes stereoscope, were invented by Sir Davis Brewster in 1847 and by Oliver Wendell Holmes in 1862, respectively.

[3] Refer `http://www.afc.gov.au/resources/online/afc_loi/presentations/gary+w.html`

[4] The first experimental stereoscopic television program was broadcasted by SelectTV, LA, CA, USA in 1953.

[5] Refer `http://www.cl.cam.ac.uk/Research/Rainbow/projects/asd.html`

efforts have been made to develop practical 3D systems but 3D technologies including holography have not met the demands for realistic displays. Most of the efforts have gone into two-view stereoscopic systems with special glasses, which have limitations in terms of providing high quality or comfortable viewing. Such systems have proved effective in some scientific applications and, to a limited extent, in 3D wide screen cinema, such as IMAX(R) 3D[6]. However, through the 90's, considerable advances in 3D display technologies and innovations in the related fields are opening a new way for the 3D systems without special glasses.

In particular, several 3DTV projects bring together both signal processing and human factors. In Europe, research on 3DTV has been initiated by several projects, such as COST230[7] and DISTIMA[8], which aimed to develop a system for capturing, coding, transmitting and presenting digital stereoscopic image sequences. The projects had been followed up by another project, PANORAMA[9], which aims to enhance the visual information exchange in telecommunications with 3D telepresence. Other noteworthy efforts have been made by the 3D HDTV project of NHK[10].

2.2 3D Perception and Stereo Geometry

So far, stereo images/video have been intensively studied in the field of computer vision because stereoscopic viewing is one basic and popular way to perceive the environment in 3D [16, 17]. The two images in a stereo pair are called stereoscopic or stereo images. A sequence of stereoscopic images is called stereo video. The main limitation of stereo images/video is that the viewing position is bound to the position of cameras. In general, 3D imaging systems provide more freedom in viewing position than stereoscopic displays. However, the term "stereoscopic" and "3D" are

[6] Refer http://www.theatres.sre.sony.com/imax/across/history/history.html

[7] Refer http://www.fub.it/cost230/welcome.htm

[8] Refer http://www.tnt.uni-hannover.de/project/eu/distima/overview.html

[9] Refer http://www.tnt.uni-hannover.de/project/eu/panorama/

[10] Refer http://www.strl.nhk.or.jp/results/annual96/3-1.html

used interchangeably because stereoscopic images/video can be easily extended into 3D.

In general, 3D perception is based on various depth cues such as light, shade, relative size, motion, occlusion, texture gradient, geometric perspective, disparity, etc. However, one of the most effective cues is the binocular depth perception based on the fact that the depth perception is obtained by viewing a scene from slightly different viewing positions. Humans perceive a scene in 3D as follows. First, the scene in 3D real world is projected onto the retina as a 2D image, where each eye views a slightly different scene. Note that the 3D depth information is lost at this stage. Then, the primary visual cortex in the brain fuses the stereo pair by a stereopsis and a prior knowledge on the 3D world. Finally, humans perceive the feeling of depth by reconstructing 3D from 2D.

Similarly, in 3D imaging systems, the function of the eyes is taken over by stereo cameras that capture a scene from slightly different positions. The depth information can be obtained based on stereo vision techniques where the depth information is calculated by triangulation with the disparity, the relative displacement, and the geometry of the stereo camera. The procedure of estimating the disparity field has been known as the *correspondence problem* or *disparity estimation*.

To generate a stereo video sequence, two video cameras are placed in parallel to take images from slightly different perspective. Figure 2.1 shows the basic structure for stereo image formation and stereo camera geometry. The center of the lens is called the camera focal center and the axis extending from the focal center is referred to as the focal axis. The line connecting the focal centers is called the baseline, b. The plane passing through an object point and the focal centers is the epipolar plane. The intersection of two image planes with an epipolar plane makes the epipolar line. Let (X, Y, Z) denote the real world coordinates of a point. The point is projected onto two corresponding points, (x_l, y_l) and (x_r, y_r), in the left and right images. The disparity is defined as the difference vector between two points in the stereo images, corresponding to the same point in an object, *i.e.*, $v = (x_l - x_r, y_l - y_r)$.

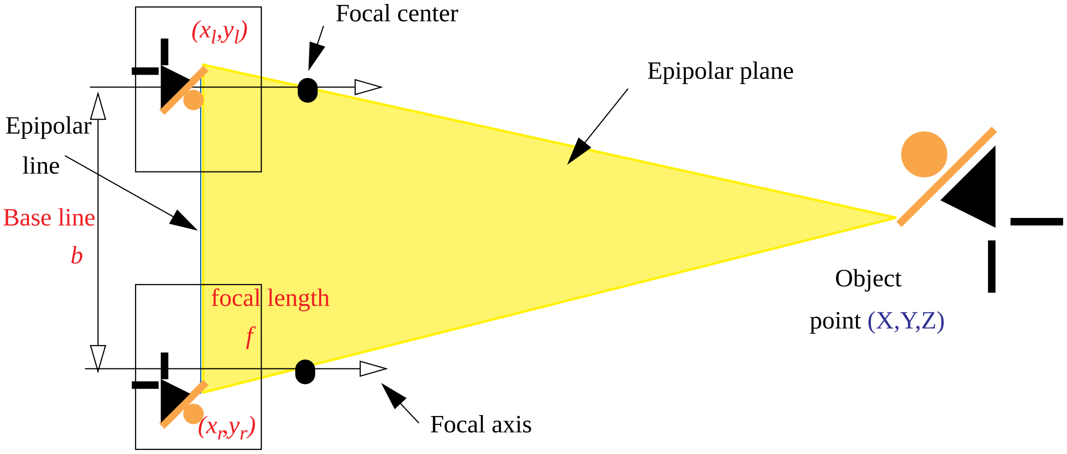

Figure 2.1: Simple camera geometry for stereo photography

In general, as shown in Figure 2.2, the converging camera configuration generates 3D distortion such as the *Keystoning error* [18]. For example, the projected squares are no longer the same size and become trapezoids or other sorts of quadrangles. These shapes are called *keystones*. If the keystoning effects are severe, then disparity estimation will generate higher estimation errors in the disparity compensated difference frame. Also, notice that the perception of 3D will be painful because the resulting depth plane is a curve rather than a straight line.

Therefore, the parallel camera configuration is preferred to the converging camera configuration. We assume pinhole cameras with parallel optical axes: the focal rays of the two cameras are parallel and perpendicular to the stereo baseline. We also assume that the two image planes are coplanar and that the two scan lines are parallel with the epipolar line (or baseline). As a result and with appropriate calibration, stereo images satisfy the following constraints.

- **Epipolar Constraint** Corresponding points in stereo images are in the same epipolar lines.

- **Similarity** Corresponding points in images have similar brightness.

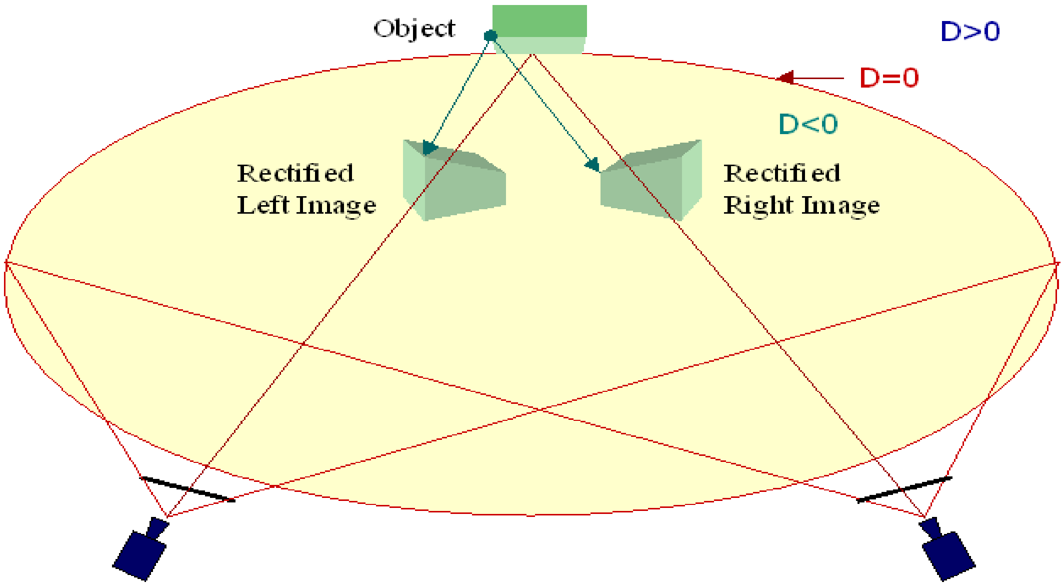

Figure 2.2: Conversing camera geometry for stereo photography

- **Uniqueness** A point in an image corresponds to only one point in the other image because one point in an object is projected onto only one point in each image.

- **Continuity and Ordering** Under the assumption of smooth object surfaces, the disparity varies continuously (or smoothly) in most parts of the image except at object boundaries or occlusion areas. The disparity is also in order except for the occlusion areas.

Finally, 3D information (X, Y, Z) can be computed by triangulation with binocular disparity and a given camera geometry as follows.

$$X = \frac{b(x_l + x_r)}{2 \times |v|}, \ Y = \frac{b(y_l + y_r)}{2 \times |v|}, \ Z = \frac{bf}{|v|}, \tag{2.1}$$

where b represents the baseline and f denotes the camera focal length. As can be seen in (2.1), the disparity can be considered as a relative depth because the disparity is inversely proportional to the depth. If the parallel axis constraint is satisfied, the search area for correspondence is restricted to a line and the matching process is accelerated significantly, *i.e*, $(v_x, v_y) = (0, y_l - y_r)$. By broadening the baseline, the accuracy of the distance measure can be increased but the common areas in the two images are decreased.

In real systems, there may be luminance differences between images in a stereo pair because the characteristics of the stereo cameras may be slightly different. In addition, there are some areas that only appear in one image of the stereo pair due to the stereo camera geometry, even though we assume the parallel axis constraint is met. Figure 2.3 shows an example of this phenomenon in stereo images, which is called *occlusion*.

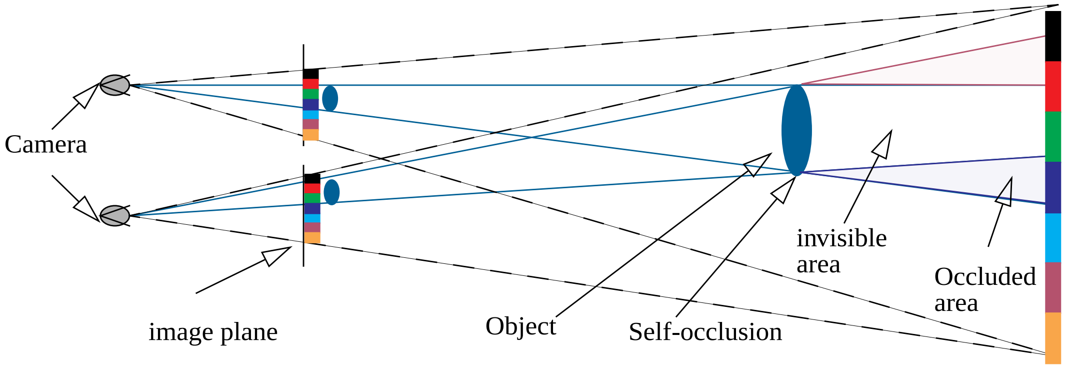

Figure 2.3: Occlusion effects. There are some regions that appear only in one image of the stereo pair due to the stereo camera geometry.

In general, the occlusion makes disparity estimation complicated. Figure 2.4 shows the disparity field variation according to the occlusion effects.

2.3 Issues in Stereo Image Coding

2.3.1 Disparity Correspondence

Most research efforts in stereo vision have been focused on an accurate disparity estimation[11]. As explained, several factors make the correspondence problem difficult. To overcome those problems and to estimate an accurate disparity field, several

[11] A comprehensive review on computational stereo can be found in [19].

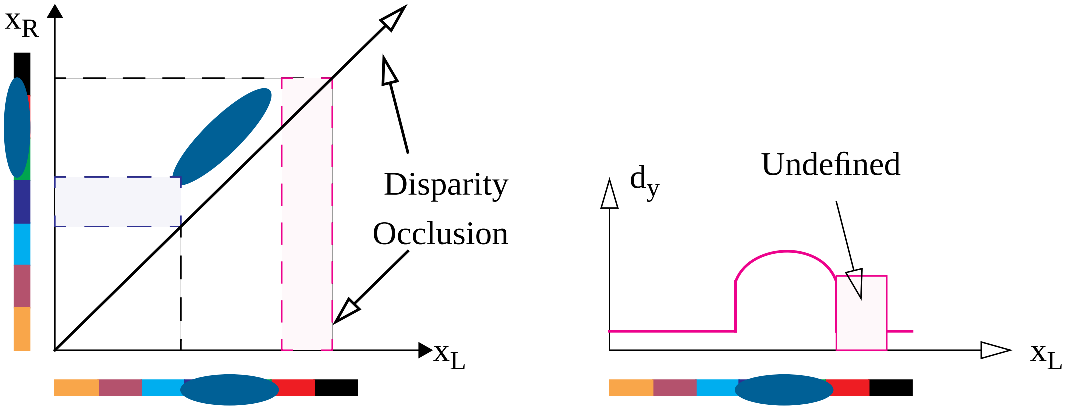

Figure 2.4: Disparity variation according to occlusion areas

schemes have been proposed, which can be grouped into two categories: (i) *area-based* and (ii) *feature-based* approaches.

In area-based approaches, pixels or regions are used to measure the similarity between stereo pair [20,21]. They yield dense disparity fields but tend to fail because of local ambiguities in the correspondence. Various improved estimation techniques have been proposed to overcome these problems. Regularization methods with smoothness constraints weaken the noise problem but they oversmooth the discontinuities such as those occurring at object boundaries [22–24]. Markov random field (MRF) models with various constraints reduce the oversmoothing problem using *soft* smoothness constrained with *line processes* [25–28]. Though the benefits of including discontinuities in the energy function are significant, they require excessive computational power to solve highly nonlinear (stochastic) optimization problems.

In feature-based methods, local cues (such as edges, lines, corners) have been used in disparity estimation [29–33]. They provide a robust disparity field because the features are more stable image properties than the original intensity image. However, feature-based schemes may work only if features are extracted in both images. They also may require interpolation to estimate a dense disparity field, because the disparity can be estimated only at the feature positions. However, interpolation is another complicated procedure due to its ill-posedness [34]. Phase-based disparity estimation is another method, which also requires additional steps to ensure the exclusion of regions with ill-defined phase [35,36].

Though many disparity estimation techniques developed in the computer vision communities may be applicable to stereo image coding, the direct adoption of those techniques may not be effective for various reasons. For example, the main emphasis of stereo vision (or/and motion analysis) has been on the accurate estimation of disparity (or/and motion) in order to reconstruct the 3D structure of the scene. An accurate displacement estimation is a key issue in stereo vision, because a disparity vector corresponds to the distance between cameras and the corresponding object point in the scene. However, the main focus of coding is the tradeoff between rate and distortion. Thus the goal of stereo image/video coding is not to estimate the true disparity but rather to achieve a high compression ratio. Therefore, it may not be worthwhile to compute a dense disparity field if the cost of handling (transmitting or storing) the disparity vector field is too high.

As a compromise, in coding of stereo images/video, fixed size block matching (FSBM) has been widely used, even though the true disparity/motion fields are obviously not blockwise constant [8,12,37]. FSBM-based methods are simple to implement and effective in terms of rate-distortion (RD) because they exploit the redundancy on the disparity field with a regular structure, which does not require additional information for the structure of the disparity field.

2.3.2 A Brief Review: Stereo Image Coding

As explained, higher encoding performance can be achieved by exploiting the inherent redundancy between two images in a stereo pair, as compared to independent coding. A simple coding for stereo images is to encode the two images independently, using conventional coding schemes or using 3D DCT [38]. Dinstein *et al.* also proposed a compression method based on the frequency domain relationship without disparity estimation [15]. A simple modification to uncorrelate two images is to encode an image and the difference between two images. However, this method is not so efficient because each object in the scene has different disparity. Therefore, further improvement can be achieved by adopting predictive coding, where a disparity vector field and disparity compensated difference frame are encoded.

Due to the similarity between stereo images and video, many of the intuitions and techniques used in video coding are applicable to stereo image coding [39]. Predictive coding with motion estimation in video coding increases the coding gain by exploiting the temporal dependency. It is possible because consecutive images in a video sequence tend to be similar. In general, disparity estimation is similar to motion estimation in the sense that they both are used to exploit the similarity between two (or more) images in order to reduce the bit rate.

However, the motion estimation schemes developed in video coding may not be efficient unless geometrical constraints for stereo imaging are taken into account. For example, if the cameras meet the epipolar constraint[12], the direction of the disparity is predominantly horizontal[13]. In comparison, motion vectors can take any direction in the 2D plane. This property simplifies the disparity estimation process, but other distinctive features of stereo images, *e.g.* occlusion, noise and 3D distortion (such as *Keystoning*) resulting from the stereo camera geometry, significantly degrade estimation/compensation efficiency [17, 18]. Note that, unlike video sequences, stereo images are projected onto two cameras and thus intensity levels between two images in a stereo pair tend to be slightly different. Note also that the occlusion areas are generated by all objects in the scene and not only moving objects as in motion estimation, as long as the objects are located at slightly different position in the 3D scene. As a result, the DCD may have high residual energy and thus the DCD frame may require relatively more rate as compared with the displaced frame difference (DFD)

[12] This constraint implies that the focal rays of the two cameras are parallel and perpendicular to the stereo baseline.

[13] If the cameras met the epipolar constraint, a particular object will appear in the two images with only a horizontal shift between its respective position. The epipolar constraint implies that focal rays of the two cameras are parallel and perpendicular to the stereo baseline

in video coding. Consequently, the efficiency of disparity compensated coding can be greatly reduced due to those features and the coding gain of disparity compensation is relatively smaller over independent coding, as compared to motion compensation [38].

Disparity estimation is one of the key steps in the stereo coding, because it helps to exploit the similarity along the disparity in the process of disparity estimation/compensation. In the predictive coding framework[14], the redundancy is reduced by compensating the target image from the reference image along the disparity vectors. Since the pioneering work by Lukacs [12], the most widely used coding methods for stereo images have been FSBM-based predictive coding[15].

Though FSBM is simple and effective to implement, disparity estimation schemes based on FSBM suffer from several well-known drawbacks: (i) inaccurate disparity estimation and (ii) annoying artifacts in the reconstructed image. In general, an inaccurate estimation is inevitable, with the inaccuracy mainly coming from: (a) the various noises, occlusion and lack of or repetitive textures, (b) a pixel accuracy in disparity estimation and (c) the uniform disparity assumption within a block. In general, FSBM with a simple error measure may not provide the smooth disparity field, and thus may result in increased entropy of the disparity field. In turn, an inaccurate estimation increases the bit rate of the disparity field.

Therefore, the efficiency of FSBM-based predictive coding can be increased by improving the efficiency of the disparity estimation/compensation. The proposed schemes to improve the encoding efficiency include: genetic algorithms [18], subspace projection methods [40, 41], extended windows [42], balanced filtering [43] and RD-based estimation [44]. The rate for the DV field also can be reduced by adopting other lossy encoding schemes (*e.g.* appropriate smoothing) for the disparity field. The central idea of achieving efficient estimation is to reduce or weaken the various

[14] In general, predictive codec consists of disparity estimation/compensation, transform/quantization, and entropy coding.

[15] Note that block, rather than feature or pixel, has been widely used, because the main focus of the coding is in the tradeoff between rate and distortion due to the limited available channel bandwidth.

noise effects by using useful constraints such as smoothness. The noise effects can be reduced by exploiting the correlation among neighboring disparity vectors. In general, the reduction of bit rate for the disparity field can be achieved by estimating a relatively smooth disparity field. Note however that, in order to maintain or improve encoding efficiency, a careful tradeoff is required between smoothness of the disparity field and the entropy of the DCD frame. For example, the disparity vector has to be selected to reduce the entropy for the disparity field, if it is similar to those of its neighbor blocks and it does not increase prediction error "too much."

In addition, an efficient method to deal with the DCD frame is essential to achieve low rate encoding because higher energy occurs along object boundary and occlusion region. For example, if the block includes object boundaries, block-based methods may suffer from visual artifacts at low bit rates, where only a few bits are assigned to the DCD frame. In particular, for images encoded at low rate coding, these artifacts usually appear along the block boundaries in the decoded target, as shown in Figure 2.5. These blocking errors can be very annoying because the human visual system (HVS) is sensitive to object boundaries, which are usually related to abrupt intensity changes. These artifacts result from different error sources: (i) disparity discontinuity due to our use of an error criterion considering only the DCD, (ii) the assumption of one vector per fixed size of block, and (iii) the quantization effect of the reference image, *i.e.*, block edge may be copied and pasted. Therefore, using overlapped block disparity compensation reduces the energy level of the disparity estimation errors without increasing the bit rate for the disparity field. In particular, the rate of the DCD frame can be reduced by combining both the subpixel accuracy and overlapped block disparity compensation [45].

Another approach to improve encoding efficiency is relaxing the *one-vector-per-block* assumption, which can overcome the disadvantage of FSBM, *e.g.* the annoying blocking artifacts in the reconstructed image. In FSBM, the higher prediction errors occur because the block boundaries do not coincide with the object boundaries. By

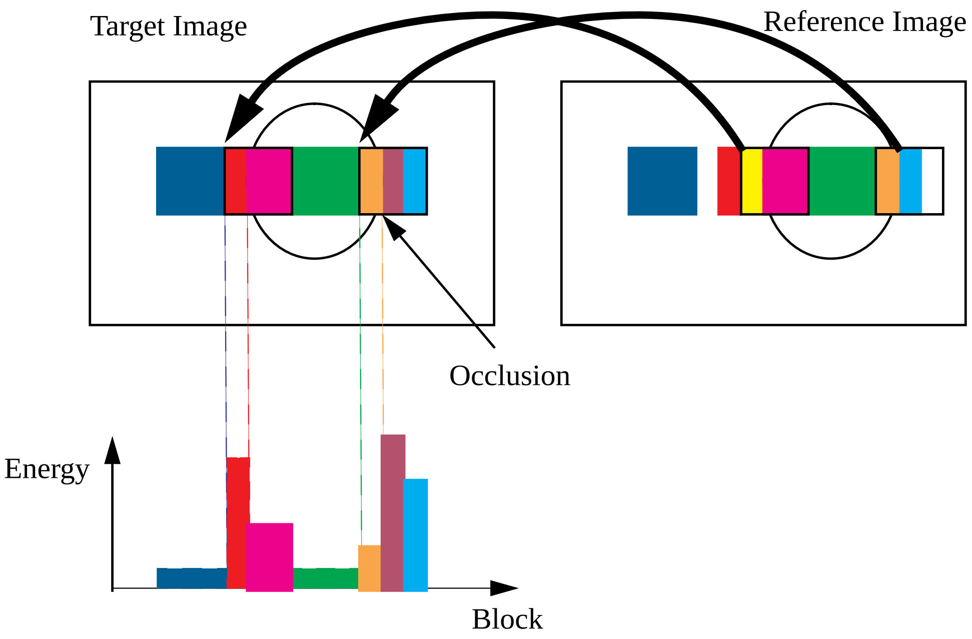

Figure 2.5: Various types of error in the DCD frame.

reducing the block size, the estimation error can be reduced, but as the block size becomes smaller the associated overhead (bit rates) required to transmit the disparity field becomes too large. In addition, smaller blocks frequently fail to provide good matching results because the estimation is subject to various noise effects and thus a less homogeneous disparity field is generated. Note that pixel-based estimation is the best way to reduce the entropy of the DCD frame. However, this comes at the cost of an expensive increase in the overhead necessary to represent the resulting disparity field. Meanwhile, increasing the block size increases the robustness against noise in the disparity estimation, but it also increases the magnitude of the estimation error. A good solution to this dilemma is a hierarchical (or sequential) block segmentation [46, 47].

Segmenting a block with higher prediction error into smaller subblocks can further reduce the rate of the DCD frame. The quadtree-based methods have been commonly used to encode the resulting disparity field [48–52]. However, the cost for reduced energy of the DCD frame is the increased side information of the disparity field. In order to increase coding gain over the block-based methods, segmentation-based algorithms have to represent the segmentation information (quadtree or boundary) and the corresponding disparity in an efficient manner.

A hybrid segmentation approach, which combines the disparity estimation based on the hierarchical block segmentation and the disparity field segmentation using an MRF model, can further improve encoding efficiency [53]. Also, the pixel-based disparity estimation with an arbitrary shape-based coding can be used to reduce the blocking artifacts [54,55]. In general, the process of segmentation simultaneously produces useful intermediate information for various applications such as scene analysis, synthesis, or generation [56]. Note however that the segmentation and its description cost are too expensive, compared to block-based schemes [3, 4, 53, 57].

In general lossy coding scenarios, quantization is an equally important problem. However, with few exceptions (*e.g.* [58]), the quantization and the bit allocation issues specific to stereo image coding have rarely been considered. Note that available conventional quantization or bit allocation schemes are mainly developed based on the assumption of completely decoupled encoding steps, *e.g.* the reference image and the target image in a stereo pair are quantized independently, and thus overall optimality cannot be guaranteed. Obviously, in the predictive coding framework, dependent quantization can further optimize the coding performance by selecting two sets of quantizers reducing quantization errors for the reference image and the DCD frame, while maintaining the total bit rate less than that of the allowed bit budget [39, 59].

A noteworthy effort in stereo image coding research has been generating intermediate views to provide additional freedom of viewing angles, without increasing rates. In general, intermediate view at the decoder can be synthesized by spatial interpolation using two decoded images in a stereo pair and disparity information. Therefore, to increase the quality of the synthesized intermediate image, a reliable occlusion, as well as disparity, estimation is essential [53, 60].

Another challenging area is measurement of 3D distortion. In 3D imaging systems, humans observe 3D scenes by combining two images together, instead of observing each image independently. Recently, image coding schemes incorporating the characteristics of human visual system (HVS) have been investigated. The spatial frequency sensitivity of HVS is measured and model as modulation transfer function (MTF) [61]. The MTF has been incorporated into transform coding and used to adjust quantization step sizes [62]. In addition, the spatio-temporal characteristics of HVS have been measured and modeled [63]. However, the measurement of 3D perception of HVS has yet to be actively researched. Obviously, simply combined distortion, $D_1 + D_2$, may not reflect the exact perceptual quality [64]. According to the suppression property of HVS, relatively lower bit rate for the target image may not significantly degrade the 3D perceptual quality [38].

2.3.3 Fixed Size Block Matching

2.3.3.1 Disparity Estimation

The basic idea of FSBM is to segment the target image into fixed size blocks and find for each block the corresponding block that provides the best match from the reference image. In general, a block minimizing estimation error is selected as a matching block. Let the target image be segmented into blocks, with a fixed size of $B \times B$ pixels. Two popular error criteria are the mean absolute error (MAE) and the mean squared error (MSE) which are defined as follows

$$\begin{aligned} D_{MAE}(i,j) &= \frac{1}{B \times B} ||f_{ij}^2 - f_{ij \oplus v_{ij}}^1|| \\ D_{MSE}(i,j) &= \frac{1}{B \times B} ||f_{ij}^2 - f_{ij \oplus v_{ij}}^1||^2 \end{aligned} \tag{2.2}$$

where f_{ij} and $\oplus v_{ij}$ denote the ij-th block in the target image and the corresponding displacement of the block, respectively.

In general, MAE, rather than MSE, is selected as a measure because MAE is more efficient in hardware implementation, while MSE yields somewhat better performance. In many standards, 16×16 blocks are used, but the block size can be increased or reduced according to the characteristics of the images. The most straightforward block matching method is the full search within the search window, known as the *exhaustive search*. It guarantees an optimal solution for given sizes of block and search window, if only the DCD frame is considered.

However, the advantages of FSBM may not be so clear once the overall coding system is considered together. In addition, a more consistent and exact disparity field is necessary for the application of intermediate scene generation, which provides look-around capability, because there is no available DCD frame in synthesizing the images corresponding to the intermediate viewpoints.

2.3.3.2 Disparity Compensated Difference

After disparity estimation/compensation, the difference between the disparity compensated and the original target image is generated. The difference is called *disparity compensated difference* (DCD), which has to be stored or transmitted together with a disparity field to improve the quality of the decoded target image. As explained in Section 2.3.3, the disparity estimation based on FSBM with MSE (or MAE) results in non-zero residual images containing high frequency components, especially in the block where the disparity estimation/compensation fails.

For DCD coding, several different approaches can be used such as pulse code modulation (PCM), differential PCM (DPCM), vector quantization, transform coding and subband coding. The simplest way is PCM, where the value of each pixel in DCD frame is quantized and encoded independently, without considering values of neighboring pixels. However, PCM is inefficient when neighboring pixels have strong correlation. DPCM exploits inherent spatial redundancy by predicting the current value using values of neighboring pixels. The difference between the value of the current pixel and the predicted value is quantized and encoded. In PCM or DPCM, an optimal scalar quantizer (SQ), such as Lloyd-Max or entropy constrained quantizer, is required to optimize the encoding efficiency [65]. Given the number of reconstruction levels, the indices of reconstruction levels are transmitted or stored. Though DPCM is relatively simple to implement, the achievable compression ratio is not so high.

A more efficient approach is to group pixels into vectors and to quantize them jointly. Note that usually this so called vector quantization (VQ) has been applied jointly with a transform or a subband coding scheme. The main advantage of VQ over SQ stems from utilizing correlation between pixels. However, finding an optimal codebook, *i.e.* reconstruction levels, is complicated.

The discrete cosine transform (DCT) is the most widely used transform for image and video coding. It has been so successful that, in current image/video coding standards, the DCT is employed for encoding of the DCD frame as well as the intra frame. Note that the basis of DCT are image independent but DCT approximate the optimum transform, Karhunen-Loeve transform (KLT), for natural images that can be modeled with a first order Gauss-Markov process (with higher correlation, $\rho > 0.9$). Chen *et al.* showed that the KLT, for the motion compensated difference frame is identical to that for the luminance image in spite of different statistical characteristics and, as a result, the DCT remained a near optimum transform for the motion compensated difference frame [66]. Another advantage of DCT is the availability of a fast implementation. Note however that the main weakness of the DCT is the fact it causes blocking artifacts at low rate coding.

Other noteworthy efforts include exploiting the statistical characteristics of DCD frame. The characteristics of motion compensated difference (MCD) frames have been studied [62, 66–72] and those works can provide insights into the encoding of the DCD frame. Based on observed statistics, many adaptive quantization schemes (with transform coding) have been reported. Connor *et al.* discussed the statistical characteristics of the MCD frame using the autocorrelation properties based on MRF theory [67]. Gonzalez *et al.* developed a minimal adaptive quantization algorithm operating in DCT domain. The algorithm is designed to optimize image quality by adapting a quantization scale factor to the local characteristics of the video while keeping the average output bit rate [73]. Puri *et al.* developed a strategy for an adaptive quantization method using a model for perceptual quality and bit rate [71]. Chun *et al.* described an adaptive quantization algorithm for video sequence coding by applying the perceptual weights according to the block-based visual activity in the DCT domain [72]. Stiller *et al.* proposed a Laplacian pyramid coding for the MCD, where they employed the classical Laplacian pyramid, a tree growing bit allocation strategy and the subsequent vector quantization [74]. Muller *et al.* proposed an embedded pyramid coding of MCD based on Shapiro's zerotree coding algorithm [75, 76].

Needless to say, a more precise modeling of the DCD frame for stereo image/video coding is very important to improve the quality of the coded image, especially at low rate coding. For stereo image coding, Moellenhoff *et al.* reported on specialized transform coding for the DCD frame, where they modified a quantization matrix and then the scanning order [58].

2.3.4 Variable Size Block Matching

Due to its simplicity and robustness, FSBM has been widely used in many video coding algorithms, including those based on standards[16]. However, as explained in previous section, FSBM has well-known drawbacks such as blocking artifacts and inaccurate estimation. An extreme example of FSBM would be a pixel based approach, which allows the reduction in entropy of the DCD frame, while increasing the rate of the disparity field by estimating a dense disparity field.

The basic idea of variable size block matching (VSBM) is to tradeoff between an efficient estimation/compensation and representation of the disparity field and the resulting DCD frame. The quadtree (Qtree) is commonly used, because the Qtree is efficient in hierarchically estimating and representing the disparity field [77]. An

[16] One exception is H.263, which allows splitting 16×16 block into 8×8 block in the "advanced prediction mode."

image or a block is assigned to a Qtree. Then, the block is segmented into four subblocks according to a given criterion. The segmentation is repeatedly applied until the size of subblock reaches 1×1 or the criterion is met. The resulting disparity field is encoded using DPCM.

Another promising approach is *region matching*, instead of block matching, which allows more efficient estimation by considering complex displacement. Obviously, region or object-based schemes are attractive because they allow the addition of various object-based functionalities. Note however that the cost of these more sophisticated schemes is the increase in computational complexity.

2.4 Tools

2.4.1 Rate Distortion Theory

In this Section we introduce some basic concepts of rate-distortion (RD) theory, which will be useful for the remainder of the dissertation. The source coding theorem states that the entropy of a source X, $H(X) = -\sum p(X) log_2 P(X)$, is the minimum rate at which a source can be encoded without information loss, and the channel coding theorem states that the rate of the source need to be smaller or equal to C for error free transmission over a channel with capacity C. Meanwhile, the RD theory represents the lower bound on the rate with a given average distortion or vice versa. Based on the RD theory the performance bound of lossy data compression schemes can be found. Note however that RD theory does not provide methods *to achieve the bound.* A detailed introduction can be found in [78].

Let a stereo pair in a stereo video sequence be a correlated random processes, *i.e.* (F_1, F_2). Then, according to Shannon's first theorem [79], the achievable bound of the minimum rate is $H(F_1, F_2) = H(F_1) + H(F_2|F_1)$. Let R and D denote rate and distortion of an image, respectively. Then, $H(F_1) \leq R(F_1)$ and $H(F_1, F_2) \leq$

$R(F_1, F_2)$. As a result, the required rate for lossy coding of the stereo pair can be represented as follows,

$$R(F_1) \leq R(F_1, F_2) = \{R(F_1) + R(F_2|F_1)\} \leq \{R(F_1) + R(F_2)\} \tag{2.3}$$

Similarly, the RD function can be represented as follows,

$$R(D_1) \leq R(D_1, D_2) = \{R(D_1) + R_{F_2|F_1}(D_2)\} \leq \{R(D_1) + R(D_2)\} \tag{2.4}$$

where $R(D_1, D_2)$ and $R_{F_2|F_1}(D_2)$ denote the joint RD function and the conditional RD function, respectively. Therefore, predictive encoding, which simultaneously considering two images in a stereo pair, achieves better RD performance over independent encoding, in general [13].

2.4.2 Optimal Bit Allocation

The aim of optimal bit allocation is to distribute "optimally" the available bit budget among different sources such that the overall distortion is minimized. In general, the bit allocation problem can be considered as an optimal quantization problem because usually a set of quantizers is available for each source.

So far, most research efforts have dealt with the problem of optimal independent quantization under the assumption that a specific selection of quantizer for a source does not affect the performances of other sources. In general stereo images/video scenarios, as well as in video coding, this is not the case because there exists strong "binocular" dependency between the two images in a stereo pair along disparity vectors. The selection of quantizers for the reference frame affects the selection for the target frame, as long as the reference frame is used to predict the target frame. Therefore, optimal dependent quantization schemes maximize overall coding performance [39, 59, 80, 81].

Meanwhile, optimal bit allocation schemes have been developed based on the operational RD (ORD) theory. In general lossy coding scenarios, only a finite number of quantizers are available, which results in only having a finite number of RD-points. Those pairs of RD points constitute the ORD function. Let Q be a set of available quantizers, *i.e.* $Q = \{q_0, \cdots, q_{N-1}\}$, where N is the number of available quantizers, *i.e.* $N = |Q|$, the cardinality of Q. Let $R(q_i)$ and $D(q_i)$ be the rate and corresponding distortion of a source for a quantizer q_i. As shown in Figure 2.6, corresponding sets of RD points can be plotted on an RD plot. Then, the ORD line is obtained by connecting those selected consecutive ORD points, where no other quantizer results in a lower or equal rate with a given distortion, or vise versa. While the RD curve is useful in showing how the performance of a real scheme approximate the optimal performance bound, ORD curve is useful in allocating bits optimally for a given scheme.

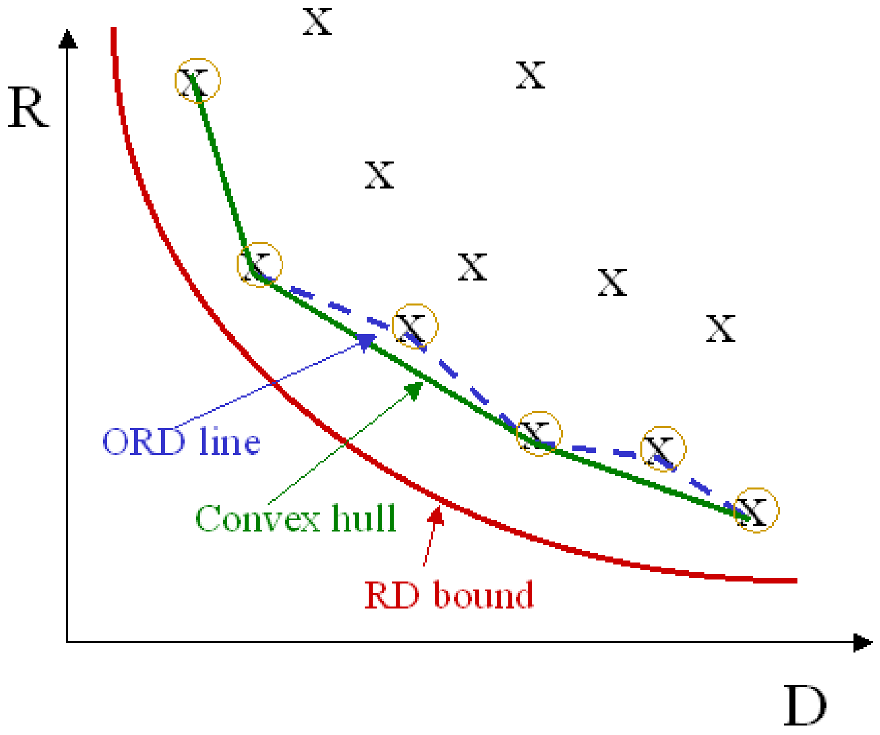

Figure 2.6: An operational RD plot. The x-mark and represents a possible RD pair. The ORD line is obtained by connecting consecutive o-marks points.

2.4.3 Lagrangian Optimization

An optimal solution to the bit allocation problem can be solved using Lagrangian multiplier approach [82]. Lagrangian multiplier method is a well-known mathematical tool to solve constrained optimization problems in a continuous framework. Note that for a discrete number of operating points, the Lagrangian method finds a solution lying on the convex hull, rather than on the ORD line.

Let the rate and distortion of each block depend on the quantization selection. Then, the rate and the distortion functions are defined as $R(Q) = \sum_{(ij)\in\Omega} r(q_i)$ and $D(Q) = \sum_{(ij)\in\Omega} d(q_i)$, respectively.

For a given bit budget R_{budget} an optimal set of quantizers that solves this problem is,

$$Q^* = \arg\min_Q D(Q), \text{ subject to } R(Q) \leq R_{budget} \tag{2.5}$$

The constrained problem can be transformed into an unconstrained problem using a Lagrange multiplier λ. For any $\lambda > 0$, an optimal solution $Q^*(\lambda)$ to the unconstrained problem is

$$Q^*(\lambda) = \arg\min_Q \{D(Q) + \lambda R(Q)\} \tag{2.6}$$

A remaining problem is how to find an optimal λ^* to optimize the quantization efficiency. For $\lambda_2 > \lambda_1$, by the optimality of $Q^*(\lambda_1)$ with $R(Q^*(\lambda_1)) > R(Q^*(\lambda_2))$, $D(Q^*(\lambda_1)) + \lambda_1 R(Q^*(\lambda_1)) \leq D(Q^*(\lambda_2)) + \lambda_2 R(Q^*(\lambda_2))$. By solving for λ_1 and λ_2,

$$\lambda_2 \geq \frac{D(Q^*(\lambda_1)) - D(Q^*(\lambda_2))}{R(Q^*(\lambda_1)) - R(Q^*(\lambda_2))} \geq \lambda_1 \tag{2.7}$$

Therefore, the ratio of the changes is bounded between two multiplier, λ_1 and λ_2. Note that $R(Q^*(\lambda))$ and $D(Q^*(\lambda))$ are, respectively, a nonincreasing and nondecreasing function of the Lagrangian multiplier λ. Therefore, with a pair of two initial λ's, (λ_1, λ_2), bisection method starts, *i.e.* $R(Q^*(\lambda_1)) \geq R_{max} \geq R(Q^*(\lambda_1))$, where R_{max} is the target rate. By selecting a $\hat{\lambda} = \frac{\lambda_1+\lambda_2}{2}$, the initial interval is bisected. Then, $\lambda_1 = \hat{\lambda}$

if $R(Q^*(\hat{\lambda}) \geq R_{max}$ and $\lambda_2 = \hat{\lambda}$, otherwise. By repeating this procedure, the bound is getting tighter and tighter. However, the bisection scheme has to be stopped using a threshold value ϵ (> 0), because there might not exist λ satisfying $R(Q^*(\lambda)) = R_{max}$. Note that R is defined on the finite set of quantizers Q.

The Lagrangian method is not always optimal because, as shown in Figure 2.6, the ORD line is not necessarily convex. Note that the Lagrangian method only finds the convex approximation, while a direct exhaustive search of constrained problem results in an optimal solution.

2.4.4 Viterbi Algorithm

The Viterbi algorithm (VA) is a deterministic forward dynamic programming scheme, which solves an constrained problem efficiently. The main advantage of VA over conventional optimization techniques is that VA can deal with discrete sets. In addition, VA yields a globally optimal solution according to Bellman's optimality principle.

We use VA to search possible solutions through a tree or trellis, while sequentially eliminating suboptimal solutions. In the tree (or trellis) each branch (or/and node) has a cost, which is additive over the path. In image/video coding, usually a block (or a frame) is assigned to a stage and other available quantity, such as a selection of quantizer or motion vector, is assigned to a node. Then, at each stage we can prune all branches arriving at each node, except the one having least cost.

Additional pruning schemes can help reduce the number of possible paths. Especially, in case of the dependent quantization problem in predictive coding, the pruning based on the so called *monotonicity property* efficiently reduces the search space without significant loss of performance [39, 80]. The monotonicity property indicates that the finer quantization for the reference frame, the more efficient quantization, in the RD sense, for the depending frame.

2.4.5 MRF/GRF Model and MAP Estimation

Geman and Geman considered images as realizations of a stochastic process that consists of an observable noise process and a hidden edge process [83]. We can apply this stochastic model to modeling the intensity image and extend it to modeling the disparity field. We model the spatial interactions among the neighboring intensity pixels (disparities) based on the discrete MRF model and Gibbs distribution. Consider a random field of intensity, $F = \{f_{ij}, (i,j) \in \Omega\}$ (or disparity, $V = \{v_{ij}, (i,j) \in \Omega\}$) defined on a discrete, finite, rectangular lattice $\Omega = \{(i,j) | 0 \leq i \leq N_x, 0 \leq j \leq Ny\}$ where N_x and N_y are, respectively, the vertical and horizontal size of the image (or the disparity field). Assume the intensity image, F (or V), is a MRF with respect to a neighborhood system $\eta = \{\eta_{ij}, (i,j) \in \Omega\}$, where η_{ij} is the neighborhood of f_{ij} (or v_{ij}) such that $(i,j) \notin \eta_{ij}$ and $(k,l) \in \eta_{ij}$, *i.e.*,

$$P\{F = f_{ij} | f_{kl}, (k,l) \in \Omega\} \quad = \quad P\{f_{ij} | f_{kl}, (i,j) \neq (k,l), (k,l) \in \eta_{ij}\} \qquad (2.8)$$

Similarly, the spatial interaction among the disparity (or motion) in the image sequences also can be defined as follows,

$$P\{V = v_{ij} | v_{kl}, (k,l) \in \Omega\} \quad = \quad P\{v_{ij} | v_{kl}, (i,j) \neq (k,l), (k,l) \in \eta_{ij}\} \qquad (2.9)$$

Fig. 2.7 shows some neighborhood systems commonly used in image processing. These can be used similarly for disparity and occlusion.

Fig. 2.8 shows two different neighborhood systems for edge processes, horizontal and vertical edges, respectively [27]. Considering the model constraints, an isolated edge is inhibited and a connected edge is encouraged even if the intensity (or disparity) changes slightly.

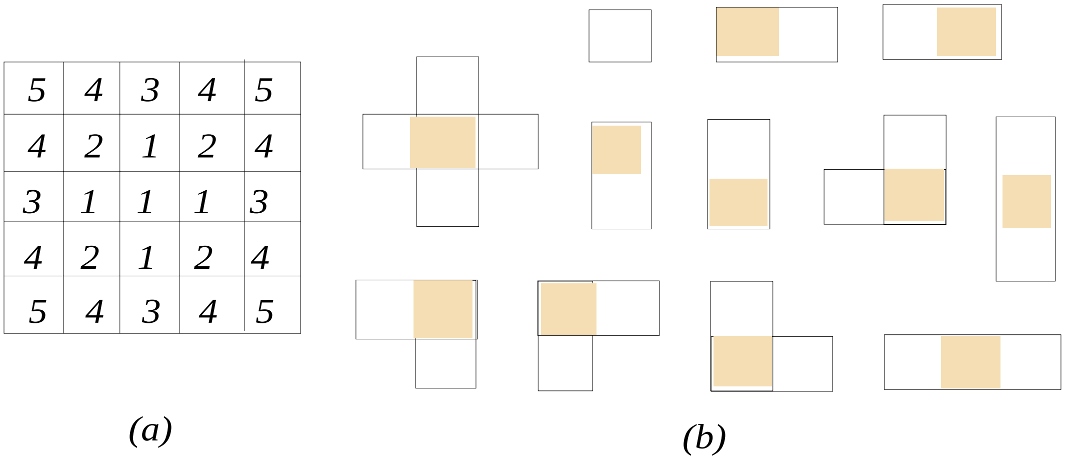

5	4	3	4	5
4	2	1	2	4
3	1	1	1	3
4	2	1	2	4
5	4	3	4	5

Figure 2.7: Neighborhood systems and cliques: (a) Geometry of neighborhoods; the number denotes the order of the neighborhood system. (b) First order neighborhood η^1 and cliques used for intensity, the disparity and the occlusion; we can quantify the effect of each clique according to the characteristics of the random fields.

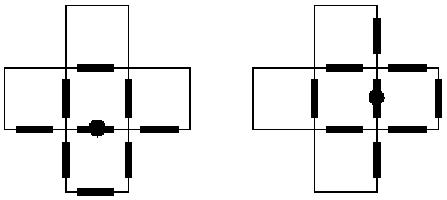

Figure 2.8: Neighborhood System for Edge Process for: (a) Vertical Edge (b) Horizontal Edge

According to the Clifford-Hammersley theorem [84], if a measure can be modeled by a MRF, then the probability mass of the measure can be represented in the Gibbs distribution form as follows

$$P(F) = \frac{1}{Z} exp\{-\frac{1}{T} U(F)\} \tag{2.10}$$

where Z is a normalization constant and T is the so called temperature which controls the sharpness of the distribution. The energy function $U(F)$ can be represented as the sum of clique potentials defined according to the neighborhood system selected. The main advantage of representing each probability in the Gibbs distribution form is that it can be formulated with energy function and the multiplication of the probabilities can be replaced by the sum of the energy equations. Therefore, the MAP estimation problem can be replaced by the problem of finding a solution minimizing the energy equation.

The main advantage of the MRF model based approach is that it provides a rigorous mathematical framework and a general model for the interaction among spatially related random variables. Another advantage of the MRF model is its ability to combine discontinuity into the energy equation. It reduces the error resulting from an oversmoothing effect by adopting the *line process*. It is easy to integrate different information such as stereo and motion [85]. It also can deal with the occlusion effect. The resulting algorithm also can be implemented in parallel due to its inherent localization property [27].

2.4.5.1 Example-I: Image Restoration and Segmentation

We can formulate an image segmentation problem as follows. For a given intensity image, G, we want to find a smooth intensity image, F, and intensity edge, L^I, such that solutions maximize the *a posteriori* probability (MAP), $P(F, L^D|G)$. We can decompose the posterior probability using Bayes theorem as follows

$$P(L^I, F|G) = \frac{P(G|L^I, F)P(F|L^I)P(L^I)}{P(G)} \propto P(G|F)P(F|L^I)P(L^I) \tag{2.11}$$

where $P(G)$ is a constant and thus can be ignored, because $P(G)$ is not a function of L^I or F.

The first term of the right side in (2.11) is called the observation (or noise) process. The degradation model can be represented in the Gibbs distribution form as follows

$$P(G|F) = \frac{1}{Z} exp\{-U(G|F)\} \tag{2.12}$$

where Z is a normalization constant. The energy functions designate the constraints of the strong similarity between the noise image and the original image. The energy function, $U(g_{ij}|f_{ij})$, can be represented as follows

$$U(g_{ij}|f_{ij}) = (g_{ij} - f_{ij})^2 \tag{2.13}$$

where f and g denote the given and the reconstructed intensity image, respectively.

The second term in (2.11) represents an *a priori* assumption on the smoothness of the intensity field, F, given an intensity edge, L^I. The *a priori* distribution for F with L^I can also be represented as Gibbs distribution form

$$P(F|L^I) = \frac{1}{Z} exp\{-U(F|L^I)\} \tag{2.14}$$

where Z is a normalization constant. The energy function $U(f_{ij}|l_{ij})$ can be represented as follows

$$U(f_{ij}|l_{ij}) = \sum_{\eta_{ij}} (1 - l_{ij}^{\eta})(f_{ij} - f_{ij}^{\eta})^2 \tag{2.15}$$

where f^η represents the neighboring pixels and l^η represents the corresponding discontinuities.

We can also decide edge process initially by the intensity difference of the noisy image. The initial discontinuity process is defined as

$$l_{ij} = \begin{cases} 1, & |f_{ij} - f_{ij}^\eta| \geq T_d \\ 0, & o.w. \end{cases} \tag{2.16}$$

where T_d is the threshold for edge decision. If the difference between the intensity and its neighborhood exceed a threshold T_d, then there is discontinuity. In this case, the smoothness constraints should not be performed across this discontinuity.

Finally, we have

$$P(L^I, F|G) \propto exp\{-U(G|F)\}exp\{-U(F|L^I)\}exp\{-U(L^I)\} \tag{2.17}$$

where each term represents a noise process, a smooth intensity field, and an intensity edge process, respectively. The overall energy function for the intensity image restoration/segmentation can be represented as equation (2.11) and the corresponding energy function can be calculated as follows

$$U(l_{ij}^I, f_{ij}|g_{ij}) = \alpha(f_{ij} - g_{ij})^2 + (1-\alpha)\sum_{\eta_{ij}}(1 - l_{ij}^\eta)(f_{ij} - f_{ij}^\eta)^2 + \gamma V_c(l_{ij}, l_{ij}^\eta)\} \tag{2.18}$$

where α and γ are weighting constants. The weighting constant α is controlled according to the noise level of the given image.

2.4.5.2 Example-II: Block-based Disparity Estimation

The disparity estimation problem can be formulated as follows. For given stereo pairs, F_1 and F_2, we want to find the disparity field, V, and occlusion, Φ, such that the solutions maximize the *a posteriori* probability, $P(V, \Phi|F_1, F_2)$. We can decompose the posterior probability using Bayes theorem. Similarly, according to the

Clifford-Hammersley theorem [84], the MAP estimation problem can be replaced by the energy minimization problem. As a result, the solutions, $X = (V, \Phi)$ minimizing the energy function $U(V, \Phi|F_1, F_2)$, are the solutions maximizing the posterior probability $P(V, \Phi|F_1, F_2)$, *i.e.*,

$$\begin{aligned}\hat{X} &= \arg\max_X P(V, \Phi|F^1, F^2) \\ &= \arg\min_X U(V, \Phi|F^1, F^2) \\ &= \arg\min_X \{U(F_2|F_1, V, \Phi) + U(V|\Phi) + U(\Phi)\} \qquad (2.19)\end{aligned}$$

where each term represents imposed constraints for the disparity estimation, *i.e.* similarity, smoothness and occlusion, respectively.

Given the above model, we can derive the overall energy function for the disparity estimation with FSBM as follows,

$$\begin{aligned}U(V, \Phi|F_1, F_2) &= \sum_{(ij)\in N} U(v_{ij}, \phi_{ij}|f_{ij}^1, f_{ij}^2) \\ &= \sum_{(ij)\in N} \{(1-\alpha)(1-\phi_{ij})||f_{ij}^2 - f_{ij\oplus v_{ij}}^1||^2 \qquad (2.20) \\ &\quad +\alpha \sum_{\eta}(1-\phi_{ij}^{\eta})(v_{ij} - v_{ij}^{\eta})^2 + \beta \sum_{c\in C_L} V_c(\phi_{ij}, \phi_{ij}^{\eta})\}\end{aligned}$$

where f_{ij}, v_{ij} and ϕ_{ij} represent a block and the blockwise disparity vector and its occlusion status, respectively. In the above equation, α and β denote the weighting constants[17]. In general first order neighborhood η^1 is used. The larger the neighborhood, the greater the influence from the neighboring disparity vectors. A set of cliques C_L and its potential are pre-specified for the occlusion.

[17] Note that the constant α is determined according to the noise level of the two images and increased according to its noise level. For example, if we set α to be zero for the noise-free images the equation will be similar to the simple BM algorithm.

Chapter 3

Optimal Blockwise Dependent Quantization

Research in coding of stereo images has focused mostly on the issue of disparity estimation/compensation, which aims at exploiting the redundancy between the two images in a stereo pair. However, less attention has been devoted to the equally important problem of allocating bits between the two images. This bit allocation problem is complicated by the dependencies arising from using a prediction based on the quantized reference images. In this chapter, we address the problem of blockwise bit allocation for coding of stereo images and show how, given the special characteristics of the disparity field, one can achieve an optimal solution with reasonable complexity, whereas in similar problems in motion compensated video only approximate solutions are feasible. We present algorithms based on dynamic programming that provide the optimal blockwise bit allocation. Our experiments based on a modified JPEG coder show that the proposed scheme achieves higher mean PSNR over the two frames (0.2-0.5 dB improvements), as compared to blockwise independent quantization. We also propose a fast algorithm that provides most of the gain at a fraction of the complexity.

3.1 Introduction

Most research efforts on stereo image/video coding have been devoted to investigating efficient disparity estimation/compensation (DE/DC) schemes to improve the encoding performance [12, 13, 41, 43, 53, 86]. As in other coding scenarios, stereo images/video can be compressed by taking advantage of spatial/temporal redundancies in each monocular image/video. However, the coding efficiency for stereo images/video can be improved even further by exploiting an additional redundancy associated with the similarity between the two images in a stereo pair, *i.e.* the "binocular" dependency. The central idea of stereo image coding based on DE/DC is to use one of the images in the stereo pair as a reference and to estimate the other image (the target)[1].

With few exceptions (e.g. [58]), the quantization and the bit allocation issues specific to stereo coding have rarely been considered. Obviously, as shown in Figure 1.3, the encoding performance also depends on making a "proper" choice of quantizers (Q_1, Q_2) and not just on the choice of the disparity vectors (V). However, the available bit allocation (or quantization) schemes are mainly developed based on the assumption of completely decoupled encoding steps, *e.g.* target and reference frames are quantized independently, and thus overall optimality cannot be guaranteed.

Here, we study the problem of optimal bit allocation for stereo image coding. Our proposed bit allocation scheme is aimed at block-based, rather than segmentation based, DE/DC techniques due to the comparative simplicity and robustness of block-based techniques. Note that we assume that the disparity vector (DV) field is estimated in "open loop", *i.e.* based on the original image rather than the quantized

[1] Many of the intuitions and techniques used in motion estimation/compensation (ME/MC) are applicable to DE/DC due to the similarities between ME/MC and DE/DC.

version, and then focus on the *quantizer allocation* to the reference and the residue images[2].

The main novelty of our work is the introduction of an algorithm for *optimal blockwise dependent bit allocation* for stereo image coding. The binocular dependency has to be taken into account because the target image (F_2) is compensated based on the quantized reference image $F_1(Q_1)$. Thus, each choice of quantizer for the reference frame results in different residual energy levels in the difference frame [13]. Given that the epipolar constraint is met[3], the binocular dependency becomes relatively simple, *i.e.* it occurs predominantly along the horizontal direction. This property not only simplifies the disparity estimation process but also allows us to find an optimal solution for our allocation problem. We first demonstrate how the optimal set of quantizers can be determined using the Viterbi algorithm (VA), and then introduce a novel method that approximates the optimal solution with limited loss in performance but much faster operation.

Note that our results may also provide some ideas for the related problem of blockwise dependent bit allocation in video coding, where choices of quantization for a reference frame affect the frames that are motion predicted from it [80]. In the case of video coding it is difficult to take into account blockwise dependencies, because motion vectors can have any direction in the 2D plane[4]. Accordingly, an optimal solution for the video case is not available and thus much of the work has concentrated on analyses of framewise dependency, *i.e.* where a single quantizer is

[2] Note that techniques developed in rate-distortion (RD) based ME in video coding [44, 87–90] could also be used in conjunction with our algorithm to estimate an optimal (in an RD sense) disparity field.

[3] This constraint implies that the focal rays of the two cameras are parallel to each other and perpendicular to the stereo baseline. Thus, if the cameras meet the epipolar constraint, then the disparity is *exactly* 1D, *i.e.* a particular object will appear in the two images with a horizontal shift between its respective positions. Even if the parallel axis constraint is not strictly met (*i.e.* the disparity is not *exactly* 1D), blocks in one row in the target image can be predicted fairly accurately from blocks located in the corresponding row in the reference frame, because the vertical disparity is confined only to ± a few pixels.

[4] In the case of motion, each block in the predicted frame depends on up to four blocks in the reference, and conversely, blocks in the reference frame affect several blocks in the target image.

allocated per frame [80,91]. Note that schemes such as [92] have addressed blockwise bit allocation but without taking into account the temporal dependency, *i.e.* the effect of a particular allocation on future frames.

Our experimental results demonstrate that the proposed scheme provides higher *mean* peak signal to noise ratio (PSNR), about 0.2-0.5 dB for the two images in a stereo pair, as compared to an optimal blockwise independent quantization. Note that finer quantization for the reference image tends to allow more efficient encoding for the disparity compensated difference frame [80]. We use this so called *monotonicity* property as a starting point to propose a fast algorithm that further reduces the computational complexity without significant loss of quality. This blockwise dependent bit allocation can be a benchmark for faster allocation schemes, or can be used in offline encoding applications or in applications where encoding is performed just once but decoding is performed many times.

This chapter is organized as follows. In Section 3.2 we formulate the problem of bit allocation and describe how to find the optimal blockwise quantizer assignments using the VA. We also discuss how to reduce the complexity of the allocation algorithm. Experimental results are provided in Section 3.3. Finally, we discuss the results and give directions for future work in Section 3.4.

3.2 Dependent Bit Allocation

3.2.1 Definitions and Notations

Let an image F_l, be segmented into N square blocks, $F_l = \{B_m, 0 \leq m \leq N-1\}$, where B_m represents the m-th block in the image. In case of a stereo pair, F_1 and F_2 denote the reference and the target images, respectively. Blocks in F_2 are denoted B'_m, to differentiate them from blocks in F_1. Let a quantizer (or quantization scale) be assigned to each block (from a finite set of available quantization choices). Then, a set of blockwise quantizers for F_1 can be represented as $Q_1 = \{q_m, 0 \leq m \leq N-1\}$, where q_m denotes a quantization index. Similarly, a set of quantizers for the disparity compensated difference (DCD) frame is represented as $Q_2 = \{p_m, 0 \leq m \leq N-1\}$. The DV field is defined as $V = \{v_m, 0 \leq m \leq N-1\}$, where v_m corresponds to the disparity for the m-th block in F_2. In the same way, the blockwise rate and the distortion can be defined, and the overall rate and the distortion are represented as the sum of the individual rates and the distortions of the blocks.

In our experiments, we use simple objective measures such as mean square error (MSE) and PSNR. Note that subjective evaluation of 3D quality is still an open problem and is not very reliable and repeatable yet. Therefore, we measure the distortions of F_1 and F_2 using MSE, *i.e.* $D_1 = (F_1 - F_1(Q_1))^2$ and $D_2 = (F_2 - \hat{F}_2(Q_1, Q_2, V))^2$, where $F(Q)$ denotes the decoded image, when quantizer Q is used. The decoded target image, $\hat{F}_2(Q_1, Q_2, V)$, can be reconstructed by adding the compensated target image with the DV field and the decoded DCD, *i.e.* $\hat{F}_2(Q_1, Q_2, V) = F_1(Q_1, V) + E(Q_2)$, where $E = F_2 - F_1(Q_1, V)$. We also measure the performance using mean PSNR for the stereo pair, defined as follows,

$$PSNR_{mean} = 10 \times \log_{10}\{\frac{255^2}{(D_1 + D_2)/2}\} \tag{3.1}$$

where D_1 and D_2 denote the MSE's of the reconstructed images, $\hat{F}_1$ and $\hat{F}_2$, respectively.

3.2.2 Optimal Blockwise Dependent Quantization

For simplicity we assume that the quantizer indices are encoded with a constant number of overhead bits per block. Note that other $1D$ dependencies such as those resulting of DPCM encoding of quantization indices could also be incorporated easily into our scheme.

Let R_{budget} be the remaining bit budget after allocating bits to the DV field. For a given DV field, V, the optimal dependent bit allocation problem can be formulated as follows[5],

$$\begin{array}{ll} \text{Given} & F_1, F_2, V, R_{budget} \\ \text{find} & \hat{X} = (Q_1, Q_2) \\ \text{such that} & \hat{X} = \arg\min_X \{D_1(Q_1) + D_2(Q_2|Q_1)\} \\ \text{subject to} & R_1(Q_1) + R_2(Q_2|Q_1) \leq R_{budget}. \end{array}$$

where we would have an independent bit allocation problem in the particular case where $D_2(Q_2|Q_1) = D_2(Q_2)$ and $R_2(Q_2|Q_1) = R_2(Q_2)$.

This constrained optimization problem can be transformed into an unconstrained problem using the Lagrange multiplier method [82,93,94] by introducing a Lagrangian cost

$$\begin{aligned} J(\lambda) &= J_1(Q_1) + J_2(Q_2|Q_1) \\ &= \{D_1(Q_1) + \lambda R_1(Q_1)\} + \{D_2(Q_2|Q_1) + \lambda R_2(Q_2|Q_1)\} \qquad (3.2) \end{aligned}$$

where the Lagrange multiplier λ is a nonnegative constant.

Figure 3.1 provides an example of why dependencies have to be taken into account [80]. Note that, for a given λ and three operational RD (ORD) points, Q_{1b} is the RD optimal quantizer for the reference image because its Lagrangian cost $J_1(Q_{1b})$ is the lowest. However, if the overall Lagrangian cost for the two images is taken into account, Q_{1a} may turn out to be the best choice for the reference image; the Lagrangian cost $J_1(Q_{1a}) + J_2(Q_{2b}|Q_{1a})$ may be smaller than the cost $J_1(Q_{1b}) + J_2(Q_{2b}|Q_{1b})$.

[5] The relative importance of D_1 and D_2 can be controlled using the weighting constant α, *i.e.* using $D_1 + \alpha D_2$ as our distortion measure. This allows us to support two different views of the depth perception process: *fusion theory* and *suppression theory* [14, 15]. Note that this modification can easily be incorporated into our framework.

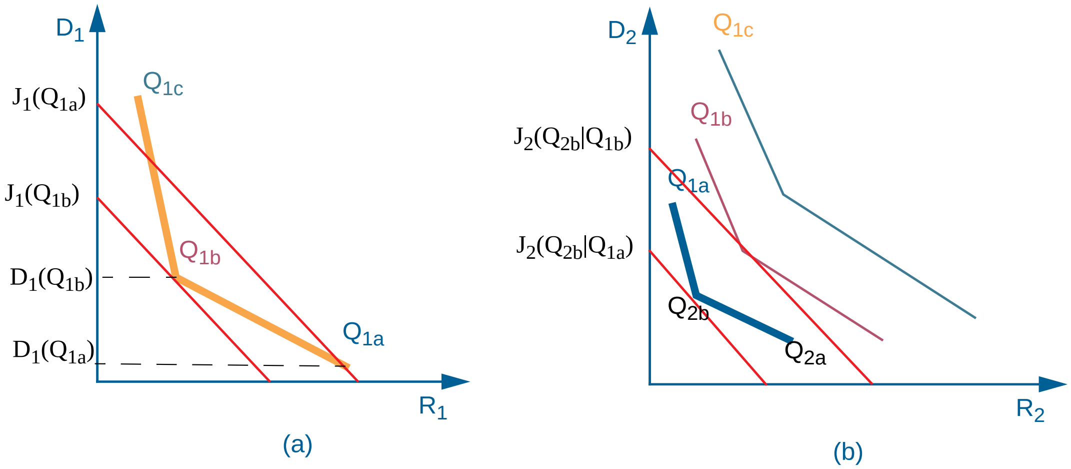

Figure 3.1: Operational RD plots in a typical dependent bit allocation scenario: (a) reference image and (b) target image. Independent bit allocation: for given λ, the quantizer Q_{1b} is optimal because the Lagrangian cost $J_1(Q_{1b})$ is smaller than for the others. Dependent bit allocation: if stereo pairs are considered together, there is a chance for the quantizer Q_{1a} to be optimal, because the total Lagrangian cost $J_1(Q_{1a}) + J_2(Q_{2b}|Q_{1a})$ can be smaller than the cost $J_1(Q_{1b}) + J_2(Q_{2b}|Q_{1b})$.

For the blockwise quantizer assignments the Lagrangian cost in (3.2) can be expressed as,

$$J(\lambda) \quad = \quad \sum_{m=0}^{N-1} \{d(q_m) + \lambda r(q_m)\} + \sum_{n=0}^{N-1} \{d(p_n|q^{\eta_1}(v_n)) + \lambda r(p_n)\} \qquad (3.3)$$

where q^{η_1} is a vector that contains the quantizer indices of those blocks in F_1 that are used to predict the current block in F_2. As shown in Figure 3.2, η_1 denotes (at most) two consecutive blocks in F_1 along the DV. Given the disparity vector v_1, the selection of a quantizer for B_1' in the DCD frame will be affected by the selection of quantizers for B_2 and B_3 in F_1. Thus a block in the DCD frame depends only on the quantizers, p_n and (q_m, q_{m+1}), *i.e.* $d(p_n|q^{\eta_1}) = d(p_1|q_2, q_3)$ in Figure 3.2. In general, the index m can be denoted as $m = n + \lfloor \frac{v_n}{|B|} \rfloor$, where $\lfloor \rfloor$ and $|B|$ represent the floor function and the width of the block, respectively.

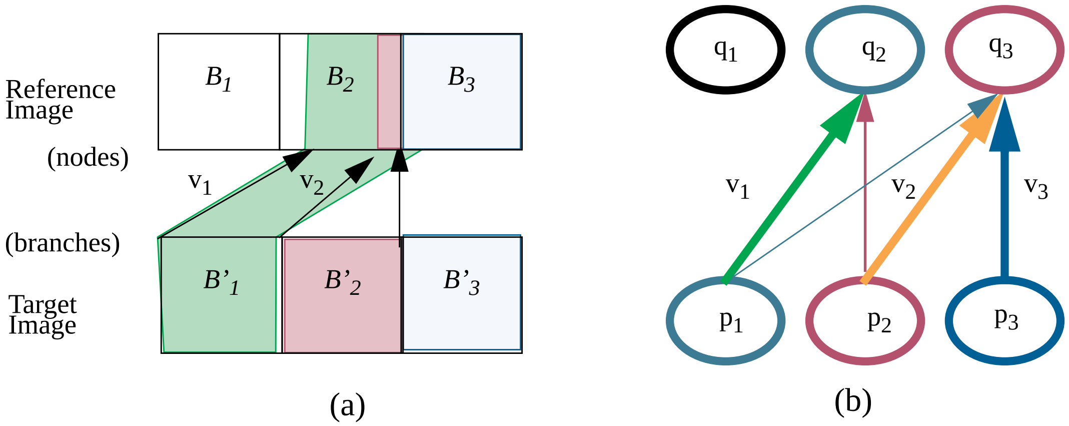

Figure 3.2: Binocular dependency between corresponding blocks along the disparity vector. At most two consecutive blocks in the reference image are related to a block in the target image. For example, a block B'_1 in the target image is compensated from two consecutive blocks, B_2 and B_3, in the reference image along the disparity vector v_1. Therefore, the distortion of the block in the DCD frame is a function of p_1, q_2 and q_3.

3.2.3 Solution using the Viterbi Algorithm

Due to the predominant $1D$ dependency, a row of blocks (ROB) in the target image depends only on the ROB in the same position in the reference image. Therefore, we only need to consider the bit allocation for pairs of ROBs[6], as other ROBs do not affect the result. Even if there is some small vertical disparity this is a sufficiently good approximation.

Let ROB_1 and ROB_2 be the ROBs in the same position in the reference image and the DCD image, respectively. From now on, when we refer to the k-th block it should be clear that this is *within the particular ROB*. We first represent all possible allocations for each pair of ROBs by constructing a *trellis*. The costs of the branches and nodes of the trellis correspond, respectively, to the blocks in ROB_1 and ROB_2. Refer to Figure 3.3 for the trellis corresponding to the example in Figure 3.2.

We now define our method more formally. Let k be the index of the stage.

[6] One from the reference and one from the target located at the same position.

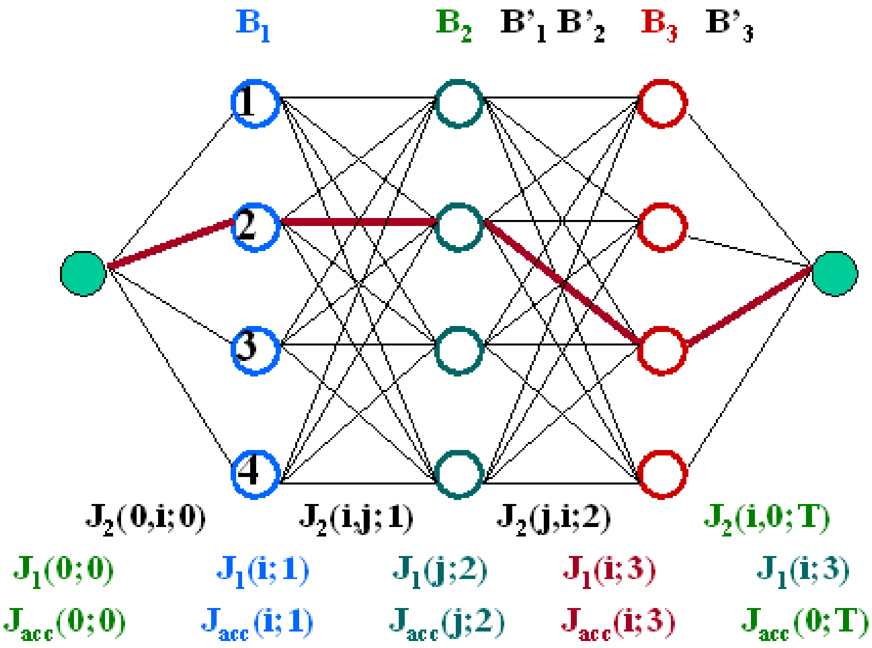

Figure 3.3: Trellis structure for blockwise dependent bit allocation. Each node in the trellis corresponds to a quantizer choice for a block in F_1 and has a corresponding Lagrangian cost. The quantizer indices are monotonically increasing from finest to coarsest. A branch linking two stages corresponds to a quantization assignment to all the dependent blocks in the DCD frame. The corresponding Lagrangian cost is attached to the branch. The darker path denotes selected quantizers using the Viterbi algorithm.

Stage: The k-th stage in the trellis corresponds to the k-th block in ROB_1. Therefore, the number of stages, K, is equal to the number of blocks in ROB_1.

Node: Each node in the k-th stage corresponds to a possible quantizer choice for the k-th block of ROB_1. The choices are ordered from top to bottom in order of finest to coarsest. Therefore, the number of state nodes per stage is $L = |q|$, *i.e.* the number of available quantizers for the reference image. Each node has a corresponding Lagrangian cost, $J_1(i;k)$ in (3.4), which depends only on the rate and the distortion of the k-th block of ROB_1 when quantizer i is used.

$$J_1(i;k) = d(q_k^i) + \lambda r(q_k^i) \tag{3.4}$$

Branch: A branch, joining nodes q_k^i and q_{k+1}^j, corresponds to the *optimal* vector of quantizers, p_n^{ij}, for the (possibly more than one) blocks in ROB_2 which depend on blocks k and $k+1$ in ROB_1. Each branch has a total Lagrangian cost

$$J_2(i,j;k) = \sum_{n \in \eta_2(k,k+1)} \{d(p_n^{ij}|q_k^i, q_{k+1}^j) + \lambda r(p_n^{ij}|q_k^i, q_{k+1}^j)\} \tag{3.5}$$

which adds up the Lagrangian costs corresponding to each of the blocks n. Note that more than one block in ROB_2 can be assigned to a given branch (this will depend on the size of the disparity search region). For example, in Figure 3.2 two blocks in ROB_2 are assigned to a branch, *i.e.* B_1' and B_2' both depend on B_2 and B_3 and thus the two Lagrangian costs corresponding to B_1' and B_2' would be added to each branch linking stages 2 and 3 in the trellis.

Path: A path is a concatenation of branches from the first stage to the final stage in the trellis. Each path corresponds to a set of quantization choices for both ROB_1 (nodes) and ROB_2 (branches). The cost of a path is the accumulated cost of branches and nodes along the path.

Trellis: The trellis is made of all possible paths linking the nodes in the first stage and the nodes in the last stage, *i.e.* all possible concatenated choices of quantizers for a given pair of ROBs in the stereo pair.

Once the trellis has been constructed, the optimal blockwise dependent quantization problem is equivalent to finding the smallest cost path from a node in the first stage to a terminal node in the last stage of the trellis. For a fixed λ, by applying the VA [95], we can obtain the best possible quantizer selection that minimizes the Lagrangian cost defined in (3.3). To find the optimal bit allocation for a given bit budget, we may need to iteratively change λ until we find λ^* such that $R(\lambda^*) - R_{budget} \leq \epsilon$, for $\epsilon \geq 0$. The desired λ^* can be selected using a fast bisection search algorithm, as in the previous chapter [82]. For a fixed λ the procedure is as follows,

Step 0: (Initialization:) Add an initial node B_0 and a final node B_T where $T = K + 1$, where K denotes the number of stages. Set $k = 0$ and $J_{acc}(0; 0) = 0$.

Step 1: At stage k, branches are added to the end of each node i (of all surviving paths) and Lagrangian costs, J_1 and J_2, are assigned to the node and the branch, respectively.

Step 2: At a stage $(k + 1)$, for each node j, an accumulated transition cost from node i, $J_{tr}(i, j; k)$, is calculated by summing the accumulated cost, $J_{acc}(i; k)$, and the transition cost, $J_2(i, j; k)$. Of all arriving branches (at most L), the one with the lowest accumulated transition cost is chosen. The resulting cost is assigned to the accumulated cost, $J_{acc}(j; k + 1)$ and the remaining branches are pruned.

$$\begin{aligned} J_{tr}(i, j; k) &= J_{acc}(i; k) + J_2(i, j; k) \\ J_{acc}(j; k + 1) &= \min\{J_{tr}(i, j; k)\}_{i=0}^{L-1} \\ J_{acc}(j; k + 1) &= J_{acc}(j; k + 1) + J_1(j; k + 1) \end{aligned} \tag{3.6}$$

Step 3: If $k < K$, then $k = k + 1$, go to *step 1* and repeat.

Step 4: The path with minimum total cost across all paths can be found by backtracking the surviving path.

In the proposed framework, the quantization choices for the k-th block in the reference image and the corresponding blocks in the DCD frame do not affect the choices for the future blocks. Thus, based on the Bellman's optimality principle, the VA provides a globally optimal solution because suboptimal paths at a given node cannot be optimal overall and can thus be pruned. Similarly, overall optimality within the stereo pair can be achieved by assigning the same λ to every pair of ROBs since each pair of ROBs is independent [80, 82].

3.2.4 Fast Algorithm Using Monotonicity

We now propose a fast algorithm based on the monotonicity property, *i.e.* the observation that finer quantization of F_1 tends to allow more efficient coding, in the RD sense, for the DCD frame [80]. For example, $J(p|q^*) \leq J(p|q)$, for $q^* \leq q$, where q^* is finer than q. If $\lambda = 0$, $d(p|q^*) \leq d(p|q)$, for $q^* \leq q$. To take advantage of this, we first consider a "ROB_1-only optimization" and then only calculate RD values for the selected nodes and branches. Figure 3.4 shows an example of the reduced trellis obtained from the trellis of Figure 3.3.

The proposed fast search algorithm is as follows.

Step 0: First, we select a pair of Lagrange multipliers, λ's, *e.g.*, (λ_1, λ_2). For example, we can choose $(0, \lambda_2)$ so that we do not eliminate the finest quantizer for ROB_1 (which tends to be good, given monotonicity).

Step 1: Then, for each λ, we set to zero the branch costs and then select, at each stage, the node, which minimizes $D + \lambda R$. Each λ will provide an optimal path (a set of nodes) in the trellis. We then restrict ourselves to only consider those paths that lie *in between* the paths selected using λ_1 and λ_2.

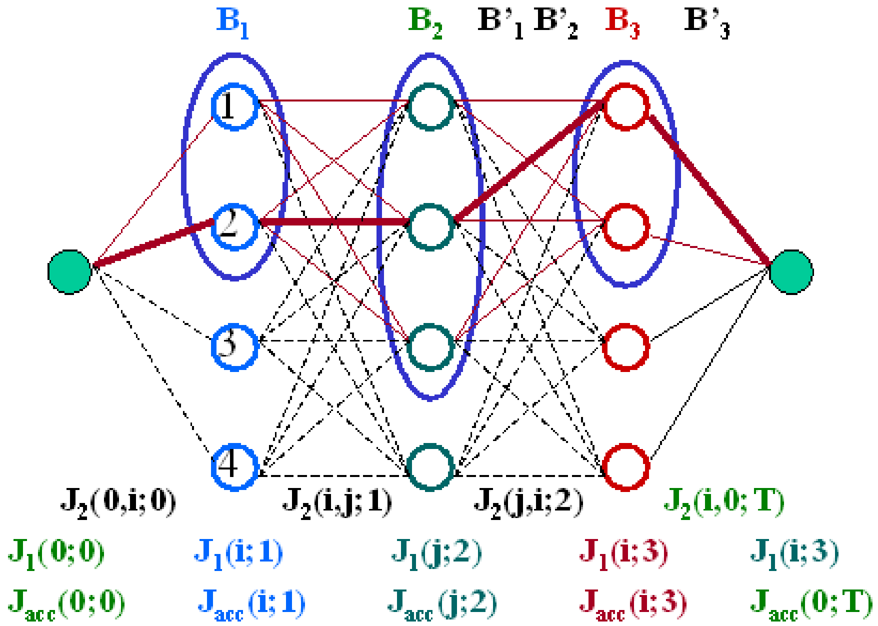

Figure 3.4: A heuristic fast search. The trellis in Figure 3.3 can be restricted using the proposed fast search algorithm. The search space is reduced to the (circled) nodes, selected by a blockwise optimization using two λ's for the reference image only. If we choose the two λ's as $(0, \lambda_2)$, then we keep the finest quantizer for ROB_1. Then, we only need to calculate RD values of the blocks in ROB_2 for the remaining (solid lined) branches.

Step 2: Finally, we use the algorithm outlined above except that we apply the VA on the pruned trellis so that only a subset of the branches representing blocks in ROB_2 need to be grown.

The proposed fast scheme reduces the computational complexity significantly. The most significant contribution to the complexity of the VA comes from having to compute the RD values in order to assign the node and branch costs. For example, if a block in ROB_2 depends on two blocks in ROB_1, each combination of quantization choices for these blocks gives rise to a different residue. Thus, we would need to compute the residues $L \times L$ times and to quantize them L times, where L is the number of quantizers. In other words, the required total number of RD values per trellis is in $O(L^3K)$, because the total number of nodes and branches per trellis are $L \times K$ and $L^2 \times K$, respectively. Let the number of remaining nodes per stage in the pruned trellis be $\tilde{L}$. In our proposed fast scheme, we need only those RD values corresponding to the remaining nodes and branches in the trellis. Thus, the required total number of RD values for the pruned trellis is in $O(K\tilde{L}^2L)$. Based on the above, if $\tilde{L}$ is small, our pruning will result in much reduced complexity and, with good choices of (λ_1, λ_2), will not affect much the final quality.

3.3 Experimental Results

In our experiments we use two stereo pairs, one synthesized and the other natural. The test images are shown in Figure B.2 and B.1, and resulting DV fields are shown in Figure 3.5[7]. The target image is segmented into blocks of size 8×8 pixels and then disparity estimation is performed using fixed size block matching. The search window sizes are $(0, 15)$ and $(\pm 2, 15)$ for the synthesized and the natural pairs, respectively.

[7] The test images are also available in
`http://escalus.usc.edu/~wwoo/Stereo`.
The original images where obtained from
Room: `http://www-dbv.cs.uni-bonn.de/~ft/stereo.html` and
Fruit: `http://www.ius.cs.cmu.edu/idb/html/stereo/index.html`

For this particular selection of the block and search window sizes, two consecutive blocks in F_1 will affect *at most* two consecutive blocks in F_2, as shown in Figure 3.3. Note that our algorithm can accommodate arbitrary search regions.

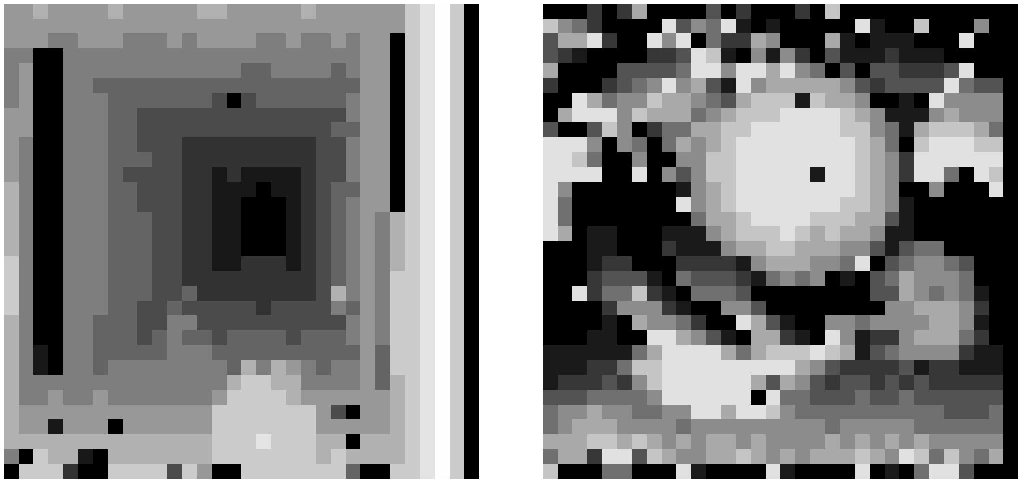

(a) (b)

Figure 3.5: Test images and DE results with 8×8 block. The DV field with FSBM for (a) Room (b) Fruit.

The resulting DV field is losslessly encoded using DPCM with a causal median predictor to exploit the spatial redundancy among neighboring DVs. The reference image and the DCD frame are encoded using a JPEG-like coder, with the only modification to the baseline JPEG [96] being that we allow each block to have a different quantization scale (QS). Consequently, the change of QS per block allows the encoder to assign different levels of quantization coarseness to each block. For each block one among eight different QS can be chosen from the set $QS = \{90, 80, \cdots, 20\}$, where increasing values indicate finer quantization. In our calculation of rate, we assume a constant overhead is used for each block.

In our experiments, we compare the RD performance of the blockwise dependent quantization scheme with those of: (i) framewise constant quantization and (ii) blockwise independent optimal allocation. Note that a constant quantization scale is used for all blocks in each image in (i), while the optimal quantization scale for each block in the two images is estimated with a fixed λ in (ii). The RD points we plot are obtained for $\lambda = \{0, 0.1, 0.5, 1, 2, 100\}$.

Figure 3.6 compares RD performance of the synthesized image. In Figure 3.6, (a) and (b) shows RD performances for the reference image, (c) compares the mean RD performance in terms of the overall bit rate and the mean PSNR.

As shown in Figure 3.6, quantization selections for F_1 affect RD performance for F_2. Table 3.1 compares the resulting RD performances for the dependent bit allocation scheme to those for the independent blockwise bit allocation scheme. In the table, "IND" and "DEP" denote the blockwise independent and dependent bit allocation schemes, respectively. Note that at the same rate, $R_{mean} = 0.727$, the dependent bit allocation scheme tends to assign relatively more bits to F_1 and achieve slightly higher PSNR gain for F_2 even though it is using lower rate, as compared to the independent scheme.

Method	λ	$R_1/PSNR_1$	$R_2/PSNR_2$	$R_{mean}/PSNR_{mean}$
IND	0.500	0.966/37.64	0.488/37.35	0.727/37.49
DEP	0.500	1.092/38.76	0.436/38.03	0.764/38.38
DEP	0.588	1.044/38.23	0.410/37.47	0.727/37.83

Table 3.1: Comparison of RD performance in terms of rate ([bpp]) and PSNR ([dB]) (Room.256).

Figure 3.7 shows the mean RD performance obtained for another stereo pair, for which small vertical disparity vectors are allowed.

According to the experimental results, at the same rate, the proposed blockwise dependent bit allocation method resulted in 0.2-0.5 dB improvement in mean PSNR for the two images in a stereo pair, as compared to the optimal blockwise independent quantization. Note that the mean PSNR gains mainly arise from the fact that the finer quantization for the reference image (F_1), increasing the rate of F_1 at the expense of decreasing the rate for the target image (F_2), improves the encoding efficiency for the target image (F_2).

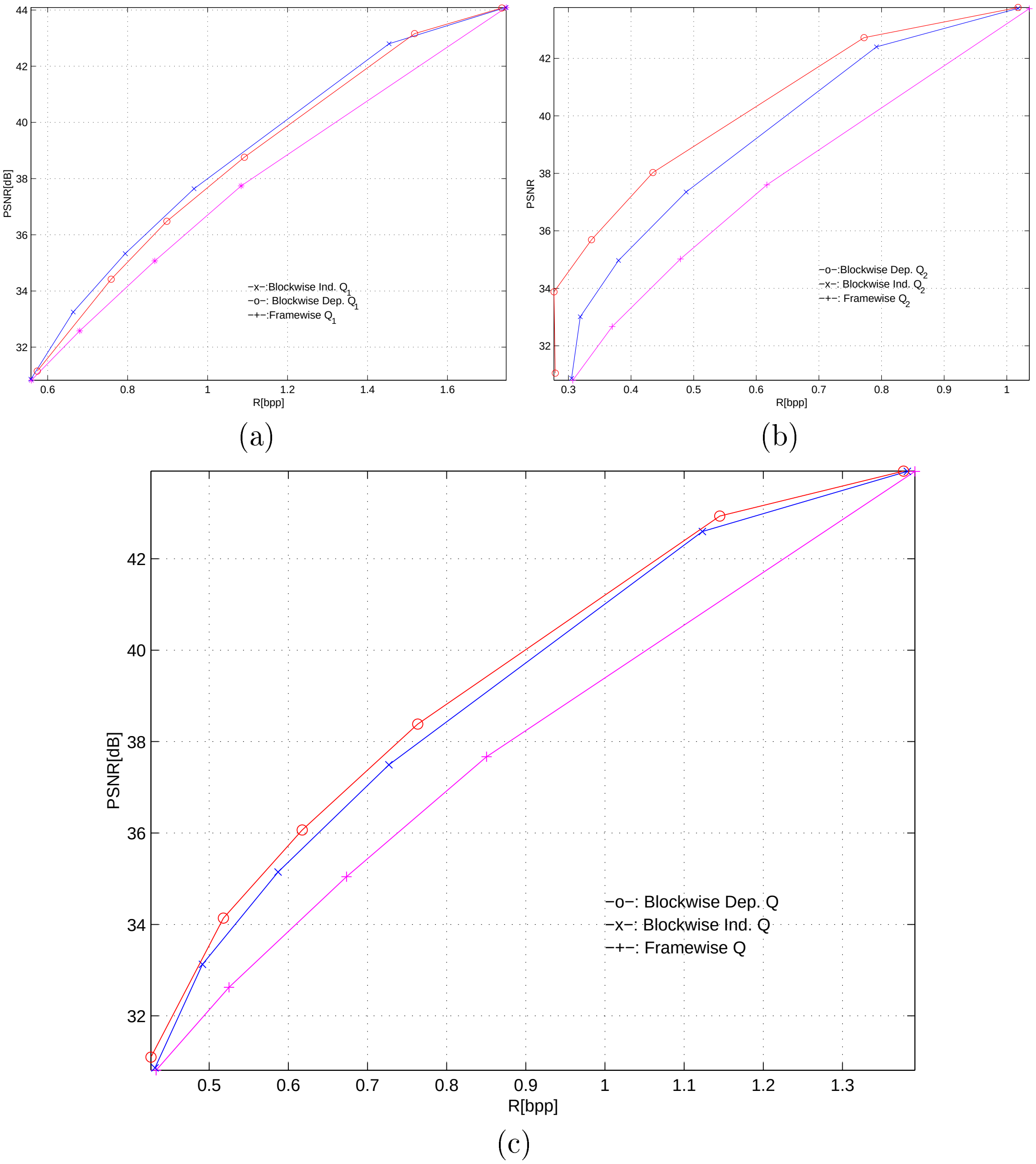

(a)

(b)

(c)

Figure 3.6: RD performance comparison (Image: room.256, Block size=8×8, $SW = 16$, $|Q| = 8$, $QS = \{90, 80, \cdots, 20\}$ and $\lambda = \{0, 0.1, 0.5, 1, 2, 100\}$). The ’+’-mark denotes the DC with framewise quantization. The ’x’-mark and ’o’-mark correspond to the DC with blockwise independent and dependent quantizations, respectively. Each point is generated with one different λ. (a) The RD performance for the reference image is similar for both types of blockwise allocation. (b) A better RD performance for the target image can be achieved using the dependent bit allocation approach. (c) The overall performance also improves when taking dependencies into account.

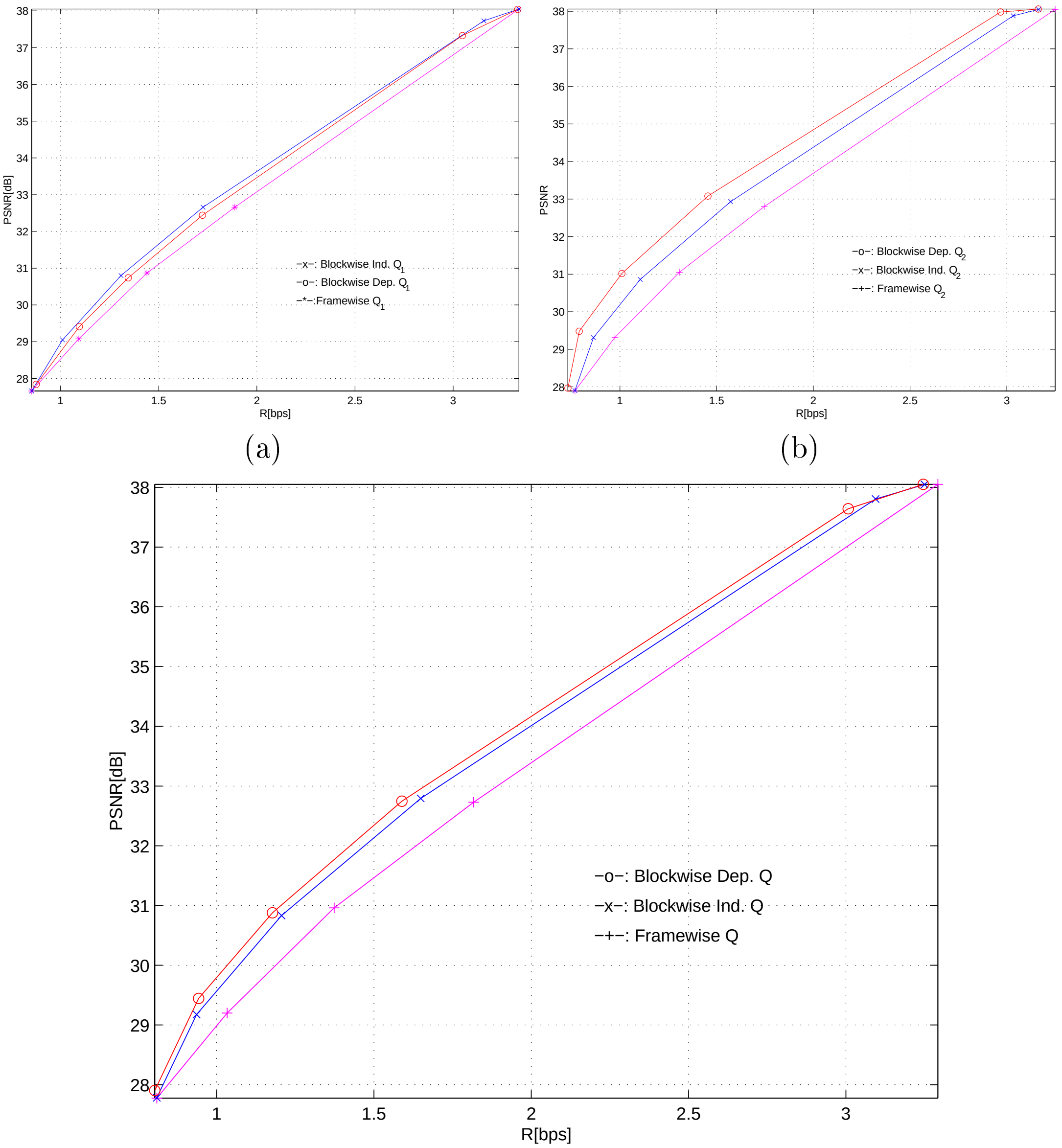

(a)

(b)

(c)

Figure 3.7: RD performance comparison. (fruit.256, Block size=8 × 8, $SW = 10$, $|Q| = 8$, $QS = \{90, 80, \cdots, 20\}$ and $\lambda = \{0, 0.1, 0.5, 1, 2, 100\}$). The '+'-mark denotes the DC with framewise quantization. The 'x'-mark and 'o'-mark correspond to the DC with blockwise independent and dependent quantizations, respectively. RD characteristics for (a) the reference image, (b) the DCD frame, and (c) the two images.

Figure 3.8 shows mean ORD curves for the reference image (points marked with x) and the dependent DCD frame (points marked with o), respectively. As shown, the monotonicity property is satisfied for the blockwise quantization, *i.e.* $J(QS_2|QS_1) \leq J(QS_2|QS_1^*)$, for $QS_1 \geq QS_2^*$. Thus if the quality of the reference frame improves, so does the DCD, for the same quantization scale QS_2, *i.e.* if $\lambda = 0$, $d(QS_2|QS_1) \leq d(QS_2|QS_1^*)$, for $QS_2 \geq QS_2^*$ [80]. Thus, the finer quantization ($QS_1 = 90$) leads to more efficient coding for the DCD frame in the RD sense so that the corresponding mean ORD curve is closer to the origin. In addition, the plot shows that, in both cases, the distortion, $d(QS_2|QS_1)$, increases monotonically as the quantization scales changes from finest to coarsest, *i.e.* from 90 to 30.

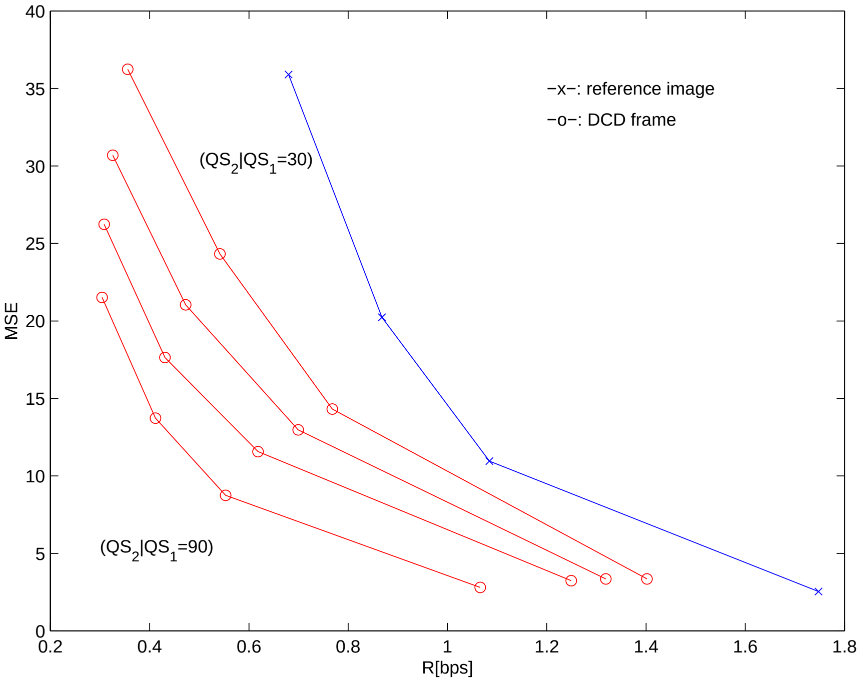

Figure 3.8: Mean ORD plots for the block in the reference image and the DCD frame. (room.256, $QS = \{90, 70, 50, 30\}$) QS_2 is changed for the DCD frame with a given QS_1. As shown, the monotonicity property is satisfied, *i.e.* $J(QS_2|QS_1) \leq J(QS_2|QS_1^*)$, for $QS_1 \geq QS_1^*$. In particular, if $\lambda = 0$, $d(QS_2|QS_1) \leq d(QS_2|QS_1^*)$, for $QS_1 \geq QS_1^*$.

Figure 3.9 shows the RD performance of the proposed fast algorithm. To keep the finest quantizers for the reference we set λ_1 to be zero and thus the selected λ's are $\{\lambda_1, \lambda_2\} = \{0, 0.5\}$, in our experiments. As explained in the previous section, we restrict the search space to the nodes in between two paths selected by the two λ's. Finally, the set of dependent quantization assignments is determined using the pruned trellis. In our example, only 61% of original nodes and 37.5% of branches remain in the pruned trellis, which results in significant savings in the computation of RD values. The resulting number of computation (and thus comparison) in the pruned trellis is about 37.5% of the original. The overall RD performance remains practically unchanged in this case, as compared to the original algorithm. Note however that we need to make a good choice for the λ range, based on the expected quality level for the overall image. Thus, in the example, we show good performance at high rates whereas the low rate points cannot be achieved since the corresponding nodes have already been pruned out.

3.4 Discussion

We have proposed an optimal dependent bit allocation scheme for stereo image coding. We have concentrated on quantization issues and assumed that the disparity estimation was performed open-loop. The proposed dynamic programming algorithm leads to an efficient bit allocation between the reference image and the DCD frame. According to our experimental results, the proposed scheme provides significant PSNR gains, *e.g.* about 1-2 dB compared to DC with the framewise bit allocations and 0.2-0.5 dB compared to DC with the blockwise independent bit allocation. In addition, we have shown a method to reduce the computational complexity and the encoding delay of the VA by exploiting the monotonicity property. Adopting reasonable RD models can further reduce the computational complexity of the proposed scheme [91]. This framework has been developed for a JPEG-like codec but it can be directly extended to an MPEG-like codec for stereo images, without the loss of generality.

Additional research is required to achieve a more complete allocation algorithm including the disparity estimation. Further study of our algorithm may lead to a

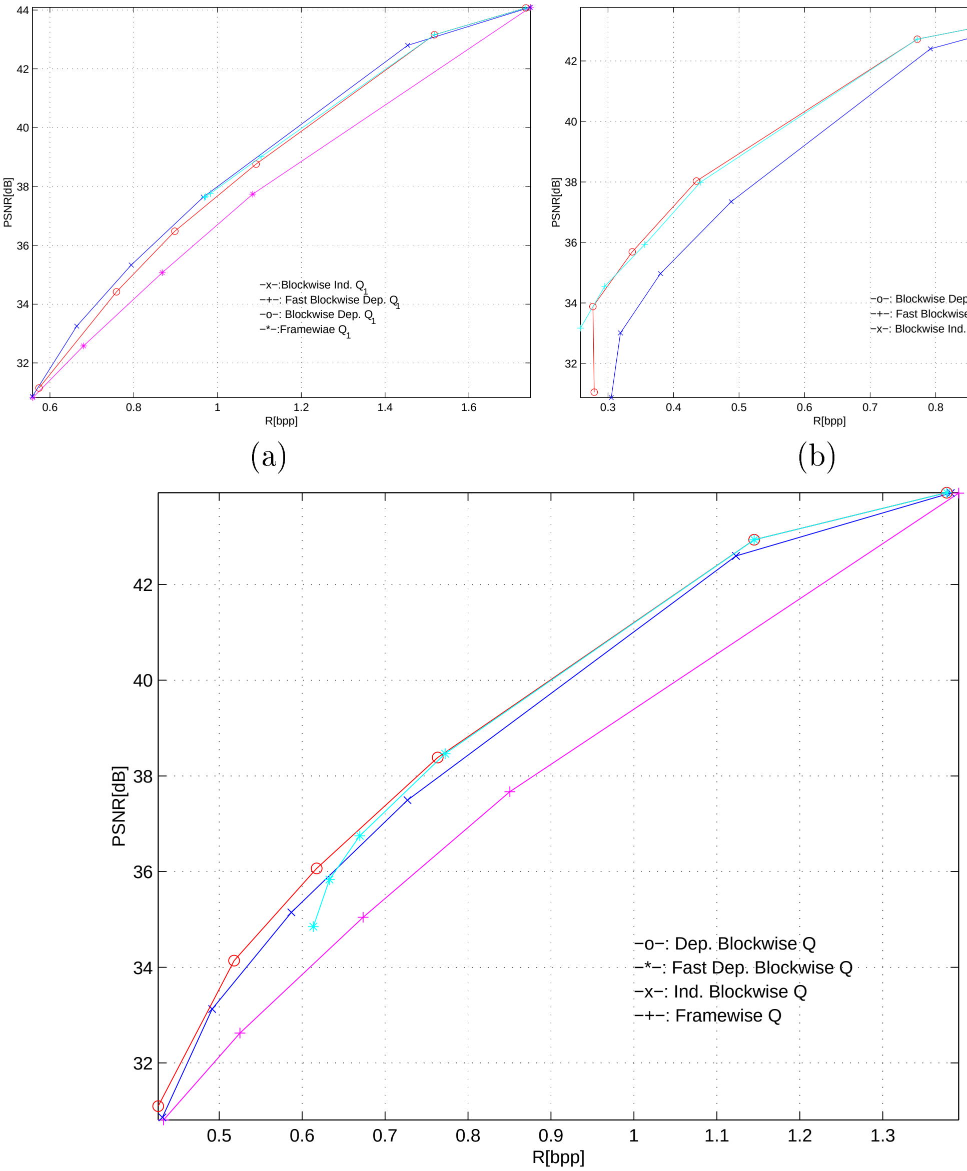

(a)

(b)

(c)

Figure 3.9: RD performance comparison of the fast algorithm. (room.256, Block size= 8×8, $SW = 10$, $|Q| = 8$, $QS = \{90, 80, \cdots, 20\}$, $\lambda_1 = [0, 0.5]$, and $\lambda = \{0, 0.1, 0.5, 1, 2, 100\}$). The '*'-mark denotes the proposed fast algorithm, which only uses 61% of the original nodes (the resulting computation corresponds to about 22.7% of the original). The '+'-mark denotes the DC with framewise quantization. The 'x'-mark and 'o'-mark correspond to the DC with blockwise independent and dependent quantizations, respectively. RD characteristics for (a) the reference image, (b) the DCD frame, and (c) the two images combined.

better understanding of the similar issues in blockwise dependent allocation for video coding, where an optimal solution cannot be achieved due to the 2D nature of the dependencies. Finally, the extension to stereo video coding [11, 44, 97], in which both temporal and binocular dependencies have to be taken into account, is another area of future work.

Chapter 4

Modified Overlapped Block Disparity Compensation

In this chapter, we propose a modified overlapped block matching (OBM) scheme for stereo image coding. The OBM scheme has been introduced in video coding, as a promising way to reduce blocking artifacts by using multiple vectors for a block, while maintaining the advantages of the fixed size block matching framework. Even though it overcomes some drawbacks of block matching schemes, OBM has its own limitations. For example, estimating an optimal displacement vector field within the OBM framework may require an iterative search procedure. In addition, OBM does not always guarantee a consistent DV field, even after several iterations, because the estimation considers only the magnitude of the prediction error as a measure. Therefore, we propose a modified OBM scheme for stereo image coding, which allows both consistent disparity estimation and efficient disparity compensation, without the need for an iterative procedure. The computational burden resulting from the iterations is reduced by decoupling the encoding into estimation and compensation. Consistent disparity estimation is performed by using a causal MRF model and a half-pixel search, while maintaining (or reducing) the energy level of the disparity compensated difference frame. The compensation efficiency is improved by both applying OBM and interpolating the reference image in half pixel accuracy.

4.1 Introduction

An efficient disparity estimation/compensation (DE/DC) has been a main focus of the research on stereo image/video coding since the pioneering work by Lukacs [12, 13, 41, 43, 53, 86]. However, the various proposed schemes only relieve those problems in part. For example, DE with a Markov random field (MRF) model can overcome the inconsistency by taking advantage of disparity information of neighboring blocks [27, 86, 98]. Subspace projection is another way of estimating a smooth DV field [41]. However, both schemes have limitations in reducing the energy level of the DCD frame. The energy level of the DCD frame can be reduced using non-integer (half or quarter) pixel-based search but that increases the rate of the DV field. Blocking artifacts also can be reduced by adopting various other methods such as post-processing, segmentation-based estimation/compensation, etc. However, many post-processing algorithms degrade the quality of the whole image as well as the block boundaries. Also, the cost to pay for the segmentation is the increase in overhead to describe the structure of the segmentation [50, 53, 57].

Another promising way to improve encoding efficiency for stereo images is adopting overlapped block motion compensation (OBMC), which has been used for video coding [99–102]. In general, OBMC reduces blocking artifacts by linearly combining multiple blocks provided by the vectors of a block and its neighbors. For practical implementations, non-iterative OBMC schemes have been proposed. For example, block matching (BM) [99] or windowed BM [103] is first applied for the motion estimation (ME), without considering the effects of neighboring blocks, and then OBMC is performed only for motion compensation (MC). However, these schemes do not always provide an optimal motion vector (MV) field for OBMC. Even the MV field itself may not be optimal because the estimation only depends on the prediction error, *i.e.* mean square error (MSE) or mean absolute error (MAE) of the block. Meanwhile, an optimal MV field estimation for OBMC requires complicated iterative schemes to resolve the noncausal spatial interaction among MVs of neighboring blocks.

In conventional approaches, to reduce complexity resulting from the non-causality problem in ME, a "two-step procedure" is usually adopted, *i.e.* an initial MV field is estimated using FSBM and then the DV field is refined to improve the encoding performance. This process repeats until the DV field converges to an optimal state. However, this iterative process makes optimal OBMC difficult in real-time applications [100]. Therefore, at the cost of slightly reduced performance, modified OBMC schemes such as raster scan OBMC [104] or checkerboard scan OBMC [105,106], have been proposed to reduce computational complexity. Note however that those schemes do not always guarantee a smooth displacement (disparity or motion) vector field. In both cases, due to the inconsistency in motion estimation, the overhead may be high in cases where the displacement field is differentially encoded using variable-length codes.

Another weakness of OBMC stems from the fixed shape of the window. Note that spreading compensation errors tends to reduce blocking artifacts, but it might degrade compensation efficiency, particularly for those blocks that can be compensated effectively without OBMC. Orchard *et al.* showed that the optimal shape of the OBMC window could be determined with the knowledge of the correlation matrix of the image [100]. However, the required computational complexity is extremely high for the adaptive window to be implemented in real-time applications.

Therefore, in this chapter, we propose an effective but non-iterative OBM scheme for stereo image coding. In the proposed overlapped block disparity compensation (OBDC) scheme, the computational complexity resulting from the iterative DE has been reduced by decoupling the encoding procedure into two steps, *i.e.* first disparity estimation and then disparity compensation. Note however that non-iterative schemes may not provide an optimal DV field for OBDC in general. Therefore, we propose an alternative DE/DC strategy to overcome the non-optimality problem. First, the *DE with a modified MRF model and half pixel search* results in a smooth DV field without excessively increasing the energy level of the prediction error and thus tends to reduce bit rate for the DV field. Then, given a smooth DV field, the *selective OBDC in half pixel accuracy* reduces blocking artifacts and energy level of the DCD frame. Note that the selective OBDC adaptively changes the shape of the OBM window to prevent the oversmoothing problem and thus lowers the computational complexity as well as the energy level of the DCD frame.

The main novelty of this research is that we introduce an OBDC scheme for stereo image coding for the first time. In the proposed OBDC, the overall encoding performance for the target image is achieved by estimating a smooth DV field, while reducing the energy level of the DCD frame, at a fraction of the computation that would be required by an OBDC based on conventional OBMC. To verify the effectiveness, we compare the RD performance of the proposed OBDC scheme with various FSBM-based DE/DC schemes such as (i) simple FSBM, (ii) FSBM with MRF model and (iii) OBDC based on OBMC. According to our experimental results, the proposed scheme achieves about 0.5-1 dB gain in terms of PSNR as well as better perceptual quality, compared to OBDC. Note that the resulting smooth DV field also helps generate intermediate-views with lower visual artifacts in the decoder. The proposed OBDC scheme can also be applicable to video coding without the loss of generality.

This chapter is organized as follows. In Section 4.2, we describe the proposed two-step hybrid scheme, the modified OBM with MRF model and half-pixel search. In Section 4.3, we provide some experimental results to compare the effectiveness of the proposed scheme. Conclusions are summarized in Section 4.4.

4.2 Modified Overlapped Block Matching

4.2.1 Notation and Definition

We define the (i, j)-th overlapping block in the target image as s_{ij}^2 and thus each target block is estimated/compensated as a windowed-sum of a block and its neighboring blocks along the corresponding DVs. In conventional FSBM, s_{ij}^2 equals f_{ij}^2 and thus each target block is estimated from only one block in the reference image along the disparity vector v_{ij}.

In general, the overlapped window W is designed to decay toward the boundaries on the assumption that blockwise estimation error increases as a pixel moves away from the block center and the increase is symmetric with respect to the block center [107]. Another property of the window is that the windowed-sum over the image is identical to the original image, *i.e.* $F = \sum_{ij} W \cdot s_{ij}$. Typical selections for the overlapped window are the sinusoidal and the bilinear windows[1]. An optimal shape for the overlapped window can also be considered but the resulting improvement is not a significant one, given the proportional increase in the computational complexity [100]. In our experiments, therefore, we adopt the bilinear window as shown in Figure 4.1 (a). For a $2B \times 2B$ window, window components corresponding to each region of a block are shown in Figure 4.1 (b)-(e).

The selected separable bilinear window W is defined as follows,

$$\begin{aligned} W(m,n) &= W_m \times W_n \\ W_m = W_n &= \begin{cases} \frac{m+0.5}{B}, & 0 \le m < B \\ W_{2B-m-1}, & B \le m < 2B \end{cases} \end{aligned} \tag{4.1}$$

where W_m and W_n denote the separable vertical and horizontal windows, respectively.

4.2.2 Disparity Estimation Using Overlapped Windows

Figure 4.2 shows the DE using overlapped window and a smoothness constraint. In general, the DV field obtained by the overlapped window is not likely to be consistent because the MSE/MAE-based prediction is sensitive to various noise effects such as intensity variation. Note that the two images in a pair may have slightly different

[1] Note that FSBM can be considered as a OBM with a rectangular function.

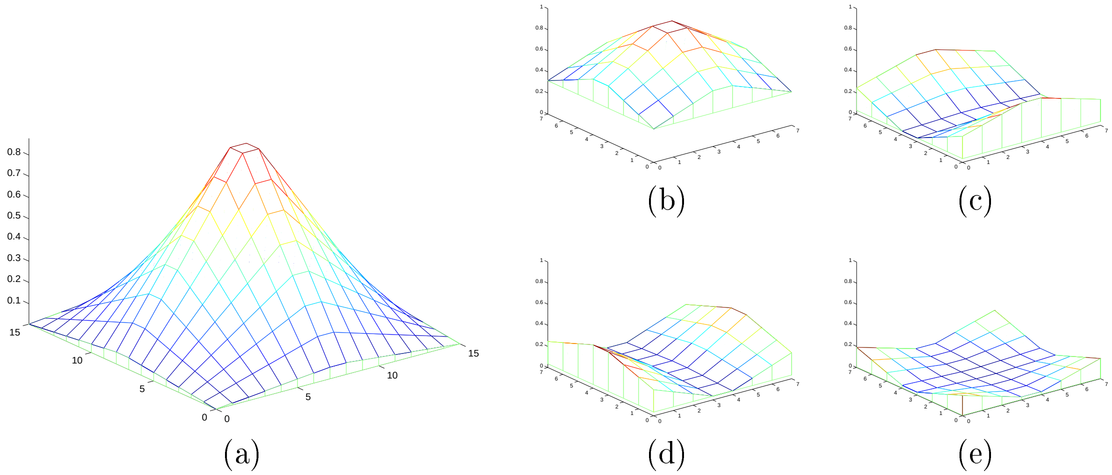

Figure 4.1: Bilinear window function for the overlapped block matching and its combined weighting matrices. (a) Bilinear OBM window (16 × 16) (b) Main ($\hat{f}^2_{ij\oplus v_{ij}}$) (c) Horizontal ($\hat{f}^2_{ij(N)\oplus v_{i-1j}}, \hat{f}^2_{ij(S)\oplus v_{i+1j}}$) (d) Vertical ($\hat{f}^2_{ij(W)\oplus v_{ij-1}}$), $\hat{f}^2_{ij(E)\oplus v_{ij+1}}$) (e) Corner ($\hat{f}^2_{ij(NW)\oplus v_{i-1j-1}}, \hat{f}^2_{ij(NE)\oplus v_{i-1j+1}}, \hat{f}^2_{ij(SW)\oplus v_{i+1j-1}}, \hat{f}^2_{ij(SE)\oplus v_{i+1j+1}}$). The capital letters (N,W,S,E) denote locations of quadrants of a block, *i.e.* north, west, south, and east, respectively.

intensity levels due to the camera noise and lighting condition. In addition, the lack of texture and/or repetitive texture may disturb consistent estimation.

Therefore, we introduce an MRF model to estimate a smooth DV field by considering the DV field and the estimation error together. In general, conventional MRF-based schemes have high computational complexity because they require several (stochastic) iterations to estimate an optimal (pixelwise) dense DV field [84]. Thus, we propose a simplified blockwise DE scheme for stereo image coding, which estimates a smooth DV field without complicated iterations by considering only blocks in a first order causal neighborhood as shown in Figure 4.3. Meanwhile, the same neighborhood is used for encoding the DV field, *i.e.* the difference between v_{ij} and the median of its causal neighborhood is encoded using DPCM. As a result, estimating a smooth DV field contributes to reducing side information, which is especially essential at low rate coding.

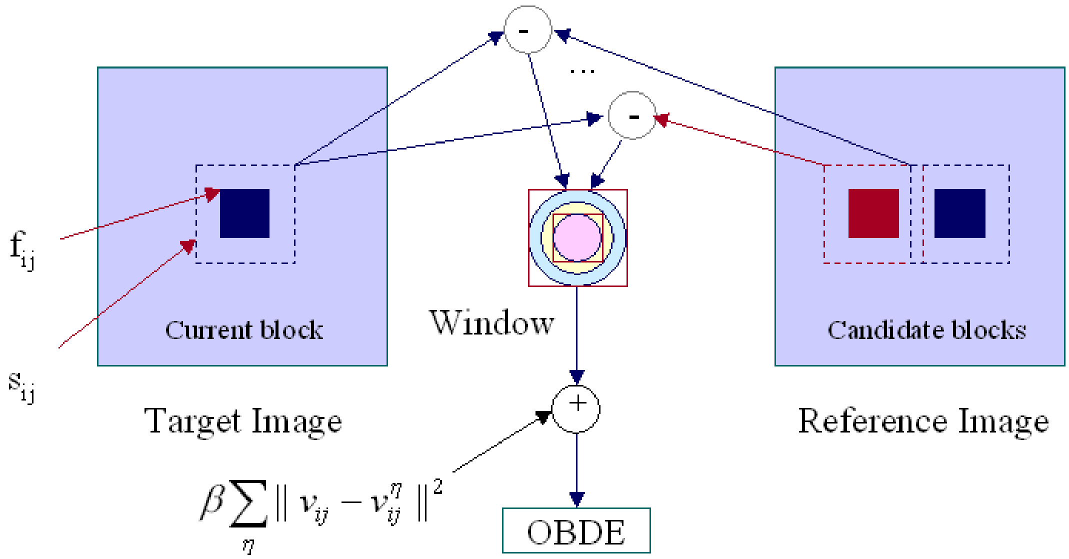

Figure 4.2: Disparity estimation based on block matching with an enlarged window. In the target image, shaded and dashed areas correspond to a block, f_{ij}, and an enlarged block, s_{ij}, respectively.

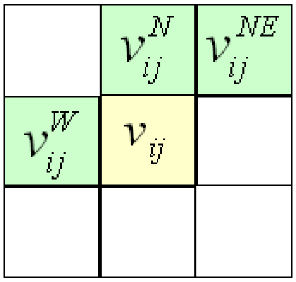

Figure 4.3: A first order causal neighborhood. The same neighborhood is used in the encoding of the DV field, *i.e.* $Diff(v_{ij}) = v_{ij} - median(v_{ij}^{W}, v_{ij}^{N}, v_{ij}^{NE})$.

We use the formulation in Chapter 2.4.5.2 for the MRF-based DE. In (2.20), we set β equal to be zero and separately determine ϕ_{ij} according to the prediction error level. Then, for DE based on overlapping block, the corresponding cost function in (2.20) has to be changed as follows,

$$\begin{aligned} U(V|F_1, F_2) &= U(F_2|F_1, V) + U(V) \qquad (4.2) \\ &\propto \sum_{(i,j)\in\Omega} \{||(1-\alpha)W \times (s_{ij}^2 - s_{ij\oplus v_{ij}}^1)||^2 + \alpha \sum_{\eta} ||v_{ij} - v_{ij}^{\eta}||^2\} \end{aligned}$$

where η denotes a neighborhood and $\alpha(> 0)$ is a weighting constant controlling the degree of smoothness. Each term of the right side in (4.2) represents the constraints of the similarity between stereo pair for a given disparity and an *a priori* assumption on the smoothness of the DV field. Note that setting $\alpha = 0$, $W = I$ and $s_{ij} = f_{ij}$ in (4.2), corresponds to conventional FSBM, which only assumes that the image intensities in the stereo pair are similar along the DV.

Also note that, in the proposed scheme, the choice of model parameters is relatively robust. For example, a small fixed weight (*e.g.* $\alpha = 0.1$) is sufficient for the smoothness term for most images because the smoothness constraint is exploited only to avoid various local minima in DE[2]. However, conventional MRF schemes, mainly employed in computer vision, require more careful selection of an "optimal" set of weighting parameters, in order to provide good results.

To further reduce the prediction error, the DE/DC is performed in half pixel accuracy. The projected images in a stereo pair are sub-sampled versions of the real scene and thus the resulting correspondence between two images may not be aligned with integer pixel location. Therefore, estimating/compensating the target image on the interpolated reference image along the disparity vectors helps to estimate a more accurate DV field and thus reduces the energy of the DCD frame. The performance can be increased by adopting more elegant interpolation methods such

[2] An optimal value of α can be selected by Lagrangian optimization.

as an approximated ideal filter or Wiener filter [108, 109]. Clearly the higher the subpixel accuracy (*i.e.* the larger displacement space), the greater the probability of finding a good match. Note however that we cannot choose an arbitrarily small value because, as the subpixel accuracy increases, both the rate for the resulting DV field and the number of candidate blocks being compared in the search area increase at the same time. In our experiments, we use bilinear interpolation, as a compromise, to obtain the half-pixel precision intensity value, as used in most video coding standards.

4.2.3 Encoding with Selective OBDC

In general, OBDC is efficient only when the energy level of the DCD block is significantly different with its neighboring blocks or when high frequency components exist in the DCD block. Thus, during the DE process, a block with higher prediction error than a threshold is selected as an OBDC candidate. The DCD is calculated by taking the difference between the predicted block and the original block in the target image, *i.e.* $DCD = f_{ij}^2 - \hat{f}_{ij}^2$. Let ϕ^0 and ϕ denote an initial occlusion and an occlusion, respectively. Then, OBDC is only considered for the block with $\phi^0 = 1$. Note that a block with $\phi_{ij}^0 = 0$ can be compensated effectively without OBDC. First, $\phi_{ij}^0 = 1$, if $|DCD| > T_\phi$, where T_ϕ denotes a threshold value. For each block with $\phi_{ij}^0 = 1$, if the energy level of the DCD using OBDC is lower as compared to block DC (BDC), then $\phi_{ij} = 1$. Meanwhile, a block having the same DV with its neighbors is selected $\phi_{ij} = 0$, since there is no RD gain by OBDC when the disparity vectors of the neighboring blocks are the same. Otherwise, *i.e* if there is no gain from BDC or OBDC, the original intensity block is encoded instead of the DCD block.

As shown in Figure 4.4, in OBDC, a target block is influenced by the nine overlapped blocks in the reference image along the corresponding disparity vectors. Thus, the whole compensation is obtained by summing up the window-operated nine blocks.

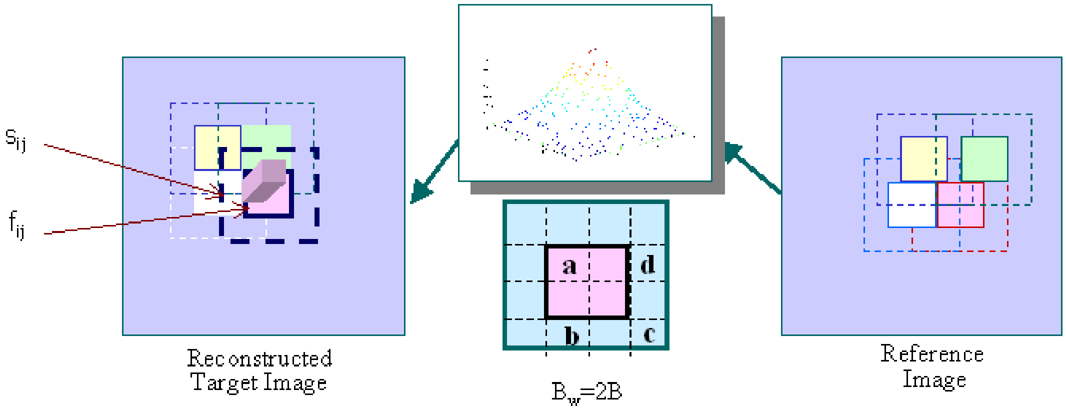

Figure 4.4: Disparity compensation based on the overlapped block matching. Colored and dashed areas correspond to a block, f_{ij}, and an enlarged block, s_{ij}, respectively.

As explained in the proposed scheme, OBDC is selectively applied to those blocks yielding higher prediction errors, *i.e.* $\phi_{ij} = 1$, while BDC is applied to all the others. This reduces computational complexity of OBDC, while preventing oversmoothing effects. Figure 4.5 shows an example of resulting window shapes, when $\phi_{ij} = 0$ and ϕ's of other blocks are one. An opposite example is shown in Figure 4.6.

Note that, as shown in Figure 4.4, in the case where the window width and height are double of those of block, *i.e.* $B_w = 2 \times B$, one quarter of a block only depends on three neighboring blocks and itself. For example, each pixel in the upper left part (NW) of the target block $f^2_{ij(NW)}$ is compensated by the weighted-sum of only four blocks as follows

$$\begin{aligned} \hat{f}^2_{ij(NW)} &= a \cdot \hat{f}^2_{ij(NW)\oplus v_{ij}} + b \cdot \hat{f}^2_{ij(NW)\oplus v_{i-1j}} \\ &+ c \cdot \hat{f}^2_{ij(NW)\oplus v_{i-1j-1}} + d \cdot \hat{f}^2_{ij(NW)\oplus v_{ij-1}} \end{aligned} \tag{4.3}$$

where (a, b, c, d) are the parts of the window W as shown in Figure 4.4. If $\phi_{ij} = 0$, the neighboring blocks are regarded as having the same disparity vectors and thus effects of neighboring blocks are ignored. Note however that the block with $\phi_{ij} = 0$ affects neighboring blocks with $\phi = 1$. These nonsymmetrical interaction prevents oversmoothing problem in part, while reducing blocking artifacts.

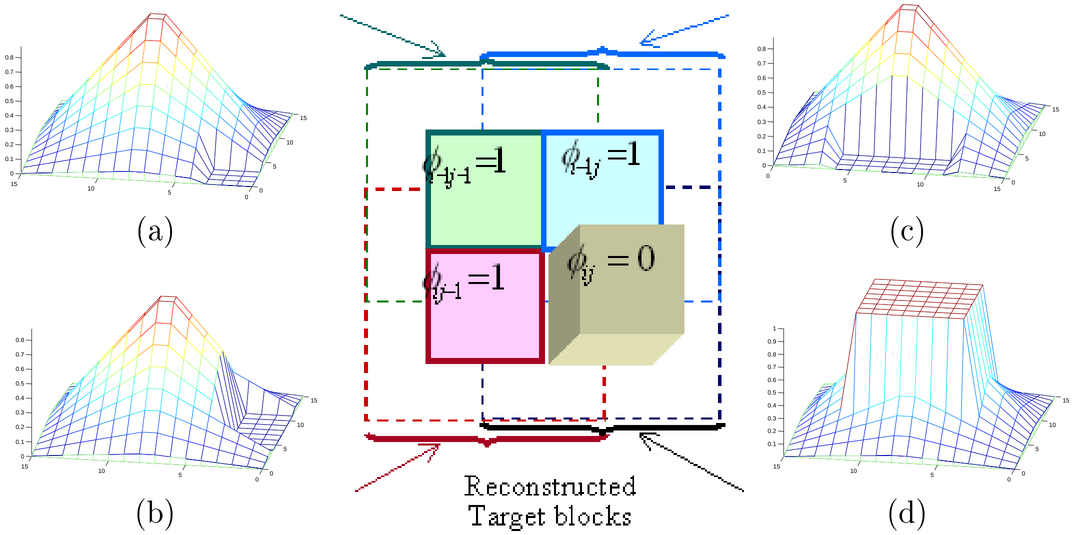

Figure 4.5: Adaptive windowing for selective overlapped block disparity compensation. Given $\phi_{ij} = 0$ and $\phi_{i-1j-1} = \phi_{i-1j} = \phi_{ij-1} = 1$, OBM windows are changed adaptively according to the ϕ's. OBM windows for (a) s_{i-1j-1} (b) s_{i-1j} (c) s_{ij-1} (d) s_{ij}.

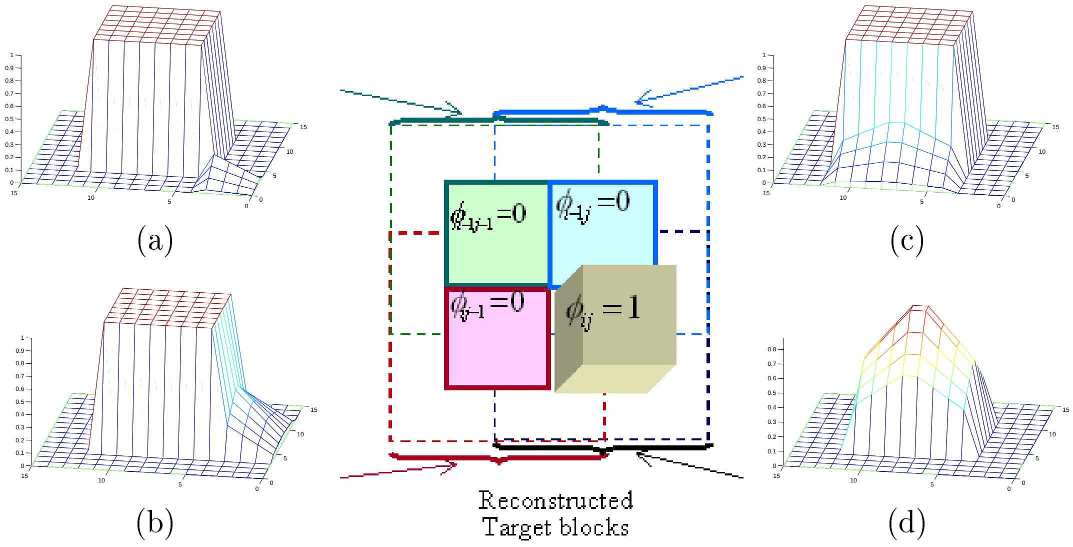

Figure 4.6: Adaptive windowing for selective overlapped block disparity compensation. Given $\phi_{ij} = 1$ and $\phi_{i-1j-1} = \phi_{i-1j} = \phi_{ij-1} = 0$, OBM windows are changed adaptively according to the ϕ's. OBM windows for (a) s_{i-1j-1} (b) s_{i-1j} (c) s_{ij-1} (d) s_{ij}.

The encoding procedure based on the proposed selective OBDC is as follows

- **Step 0** The reference image is independently encoded using JPEG.

- **Step 1** The disparity is estimated using an enlarged bilinear window with $B_w = 2B$. The window function W is operated on the disparity-predicted difference, without considering DE errors of neighboring blocks, *i.e.* $e_{obm;ij} = ||W \times \{s^2_{ij} - s^1_{ij \oplus v_{ij}}\}||$. The corresponding DE cost is defined by adding a smoothness constraint as shown in (4.2). The estimation is performed in half-pixel accuracy.

- **Step 2** Given a DV, a block is determined as an OBDC candidate, if the energy level of the difference, $DCD = f^2_{ij} - \hat{f}^2_{ij}$, is larger than the threshold. If $|DCD| > T_\phi$, $\phi^0_{ij} = 1$. Otherwise, $\phi^0_{ij} = 0$.

- **Step3** After DE with windowed BM, for each block with $\phi^0_{ij} = 1$, the DV is refined by considering OBDC. If the resulting DCD has less energy than that of BDC, the block is selected as OBDC block, *i.e.* $\phi_{ij} = 1$. If there is no gain from either BDC or OBDC, the block is replaced with the original intensity block.

- **Step 4** OBDC is selectively performed for those blocks with $\phi_{ij} = 1$ by summing up all windowed compensation blocks based on (4.3).

- **Step 5** The resulting DV field and DCD frame are encoded using DPCM and JPEG, respectively. For DPCM of the DV field, its median is selected from the pre-defined causal neighborhood.

At the decoder, the reference image is decoded first and then the target image is reconstructed according to ϕ_{ij}, *e.g.* by performing OBDC, if $\phi_{ij} = 1$ and BDC, otherwise. The final target image is reconstructed by adding information from the DCD for those blocks that have been predicted.

4.3 Experimental Results

In this experiment, the right image is selected as reference image and then a constant quantization factor ($Q_1 = 80$) is assigned for that reference image. Exhaustive search is performed within a search range of $[0, \pm 15]$ pixel in half-pixel accuracy. For the images that do not satisfy the parallax constraints, we search ± 2 pixels in vertical direction. In order to test the effectiveness of the proposed algorithm, we have simulated its performance for two pairs of stereo images; a synthesized scene, *Room*, and a natural scene, *Aqua*. The image sizes of the pairs are 256×256 and 288×360, respectively. The used stereo pairs are as shown in Figures B.2 and B.3[3].

First, we investigate how the block size affects the RD performance. Figure 4.7 compares the resulting DV fields of the *Room* image, which are obtained from FSBM for six different block sizes, from 32×32 to 1×1. Note that as the block size is reduced the resulting disparity field appears to be noisier, even though those DV fields reduce the estimation errors. The smaller block sizes also result in increase of the rates required to transmit the DV fields and thus may not be useful in practice.

Figure 4.8 shows the corresponding RD curves with different block sizes. The performance is measured in terms of the bit rates of the encoded images and peak signal to noise ratio (PSNR). As expected, DE/DC-based coding provides better coding performance than two independent coding (JPEG) of each image, because DE/DC-based coding takes advantage of the binocular redundancy in a stereo pair. However, obviously, as we reduce the block size($\leq 2 \times 2$), the bit rate of the DV field increases while the estimation error is reduced. As a compromise between the overhead and the energy of the estimation error, we choose a block size of 8×8 for DE in the following experiments.

Figure 4.9 compares the DV fields of for various disparity estimation methods: (i) FSBM, (ii) DE with MRF (in [86]), (iii) DE with OBM, (iv) MRF with half-pixel

[3] The decoded images and the used source codes (based on JPEG coder), are available at `http://escalus.usc.edu/~wwoo/Stereo/`

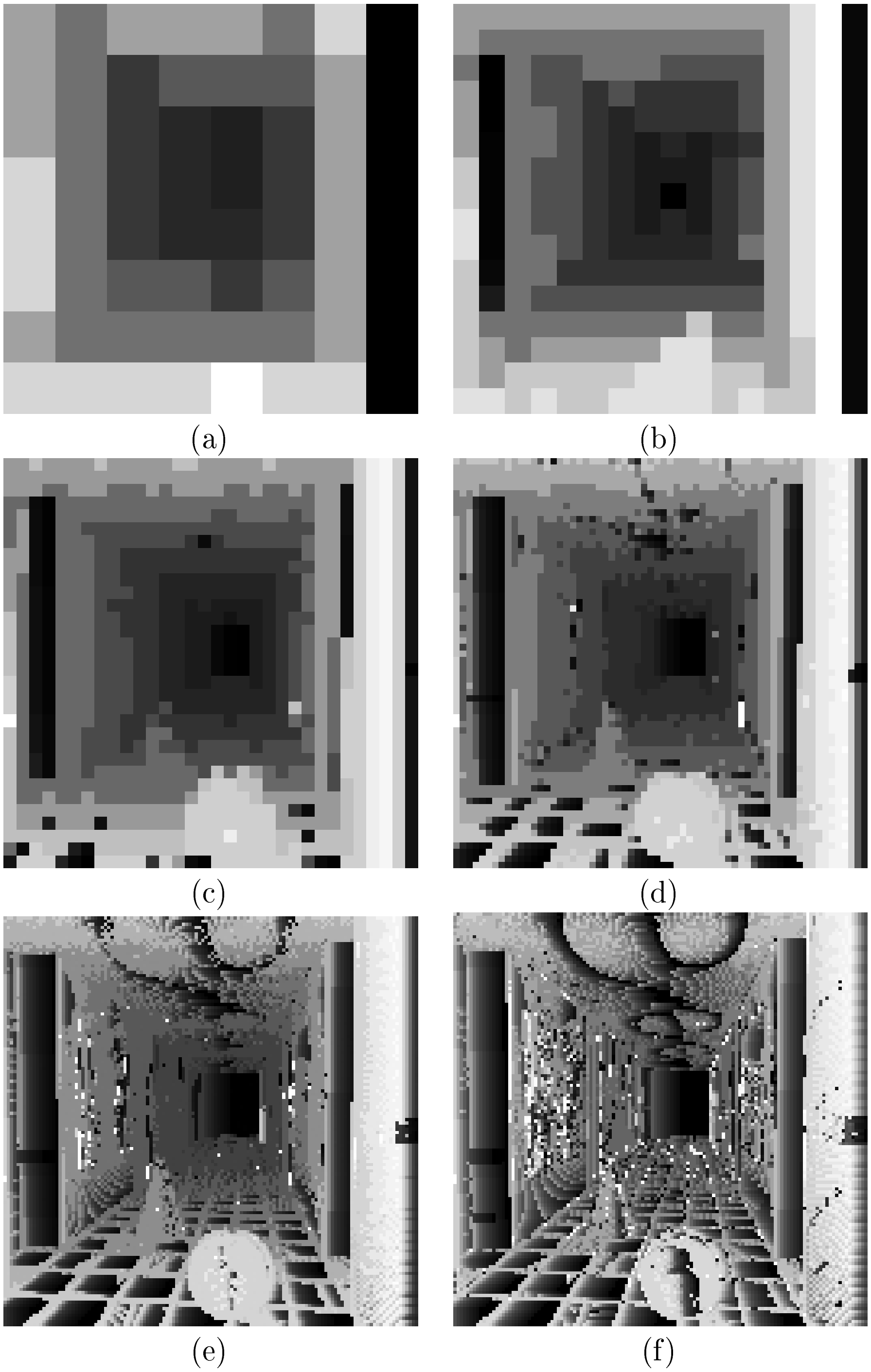

Figure 4.7: Disparity vector field using a simple FSBM with different size of block (*Room*). (a) 32 × 32 (0.003 bps) (b) 16 × 16 (0.012 bps) (c) 8 × 8 (0.046 bps) (d) 4 × 4 (0.169 bps) (e) 2 × 2 (0.725 bps) (f) 1 × 1 (3.151 bps)

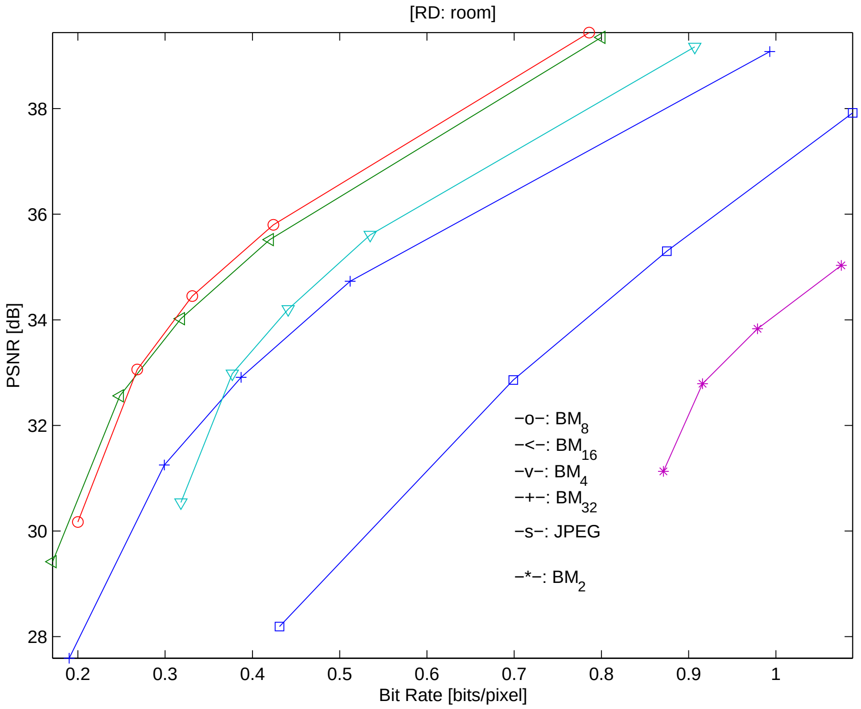

Figure 4.8: RD plot of FSBM with different block sizes. In the plot, '-s-' denotes a square-mark line, and '-<-' and '-v-' denote the direction of triangle in the triangle-mark line. The subscript represents the block size. Note that the RD performance of the smaller block (*e.g.* 2×2) is worse than that of JPEG, because the rate for the DV field is too high.

search, (v) OBM with half-pixel search and (vi) the proposed scheme (OBM with MRF and half-pixel search). As expected, the MRF-based DE estimates a smoother DV field by the tradeoff between the spatial correlation in a stereo pair and the smoothness in the DV field. The proposed hybrid method provides the most smooth and consistent DV field.

Figure 4.10 (a) and (b) compare the corresponding RD plots for the two stereo pairs, *Room* and *Aqua*, respectively. The proposed selective OBDC scheme is compared to FSBM, MRF and OBMC in terms of PSNR and bit rate of the target image. The results of JPEG without disparity compensation are also provided for reference. Note that for the natural image pair (*Aqua*), the RD gain of FSBM is relatively small, compared to those of *Room*.

As expected, the proposed selective OBDC in half-pixel accuracy results in an improved overall encoding performance, *i.e.* a lower bit rate for the DV field and DCD frame while maintaining a PSNR gain. The modified MRF model-based DE maintains the energy level of the DCD frame (or slightly increases according to α), while estimating a consistent DV field using smoothness constraint within causal neighbors. Then, the estimation/compensation in half-pixel accuracy reduces the energy level of the DCD frame. Note that the smoothness term also reduces the increase in rate of the DV field due to the half-pixel search. Selective OBDC reduces oversmoothing problem as well as blocking artifacts by summing the neighboring compensated blocks using the changing OBM window. According to our experimental results, the proposed modified OBDC scheme obtains a higher PSNR, about 0.5-1 dB, as well as better perceptual quality, over conventional OBMC schemes. In addition, selectively applying OBDC reduced the computational complexity over OBMC.

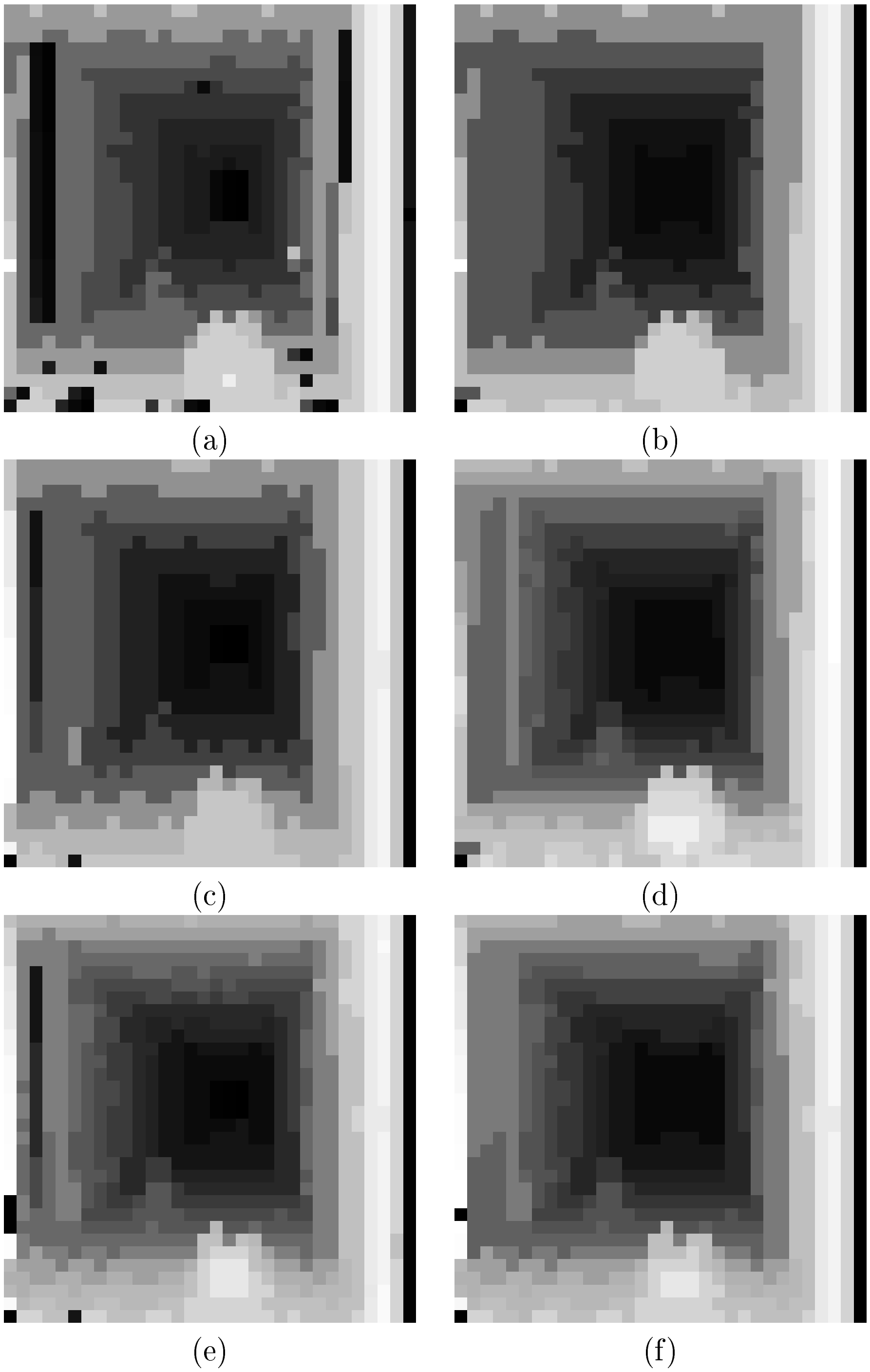

Figure 4.9: DV fields for various disparity estimation methods: (a) FSBM (0.046 bps), (b) DE with MRF (0.032 bps), (c) DE with OBM (0.038 bps), (d) MRF with half-pixel search (0.042 bps), (e) OBM with half-pixel search (0.065 bps) and (f) OBD with MRF and half-pixel search (0.060 bps). The combined method provides the most smooth and consistent DV field.

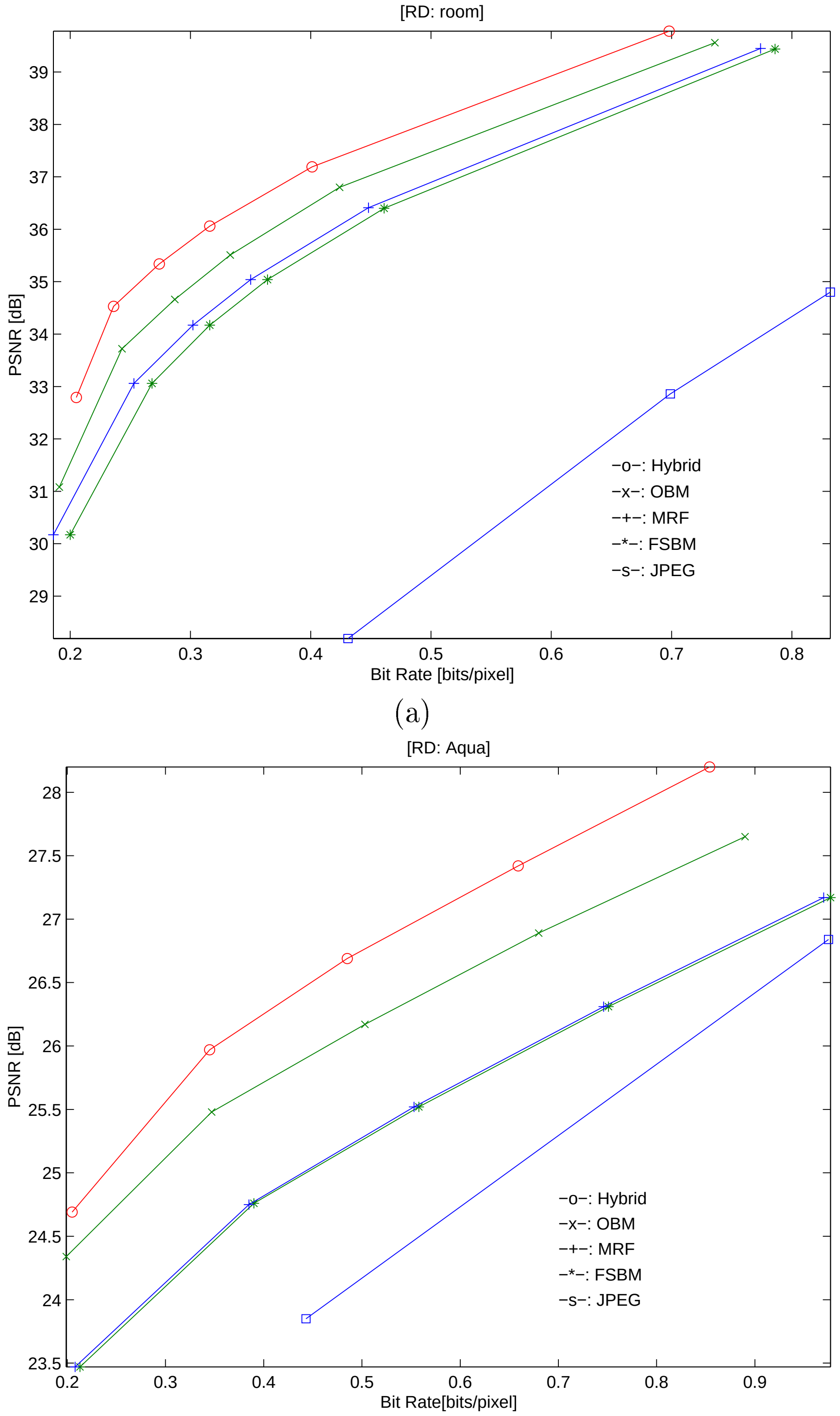

(a)

(b)

Figure 4.10: The resulting RD plots. (a) *Room* (b) *Aqua*. Various DE/DC methods (block size of 8 × 8, quality factor for the reference image Qf_1=80): The proposed hybrid scheme is compared with JPEG, FSBM, FSBM with MRF, and OBM. In the plot, '-s-' denotes the square-mark line.

4.4 Discussion

We presented a novel hybrid DE/DC scheme for stereo image coding. As expected, MRF-based DE allows estimating a smooth DV field. Also, selective OBDC in half-pixel accuracy results in better compensation by reducing the energy level of the DCD frame as well as the blocking artifacts. According to our experimental results, the proposed OBDC scheme provides a higher PSNR as well as better perceptual quality over other FSBM schemes such as MRF or OBMC, encoded at the same rate. The results of the proposed selective OBDC schemes also can be applied into video coding without the loss of generality. It is also worth noting that obtaining a smooth disparity is useful for multi-view video coding since the robustness against noise can help reduce the temporal redundancy between two consecutive disparity fields. However, there remain several problems to be resolved. The overall encoding performance could be improved by combining the proposed DE scheme and the dependent bit allocation scheme proposed in [39, 59].

Chapter 5

MRF-based Hierarchical Block Segmentation

In this chapter, we propose a novel quadtree-based disparity estimation/compensation (DE/DC) algorithm for stereo image coding. Variable size block matching (VSBM) is a way of overcoming those well-known limitations of fixed size block matching (FSBM), such as inaccurate disparity estimation and blocking artifacts in the decoded target image. However, VSMB may suffer from the inconsistency problem in disparity estimation especially as the subblock becomes small. In addition, the resulting disparity compensated difference frame contains high frequency components along subblock boundaries as a result of block segmentation. Therefore, we propose a hybrid quadtree-based DC/DC scheme, where DE with MRF model-based VSBM allows estimation of a consistent disparity field. The combination of RD cost-based block segmentation and selective overlapped block disparity compensation improves the encoding efficiency over conventional VSBM schemes. According to the experimental results, the proposed block segmentation scheme achieves a higher PSNR gain, while generating a relatively consistent disparity field, as compared to conventional VSBM schemes. The proposed scheme also yields fewer visual artifacts along object boundaries.

5.1 Introduction

As with in the video case, block-based predictive coding has been widely used to encode stereo images/video. However, as explained in Chapter 4, inaccurate estimation is inevitable in fixed size block matching (FSBM). Besides, FSBM may introduce the annoying blocking artifacts in the decoded target image at a low rate coding, where only few bits are employed to encode the disparity compensated difference (DCD) frame. Since Lukacs [12] introduced FSBM in stereo image coding, various block-based DE/DC schemes have been studied to reduce the well-known drawbacks of FSBM [41, 45, 86, 110]. Nevertheless, conventional FSBM-based approaches only relieve few of the problems.

An alternative is a hierarchical approach relaxing the *uniform-disparity-per-block assumption* [51,53,111,112]. In term of the DCD frame, it is desirable to segment an image into smaller blocks to reduce the entropy of the DCD frame. However, it may not be worth computing a dense disparity field, if the cost of transmitting or storing the DV field is too high. On the other hand, the number of blocks could not be too few because larger blocks result in higher estimation errors. As a compromise, variable size block matching (VSBM) has been introduced in image/video coding. A main advantage of VSBM is that larger blocks are used in homogeneous areas (background or inside of object) and smaller blocks are used in object boundary areas. Thus, the disparity compensation can be performed properly, even if the initial block contains several objects with different disparity vectors or contains an occlusion area. The representation of the resulting disparity vector (DV) field generally relies on a binary tree [113] or a quad tree [46, 48, 50, 77, 114].

However, like FSBM, the quadtree-based VSBM has similar limitation in a consistent DV field estimation. In general, block segmentation is determined by various intuitive *ad hoc* criteria such as threshold, features, local variance of the DCD, local motion activities and/or rate-distortion (RD) [47,48,111,113,115–119]. However even if RD-based segmentation approaches are used, the segmentation may not take into account the consistency of the displacement. As a result, DE with smaller blocks suffers from the noise effects or aperture problem[1]. Consequently, the neighboring blocks may have many different vectors, resulting in inefficient encoding for the DV field, because each vector minimizes only the prediction error of the block. Usually, smaller blocks such as 2×2 or 1×1 are very sensitive to noise and thus, in conventional VSBM, 8×8 (or 4×4) is considered as the smallest block[2]. In addition, the segmentation of the block into smaller subblocks may result in the DCD frame containing high frequency components, within the initial block, along subblock boundaries. As a result, DCT for those subblocks may not efficient because the segmented block requires more bits to encode those high frequency components.

Therefore, we propose a novel quadtree-based disparity estimation/compensation scheme to overcome those weaknesses of VSBM. The proposed scheme consists of three components: (i) disparity estimation using an MRF model, (ii) hierarchical block segmentation by the quadtree pruning based on the simplified RD cost and (iii) selective overlapped block disparity compensation (OBDC) for the segmented subblocks. The novelty of the proposed VSBM scheme is that the hierarchical disparity estimation with MRF model allows estimating a consistent DV field, *i.e.* a relatively smoother DV field. Obtaining a smooth DV field is beneficial as it reduces the rate for the DV field itself and segmenting blocks based on the RD cost improves the encoding efficiency. In addition, the selective OBDC for the segmented subblocks improves the encoding efficiency by reducing blocking artifacts within segmented blocks. The main improvement over the OBDC scheme proposed in Chapter 4 comes from the fact that we segment the occlusion blocks according to the predefined RD cost and thus we use overlapped windows with different sizes and shapes for those segmented subblocks. For selective OBDC, no side information is required because a quadtree

[1] In areas without significant features (or with repetitive features), a smaller block usually suffer from many local minima within search window during displacement estimation.

[2] Note that in H.26x, for each macroblock block, the segmentation is preset only one time (from 16×16 to 8×8), which may not be suitable for object-based coding such as MPEG-4.

already contains block segmentation information. Consequently, the proposed scheme allows more accurate disparity estimation/compensation along the object boundaries and thus reduces the visual artifacts along the object boundaries while maintaining encoding efficiency of the target image.

The proposed VSBM scheme is also of general interest in image analysis or synthesis/generation as well as image coding by producing useful intermediate information for various applications. For example, in new standards such as MPEG-4, the proposed scheme can help object-based segmentation of the image by combining both the intensity and the disparity information together. In video coding, the motion information has been used to estimate the boundaries of moving objects according to motion homogeneity, under the assumption that the objects have rigid motion. Thus, the applications have been restricted to simple video-phone-like sequences [120]. Meanwhile, in stereo images, an image can be segmented into different objects because not only moving objects but also all objects within the scene have different disparity vectors.

According to our experimental results, the proposed scheme provides higher RD performance as well as better perceptual quality, while also being computationally efficient. To prove the effectiveness, we compare the proposed scheme with a simple VSBM scheme. According to our experimental results, the proposed scheme results in an improved peak-signal-to-noise-ratio (PSNR) gain, about 0.5-1.5 dB, as well as better perceptual quality, as compared to simple VSBM, which segments blocks based on threshold values.

This chapter is organized as follows. In Section 5.2, we briefly explain the main components of the proposed scheme, *MRF model-based disparity estimation* and *RD-based block segmentation.* The proposed encoding procedure is described in Section 5.3. In Section 5.4, we provide some experimental results to compare the effectiveness of the proposed scheme. The conclusion is made in Section 5.5.

5.2 Variable Size Block Matching

5.2.1 DE with MRF Model for VSBM

In VSBM, each block is successively subdivided into quadrants until no further division is necessary. The basic idea of VSBM-based coding is that the subblocks are encoded only when they *significantly* improve encoding efficiency over their upper block. The main advantage of the hierarchical DE with MRF model is that it can overcome the mismatching problem (inconsistency of the DV field) by considering blocks in upper level as well as neighboring blocks, while maintaining encoding efficiency.

To estimate a smooth DV field, we consider the DV field as a coupled MRF model consisting of disparity process and occlusion process. We can similarly formulate DE problem as we did in Chapter 4 and in [86, 110]. The main difference is that we define a neighborhood in hierarchical layers as shown in Figure 5.1. We first derive an energy equation for hierarchical block matching based on the MRF model, which allows us to find a smooth DV field. In order to achieve an efficient estimation of the DV field, we can impose some useful and realistic constraints on the DV field, such as similar intensity level between the two corresponding images in a stereo pair, smooth disparity field, occlusion field, etc. Note that we only segment occlusion block to improve the overall encoding efficiency.

For the proposed VSBM, (2.20) has to be changed as follows,

$$\begin{aligned} U(V,\Phi|F_1,F_2) &= \sum_{i\in N}\sum_{k=0}^{K-1}\{(1-\alpha)(1-\phi_i^{lk})||b_{2i}^{lk}-b_{1i}^{lk\oplus v^{lk}}||^2 \\ &\quad +\alpha\sum_{\eta_{lk}}(1-\phi_i^{\eta_{lk}})(v_i^{lk}-v_i^{\eta_{lk}})^2+\beta\sum_{c\in C_l}V_c(\phi_i^{lk},\phi_i^{\eta_{lk}})\} \end{aligned} \tag{5.1}$$

where b^{lk} denotes the k-th block in the l-th level of the segmentation, where $K=4^l$ for the quadtree-based segmentation. Similarly, v^{lk} and ϕ^{lk} denote the disparity vector and the occlusion status of b^{lk}.

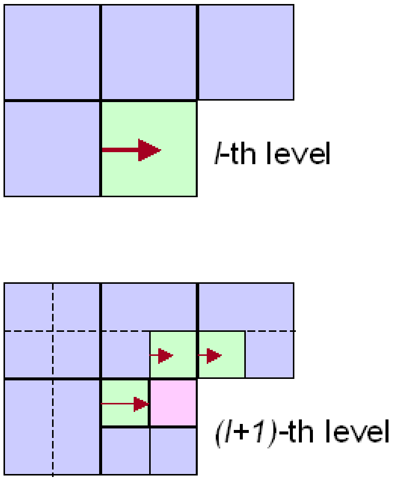

Figure 5.1: Neighborhood System For VSBM. We use 1^{st} order neighborhood system. The larger neighborhood, the greater the influence from its neighborhood.

The first term of the right side in (5.1) represents the constraints of the similarity between two images in a stereo pair for a given disparity and occlusion. Note that the block containing multiple objects or object boundaries results in erroneous matching. If the block in F_1 fails to be compensated from a block in F_2, the block is selected as an occlusion candidate and then segmented further into subsequent subblocks. Note that if we ignore the occlusion and the smoothness terms, the above algorithm simply becomes the conventional block matching.

The second term in (5.1) represents an *a priori* assumption on the smoothness of the DV field, V, given the occlusion, Φ, which will be used to tradeoff between the smoothness and the estimation error. We assume that the real disparity field is smooth except for the object boundaries (due to occlusion) that are related to the depth discontinuities. Note that generating a smooth disparity field not only mitigates the effects of noise, but also increases the encoding efficiency for the disparity, because similar disparities in adjacent blocks results in lower entropy. For VSBM, we define a neighborhood system in a hierarchical structure as shown in Figure 5.1.

The last term in (5.1) denotes an occlusion process. We can impose an *a priori* assumption on the occlusion field such as connected occlusion. The isolated occlusion is inhibited. In this experiments, we set β to be zero and then decide the initial candidate by comparing the magnitude of the mean absolute error (MAE) of the block with a pre-selected threshold. The detailed occlusion block selection procedure is explained in Chapter 4.

Finally, we selectively apply VSBM and OBDC for those occlusion blocks.

5.2.2 RD-based Hierarchical Block Segmentation

In order to achieve better overall coding performance than the FSBM-based methods, further segmentation of an occlusion block has to be performed in an efficient manner. An optimal hierarchical block segmentation can be searched in the RD-plot using a Lagrange multiplier ($\lambda \geq 0$), by minimizing a cost function according to the available bit budget, R_{budget}, or allowable distortion, D_{budget}. In general, RD-based segmentation can be considered in various aspects. First of all, all the blocks in an image can be considered simultaneously to achieve a global optimization [39]. Also the buffer-constrained optimal block segmentation can be performed for groups of blocks [81, 121]. In this chapter, we perform the block segmentation for each block on the assumption that minimizing the cost of each block also minimizes the global coding cost [48, 82].

Quadtree can be constructed by using *top-down* or *bottom-up* approaches. In this chapter, we adopt a *top-down* approach, where a hierarchical block segmentation can be performed using the Lagrangian cost. For blockwise segmentation, the number of possible trees can be approximated as $S \cong 2^{4^l}$, where l denotes the depth of a tree. For example, for $l = 4$ (from 32×32 to 2×2), $S \cong 2^{256}$. Therefore, the optimal segmentation based on exhaustive search is too computationally expensive. To reduce the complexity, we adopt a tree-pruning technique.

Let T and P, respectively, be sets of full trees and pruned trees, *i.e.* $T_2 = \{T_{2i}, 0 \leq i < N\}$ and $P_2 = \{P_{2i}, 0 \leq i < N\}$. In VSBM, an initial block f_i is assigned to the root node of T_i or P_i. In quadtree-based VSBM, an initial block (the usual size is 32 × 32 or 16 × 16) is segmented into a l-level hierarchical structure, where the block size of a subblock is $B \cdot 2^{-l} \times B \cdot 2^{-l}$. The number of subblocks is $K = 4^l$, where l denotes the level (or depth) of tree and the maximum level is $L = log_2 B$. The subsequent subblocks are assigned to the children nodes, consisting of leaf and internal nodes. A leaf node is defined as a node without children. Meanwhile, a node with children is called an internal node. The pruned tree is represented by using a sequence of bits, where "0" and "1" are used to indicate an internal or a leaf node, respectively.

In general, for a block segmentation considering the rate and distortion, the cost of the pruned tree P^* is less than that of the full tree T, *i.e.* $C(P^*) \leq C(T)$, where $R(P^*) \leq R(T)$ and $D(P^*) \geq D(T)$. To achieve an efficient segmentation, the decision of block segmentation can be made by comparing the Lagrangian costs of the parent and children nodes. We first define a blockwise Lagrangian cost c^l for the hierarchical segmentation as follows,

$$c_i^l = \sum_{k \in c_i^l} \{d_i^{lk} + \lambda r_i^{lk}\} \tag{5.2}$$

where d^{lk} and r^{lk} denote the distortion and the rate of the block, b_i^{lk}, respectively. Lagrange multiplier ($\lambda \geq 0$) controls the weight between d and r. Note that the rate r^l for the blocks in l-th level is defined as a sum of bit rates, $r(v^l) + r(dcd^l)$, where v and dcd denote disparity vectors and the resulting DCD of the block.

For the quadtree-based segmentation, the required bits are increased four times for each segmentation, if we assume the DV field is encoded with fixed length code. The required bits for a DV are (at most) $\frac{\lceil \log_2 W \rceil}{B \times B} \times$ [bits/pixel], where W denotes the maximum range of the search window and $\lceil \rceil$ represents a ceiling function. The rate for the tree also has to be counted in calculation of the rate $r(v^{lk})$. The tree structure is encoded by a sequence of bits representing the status of the tree node, *e.g.* "0" and "1" denote a leaf node and a internal node, respectively as shown in Figures 5.2. As a result, 4 bits are required to describe the segmentation in the quadtree, if the block is segmented.

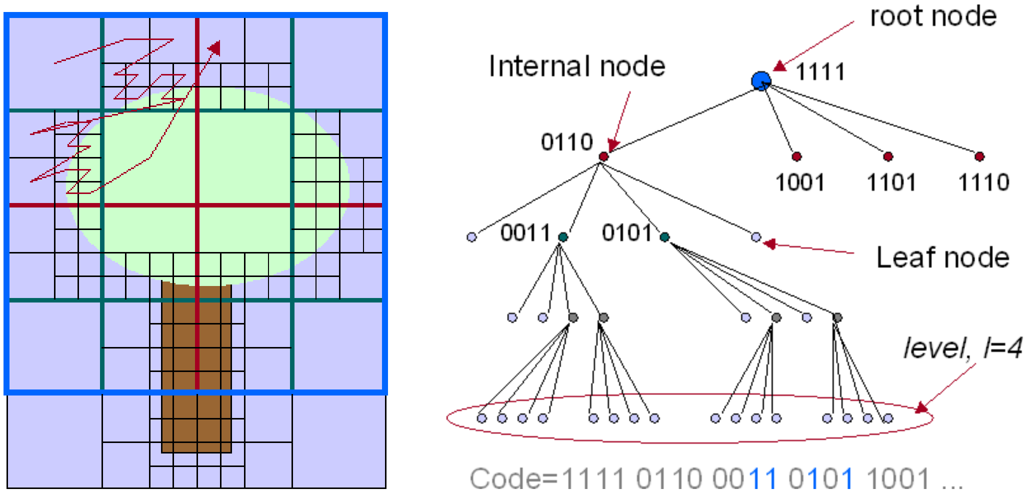

(a) (b)

Figure 5.2: Quadtree-based block segmentation and encoding. (a) DPCM of DV field (b) Quadtree Construction. A leaf node and a internal node are denoted by "0" and "1", respectively.

In (5.2), by segmenting a block the rate for the DV, $r(v^l)$, is a monotonically increasing functional, *i.e.* $r(v^l) < \sum r(v^{l+1})$,. Meanwhile, the rate for the DCD, $r(dcd^l)$, and the distortion d^l are monotonically nonincreasing functionals, *i.e.* $r(dcd^l) \geq \sum r(dcd^{l+1})$ and $d^l \geq \sum d^{l+1}$. The block segmentation is performed, only if the gain from the reduced distortion is greater than the increased rate, *i.e.*, $c^l > c^{l+1}$, which corresponds to

$$\nabla d^l - \lambda \nabla r(dcd^l) > \lambda \nabla r(v^l) \tag{5.3}$$

where

$$\left\{ \begin{array}{l} \nabla d^l = d^l - \sum_{k=0}^{3} d^{l+1k} \\ \nabla r(dcd^l) = \sum_{k=0}^{3} r(dcd^{l+1k}) - r(dcd^l) \\ \nabla r(v^l) = \sum_{k=0}^{3} r(v^{l+1k}) - r(v^l)\} \end{array} \right. \tag{5.4}$$

where ∇d and ∇r denote the distortion and the rate decreases, respectively. The distortion d^l of the blocks in l-th level is calculated using MSE (or MAE).

In this chapter, we assume that fixed length coding for $r(v)$ and ignore $r(dcd)$. We also use the MSE of the DCD for $d(dcd)$, instead of the quantized DCD. Note however that the results are still superior to those of threshold-based VSBM schemes, although the above assumptions and simplifications lead to suboptimal solution in terms of encoding efficiency. In conventional RD-based segmentation schemes, the computational cost of RD values is very expensive and thus, in place of computing the real bit rate, the rate is either replaced by the entropy, approximated by using a stochastic model [47, 116] or linear function [118]. Especially with conventional approaches, the calculation of $r(dcd)$ is complicated and yet the results are still suboptimal because the DCD is nonstationary. Therefore, based on the observation that $r(dcd)$ depends on $d(dcd)$, we ignore $r(dcd)$ and consequently only consider the two terms in (5.3), *i.e.* ∇d and $\nabla r(v)$.

The corresponding block diagram of the Qtree-based block segmentation scheme is shown in Figure 5.3.

5.3 Encoding Procedure

In this Section, we explain the procedure of the proposed hybrid coding scheme. The basic procedure is as follows. First, the F_1 is encoded in intraframe mode using transform methods such as DCT or wavelet transform[3]. Then, using (5.1), we estimate the DV field by tradeoffs between the similarity of intensities and the smoothness of the disparity field. We determine the block segmentation using (5.4). Finally, we apply OBDC only for those segmented blocks to reduce the blocking artifacts and to improve encoding efficiency of the DCD frame.

[3] Note that we do not encode the F_1 based on segmentation since the quality of the reconstructed image highly depends on that of the reference image and generally conventional transform methods provide better performance at higher bit rates than segmentation based coding does.

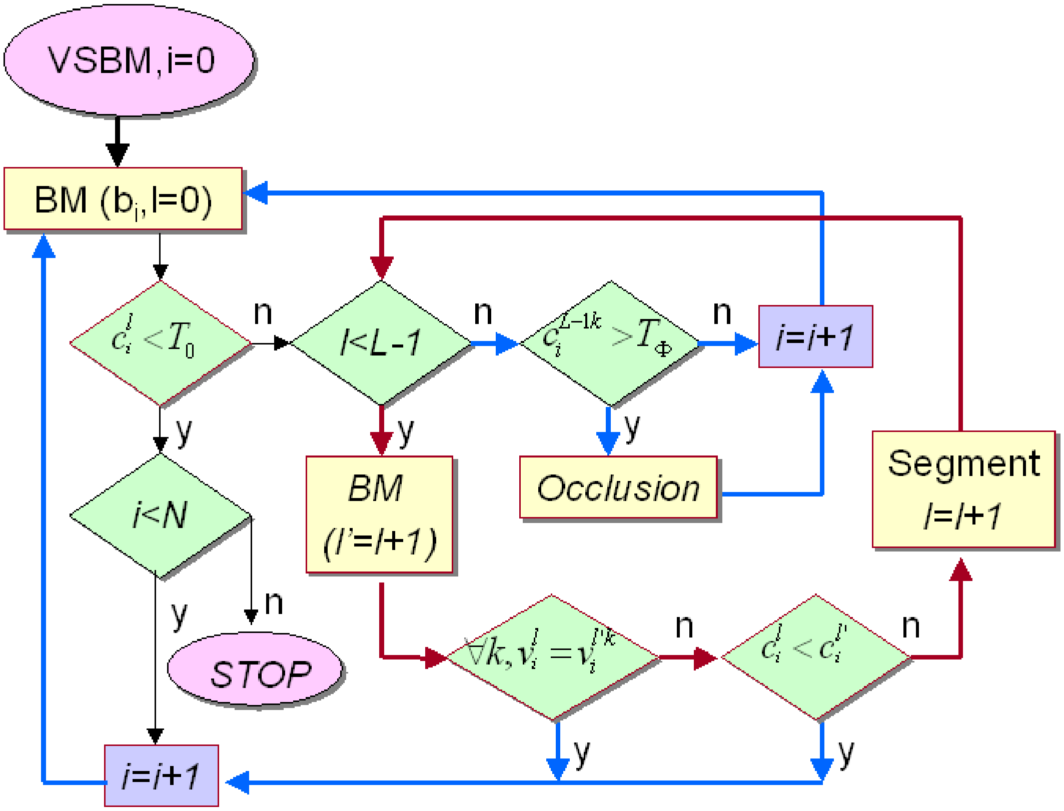

Figure 5.3: Flow chart of Qtree-based disparity estimation by comparing RD costs between blocks in consecutive layers .

The formal procedure of the proposed scheme is as follows.

- **Step 0** F_2 is segmented into initial blocks, *i.e.* 32×32 or (16×16). The segmentation level, $l = 0$.

- **Step 1** For each block in F_2, the best matching block is estimated in F_1 within the search window using (5.1). Go to next block, if the resulting MSE of the DCD is smaller than a threshold, T_ϕ. Otherwise, set $\phi_i = 1$ and go to step2 for further segmentation. A block containing high prediction error in the DCD block is considered as an occlusion block.

- **Step 2** At $l = l + 1$, for each subblock, a DV is estimated using energy function in (5.1). Outliers in DV fields are reduced in this process using MRF-based cost function to estimate a smooth DV field.

- **Step 3** If the DV's are the same as those generated in the upper level, we do not need to further consider segmentation. Otherwise, the given DE costs are compared to determine using (5.3), whether the block should be segmented. The block is segmented if the coding cost of the subblocks is lower than that of the block, *i.e.* $c^{l+1} < c^l$. Segmentation is repeated until the coding cost of the block is smaller than that of segmented subblocks or the block size is reached the preselected size, *i.e.* $k = L - 1$.

- **Step 4** This process is repeatedly applied to the blocks in the target image. If $i < N$, go to step1. Otherwise, stop.

- **Step 5** For the resulting DV field, based on the Qtree, OBDC is selectively performed for the occlusion blocks (with $\phi = 1$).

The resulting Qtree, the DV field and the DCD frame are encoded for subsequent transmission or storage. The DV vectors of subblocks, as shown in Figure Figure 5.2, are ordered in a Z shape. The DVs are then ordered in row by row and later encoded using DPCM. After selective OBDC, the smoothed DCD frame is encoded using

JPEG and then stored or transmitted to improve the overall quality of the decoded image. Notice that no side information is needed for the selective OBDC since the information is already contained in the quadtree.

The decoding is the inverse of the encoding process. At the decoder, the reference image is first decoded. Afterwards, the target image is reconstructed using the reference image and the side information such as disparity with occlusion and compensated error.

5.4 Experimental Results

To show the effectiveness of the proposed scheme, DE/DC with hierarchical block segmentation, we test our algorithm on a synthesized image pair, *Room*, and a natural image pair, *Aqua*, as shown in Figures B.2 and B.3. The search window is $(\pm 2, \pm 16)$. Then, the results are compared with those of the FSBM and VSBM. The performance is measured in terms of the bit rate and the peak signal to noise ratio (PSNR) of the target image.

First, the effects of block size are measured in terms of MSE and bit rate. As shown in Figure 5.4, as the block size is reduced for DE, the MSE between the disparity estimated block and the original block is linearly decreased. However, as shown in Figure 5.4 (b), the bit rate required to transmit the DV field is increased, simultaneously. Another noteworthy observation is that, as shown in Figure 5.4 (c), if the block size of DE becomes smaller that the block size of DCT (*e.g.* compare the RD performance for both 8×8 and 4×4), decreasing block size does not always increase the encoding efficiency, due to block boundary effects of smaller blocks, even though the smaller block decreases the MSE of the DCD frame. Note that in our experiments DCT is performed on the 8×8 block and thus the DCD resulting from FSBM with 4×4 block may not be efficient in the RD sense, which is one of the main motivations of introducing OBDC for the segmented subblocks.

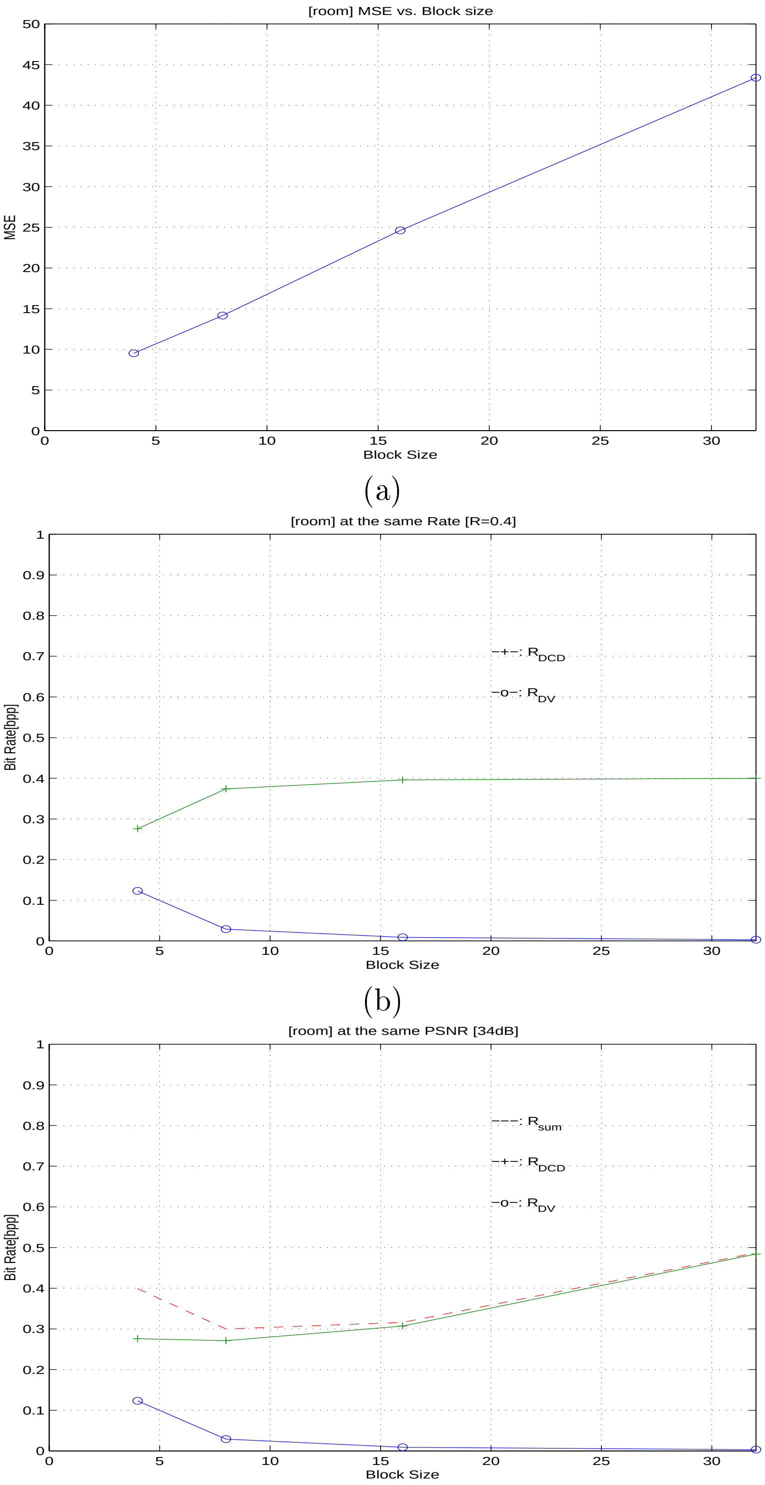

(a)

(b)

(c)

Figure 5.4: Effects of block size. (a) MSE vs. block size. (b) Bit rate vs. block size rate (at the same rate, 0.4 [bpp]). (c) Bit rate vs. block size (at the same PSNR, 34dB).

Figure 5.5 compares the disparity estimation results of the proposed scheme versus those of threshold-based VSBM. Figure 5.5 (a) and (b) show DV fields based on the FSBM. The resulting DV field of FSBM has a blocky appearance, as we are limited to a single disparity vector per block. The errors occur, as expected, along the object boundaries for the FSBM, where a different estimate for object and background is needed. The disparity field in Figure 5.5 (c) and (d) show DV fields based on the VSBM. As shown, VSBM shows inconsistencies in the DV field, as the sublock size becomes small. As shown in (d), MRF-based DE in VSBM allows a consistent DV field estimation.

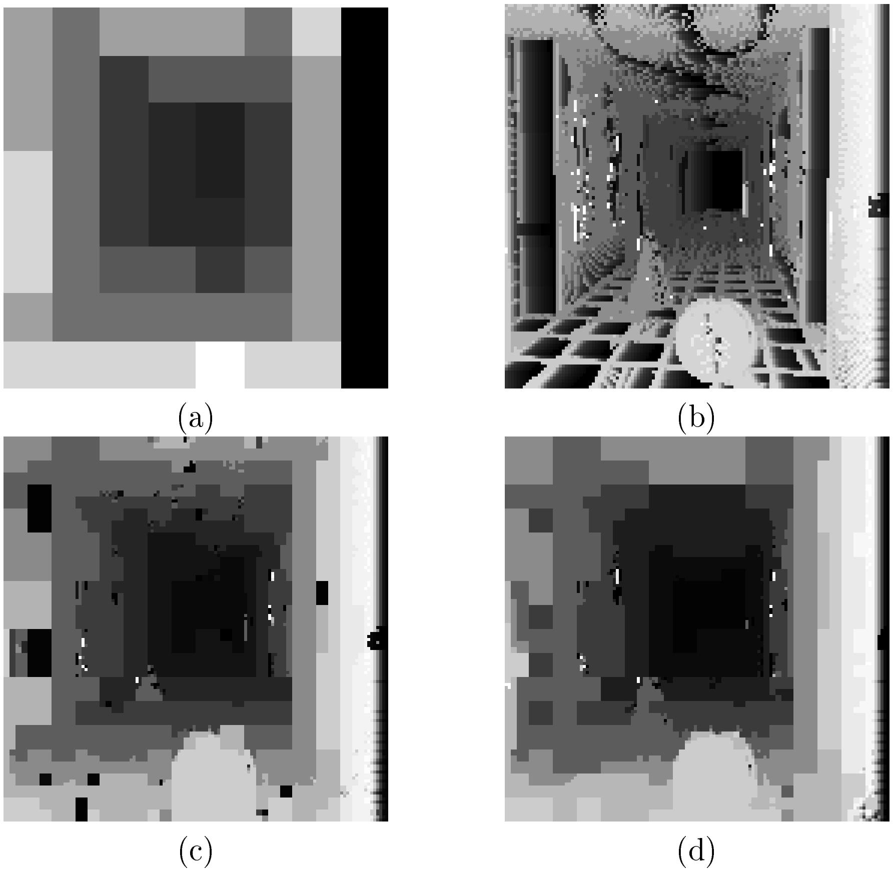

Figure 5.5: Results of the disparity estimation for the synthesized image, *Room*. (a) DV field with the FSBM (32×32) (b) DV field with the FSBM (2×2) (c) DV field with the VSBM (32×32 to 2×2) (d) DV field with the proposed VSBM (32×32 to 2×2)

As expected, the proposed MRF model-based DE scheme estimates a relatively smooth and accurate DV field, which can be used to generate intermediate scenes in the virtual environment while reducing the disparity compensated error. The resulting smooth disparity field reduces the bit rate for the disparity field itself. Figure 5.6 shows similar results for the natural images, *Aqua*.

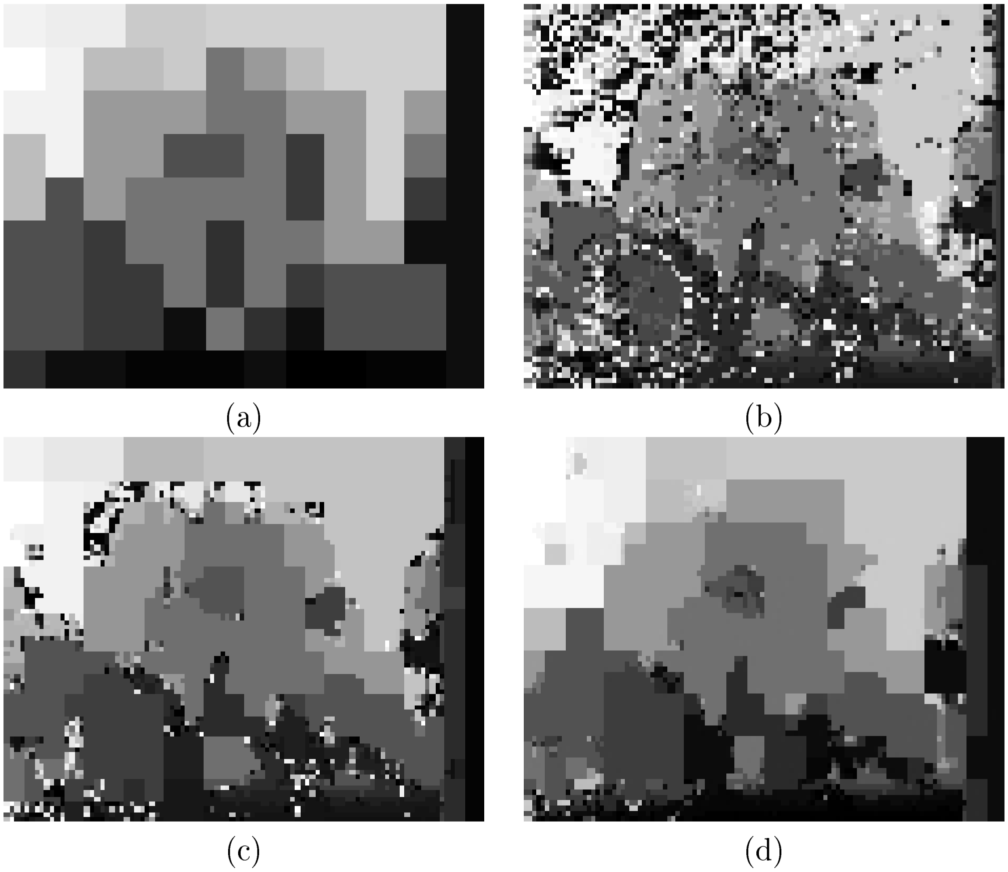

(a) (b)

(c) (d)

Figure 5.6: Results of the disparity estimation for the natural image, *Aqua*. (a) DV field with the FSBM (32×32) (b) DV field with the FSBM (4×4) (c) DV field with the VSBM (32×32 to 4×4) (d) DV field with the proposed VSBM (32×32 to 4×4)

Figure 5.7 (a) and (b) show the corresponding RD plots of both target images in the pairs of stereo images. In the experiments, we fix the reference image and only measure the RD performance for the target images in the stereo pairs. The DV fields are encoded using Qtree and the DCD frames are encoded using JPEG. The performance is measured in terms of PSNR. As shown, the proposed scheme achieves a higher PSNR performance in both test images. Note however that the RD gain of VSBM mainly comes from selectively segmenting the blocks according to some "good" RD criteria.

According to our experimental results, the proposed hybrid VSBM method improved overall encoding performance for the target image in a stereo pair. The DE using (5.1) estimates relatively accurate and more consistent DV fields, which results in less bit rate for the DV. The block segmentation using (5.3) reduces the energy levels of the DCD frame. The encoding efficiency has been further improved by selectively applying OBDC for occlusion blocks, which significantly reduces the compensation error along the object boundaries. In terms of PSNR, the proposed scheme achieved 0.5-1.5 dB higher PSNR, as compared with conventional VSBM, at the same bit rates. In addition, the reconstructed image based on the proposed scheme resulted in fewer annoying blocking artifacts, by reducing the blocking errors along the subblocks using OBDC, the main drawback of the VSBM as well as FSBM methods.

5.5 Discussion

We have proposed a hybrid coding scheme for stereo images, hierarchical DE/DC with MRF model and selective OBDC. According to our experimental results, the proposed scheme simultaneously solves the well-known problems of VSBM as well as FSBM. The MRF-based hierarchical disparity estimation provides a smooth DV field and the hierarchical block segmentation based on approximated RD cost reduces the energy level of the DCD frame. Selective OBDC further reduced the energy level of the DCD frame and blocking artifacts along subblock boundaries. As a result, the proposed algorithm provides a higher PSNR as well as a better perceptual visual quality.

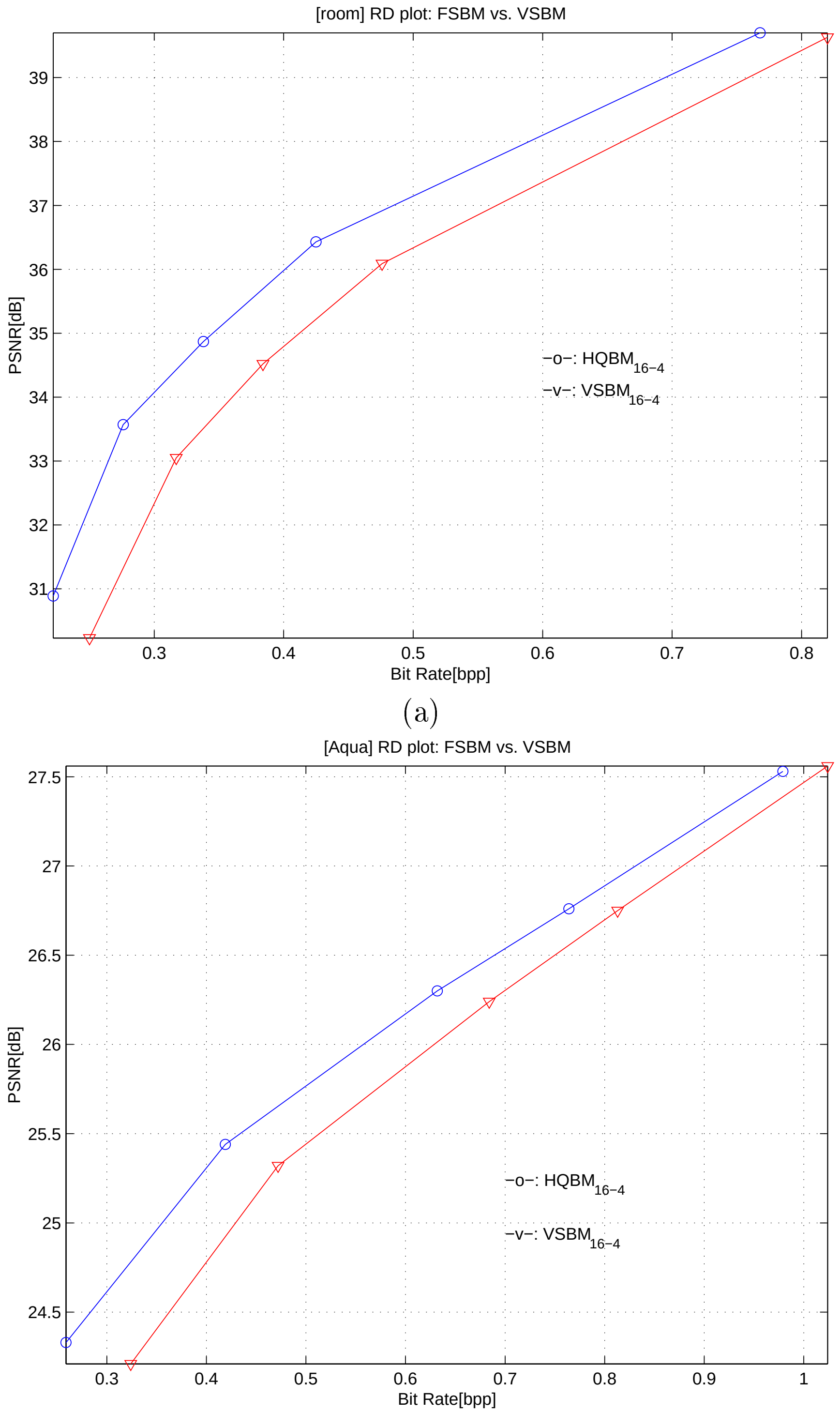

(a)

(b)

Figure 5.7: R-D Plot of reconstructed target images in the stereo pairs. (a) *Room* (b) *Aqua*.

This research will be extended to the intermediate view generation (or synthesis) to provide the look-around-capability at the decoder. The RD-based contour representation of the segmented region remains a crucial future work because the RD-based shape coding will be an important technique for object-based coding, providing various functionalities such as interactive manipulation of objects.

Chapter 6

Summary and Future Extensions

6.1 Summary

In this research, the main focus has been on the efficient representation of stereo images, which is a simple way providing the 3D-depth information on a flat 2D screen. The transmission of stereoscopic images or sequences over existing channel requires a very low rate coding of the additional stream in order to maintain the quality of the reference image sequence. Such high compression ratio can only be achieved by imposing structure to the additional sequence and taking advantage of the high tolerance of the human visual system. The easiest extension would have been to simply encode the reference image/sequence using JPEG/MPEG-type scheme and the other image/sequence using disparity compensation method. To further improve encoding efficiency, we have proposed various encoding schemes within predictive coding framework through this dissertation.

In Chapter 2, we surveyed various issues on 3D imaging systems and briefly reviewed research on stereo image/video coding. We then formulated the stereo image coding problem using the dependent coding framework, consisting of estimation/compensation, quantization, and rate control. Using the open loop coding system, we decoupled the complicated joint optimization problem into two independent problem; an efficient disparity estimation and an optimal dependent quantization.

We first proposed a blockwise dependent quantization scheme in Chapter 3. With a given DV field, we increased the coding efficiency in quantization by taking into account the binocular dependency between the stereo pairs. The special dependency of the stereo images was exploited to reduce the computational complexity. By exploiting the predominant horizontal dimensional dependency, a compact dependency tree was constructed per pairs of ROBs and then the optimal sets of quantizers had been selected using the Viterbi algorithm. On the assumption of monotonicity property, we also proposed a fast search algorithm for dynamic programming.

In Chapter 4 we explained the FSBM-based disparity estimation and its well-known limitations. We then proposed a hybrid scheme to overcome those limitations. The proposed hybrid scheme, MRF model-based disparity estimation and selective overlapped block disparity compensation, provided a higher PSNR gain as well as fewer visual artifacts. The MRF model helped provide smooth disparity field, while maintaining the entropy of the disparity compensated difference. The selective OBDC reduced the blocking artifacts in the reconstructed target. The incorporated half-pixel accuracy further improved the encoding efficiency.

In Chapter 5, we introduced the disparity estimation/compensation schemes based on the VSBM to further reduce the entropy of the disparity compensated difference. In the proposed method, the DV field was first estimated based on the MRF-based cost function. Then, hierarchical block segmentation was performed by comparing the RD costs of a block and its subsequent subblocks. Subsequently, overlapped block disparity compensation is selectively performed for the occlusion blocks. Finally, the resulting Qtree and the corresponding DV field were encoded. The DCD frame was also encoded to improve the quality of the decoded target image.

6.2 Future Extensions

Stereo images can be encoded efficiently by combining the disparity estimation and the blockwise dependent quantization. These schemes can be extended easily into stereo video coding. Based on the proposed algorithms in this thesis, the following works are possible extensions.

6.2.1 Object-Oriented Segmentation Using Stereo Images

Object-oriented image segmentation is a key step in the upcoming new standards such as MPEG-4 and MPEG-7. So far, a wide variety of image/video coding methods have been developed but the main research activities on image/video coding have concentrated on the first generation codec. Available first generation coding schemes mainly exploit statistical redundancies of the image data and change parameters of algorithms based on the blocks. The current image/video coding standards (JPEG, H.26x, MPEG-1/2) belong to this category. However, most of these methods have reached their limits in compression performance and have limitations when dealing with real objects in a scene. They may fail to provide an acceptable quality, especially at low rate coding, because annoying block artifacts become noticeable. Therefore, more flexible approaches are required.

Therefore, a novel object segmentation scheme using stereo images can help separate objects (or areas of interest) from a scene under assumption that pixels within a rigid object have similar disparity vector. This scenario works under assumption of 3D infrastructures, which require, at least, two cameras for 3D image/video capture [122]. Note however that even in 2D infrastructure, it provides look-around capability based on intermediate scene synthesis [123].

6.2.2 RD-based Contour Coding

The main goal of segmentation-based coding is an efficient representation of images, *i.e.*, achieving the best visual quality for a given bit budget. An image can be segmented into homogeneous regions and the segmented image can be represented by the contours (or shapes of segmented regions), the textures (intensities) and the segmentation errors, which then have to be encoded. The very same observed ideas can be used to segment a disparity field or a motion vector field. the segmented regions can be represented by global object descriptors such as the surface area, the perimeter, the center of mass, the length and width, or the convexity. These type of parameters are useful for object recognition and classification but not for coding since such low precision descriptions do not allow for a good reconstruction.

Other popular ways to represent the segmented regions are the region description methods and the boundary description methods. In [53], we proposed a VSBM scheme using the MRF model. The resulting DV field was segmented and encoded using the chain coding method. To further increase the encoding efficiency, we need RD-based contour coding, which is a major problem in object-based coding. In general, boundary also can be encoded using a lossy scheme and a lossless scheme [124–126]. Schuster *et al* [127, 128] proposed a RD-based boundary approximation using spline and chain coding but they ignored the rate of the texture, which also has to be considered. In addition, the bit allocation problem for the segmentation-based coding is important. The bit budget has to be distributed between the contour description and the segmentation error.

6.2.3 Blockwise Dependent Quantization for Video

The framework proposed in Chapter 3 can be directly extended into video coding without the loss of generality. However, the temporal dependency is more complicated because the direction of motion can be anywhere in 2D.

6.2.4 Joint Estimation of Motion and Disparity

Stereoscopic video consists of two image sequences, each sequence for a corresponding eye. Therefore, there exists temporal redundancy between consecutive disparity map sequence, which can help motion estimation of the reference sequence. It means that the motion and the disparity have to be estimated jointly, which provide the consistent motion and disparity fields. Basically, disparity vector field can help estimate motion vector field and vice versa. Therefore, it is interesting to combine information these two field to increase reliability and to compensate the weakness of each method [5,56].

6.2.5 Multi-view Images and Intermediate-view Generation

The ideal 3D system has to provide images in space to allow for walking around and viewing the object from all sides. In this sense, stereoscopic images are not the same as 3D images because the viewing angle is strictly restricted to the position of stereo cameras. These look-around capabilities can be achieved by multiview images. To provide the *look-around* capability, the cameras have to move synchronously with the viewers head, which is awkward. One solution is to use more cameras. However, it also requires either a feedback signal from the end user to encoder or an increase in the amount of data. the generation of intermediate scene at the decoder according to the movement of head is one simple solution to this problem. Using the concepts we used in the stereo image compression, we can synthesis the intermediate views.

Appendix A

3D Display Techniques

The basic idea of 3D display is to present simultaneously each image in a stereo pair to the corresponding eye, *i.e.* to provide separately the left and right images to the left and right eyes of the viewer, respectively. There are several ways to view 3D scenes: Free-viewing, stereoscopic display, head-mounted display, autostereoscopic display and holography. Note however that the two basic types are those that require wearing glasses (stereoscopic display) and those that do not require wearing glasses (autostereoscopic display).

A.1 Free Viewing and Stereoscope

The basic method for viewing pictures in stereo without special viewing devices is called free-viewing. For example, 3D effects can be perceived by putting viewing direction in parallel or crossing eyes to see the corresponding image, respectively. Unfortunately, some people have problems in concentrating their eyes on stereo images. There may also be side effects such as eye stain, blur, and headaches to some viewers. The classical stereoscope can help alleviate these pain in perceiving 3D by removing the crosstalk between left and right eye views.

A.2 Stereoscopic Display

To perceive 3D scene on a 2D display monitor we have to produce or synthesize 2D images by means of superimposing or temporal multiplexing.

- **Anaglyphs and Pulfrich:** Another popular and inexpensive method is *anaglyphic display (1850's)* which is the oldest type of 3D viewing (red/blue) glasses. Anaglyphs provide alternative method to represent stereo images, where two views are encoded in different colors and then each eye sees the corresponding image through different color filter. For example, with anaglyph techniques, the red (or cyan) filters must coordinate with the blue (or green) of the image. The next key is *cancellation*, which is the ability of the red filter to

NOT see a red image, and the blue filter to NOT see the blue image. This is the weakest aspect of anaglyphs because it destroys the original color because the color is used as a selection mechanism. Pulfrich is based on the same method except colors of lenses (dark/clear lenses).

- **Polarized display:** Polarized (gray lenses) display is a more sophisticated technique, where the two images in a stereo pair are encoded in orthogonal polarization and then each eye sees the properly intended image through perpendicular polarizing filters (or glasses). Polarization preserves color but is sensitive to crosstalk (when the left eye sees the image for the right eye or vice versa), because it utilizes the relative orientation of the polarized light. It is used for projection situations such as theatrical 3D movies or in special venue displays. These are comparatively expensive to manufacture because of two things: the lens material and the handling of polarized images.

- **Head Mounted Display (HMD):** HMD is the best ALTERNATIVE where the realism is not a concern, such as certain classes of video games. The resulting the very low resolution is one of its major drawbacks.

- **Sequential Display:** The stereo image is displayed in time multiplexed sequence and the synchronization signal is passed to the shuttle glasses worn by the viewer. The glasses are equipped with liquid crystal shutters switching from opaque to clear: a shuttle alternately opens and closes in front of each eye as the image changes on the monitor. For example, one of the lenses, the left one, is made opaque (closed) so that the viewer can only see the right image on the monitor through the right lens. Then, the situation is reversed, *i.e.* the right lens is made opaque while the left view is displayed on the monitor. If the images are displayed rapidly enough, then each eye perceives a different image from viewing the same monitor. For example, for a NTSC-based monitor with a refresh rate of 60 Hz, each eye sees the image at a refresh rate of 30 Hz. Therefore, for the flicker-free 3D display a 120 Hz system is desirable.

A.3 Autostereoscopic Display

What autostereoscopic implies is a form of stereoscopic display that requires no glasses or other aids for the viewer. With the advent of modern electronics, many methods have become feasible, where each eye received a separated image.

Parallax Barrier Screen (PBS) and Lenticular Display: The picture behind the PBS is composed of 2D images from different viewing angles. Pixels for the left and right images are displayed simultaneously in alternative columns. Each eye sees the corresponding image through the appropriate stripes without special glasses. Lenticular Monitor uses cylindrical lenses, which is geometrically similar to PBS but provides superior optical efficiency.

The real limitation, however, of both autostereoscopic displays is in the image quality. For example, the angular field of view is limited and each eye must be very precisely positioned relative to the display. To meet those requirements, the display system may require high display bandwidth, which is complex and expensive.

A.4 Hologram

To overcome fixed viewer position problems, 3D images have to be drawn into real space. The most popular technique in depicting 3D scenes in space is holography. Holograms are generated by splitting a laser light bundle in two parts, of which the reference ray reaches 2D media (film) directly and the other is reflected from the object onto the film. To record 3D images the film keeps only a phase difference, the interference pattern of coherent laser beam (bright and dark lines holding the coded spatial information), instead of a recognizable image. The 3D volume is displayed directly into space without any stereoscopic tricks by the diffraction phenomenon when the hologram is lit appropriately. They are fascinating new technologies but far from practicality yet because of the huge amount of data. For example, an object of a cubic ($10 \times 10 \times 10$ cm) with a 30 degree viewing angle requires a 25 Gbytes. Real time video holography requires a further improvement in coding technique.

Appendix B

Stereo Images

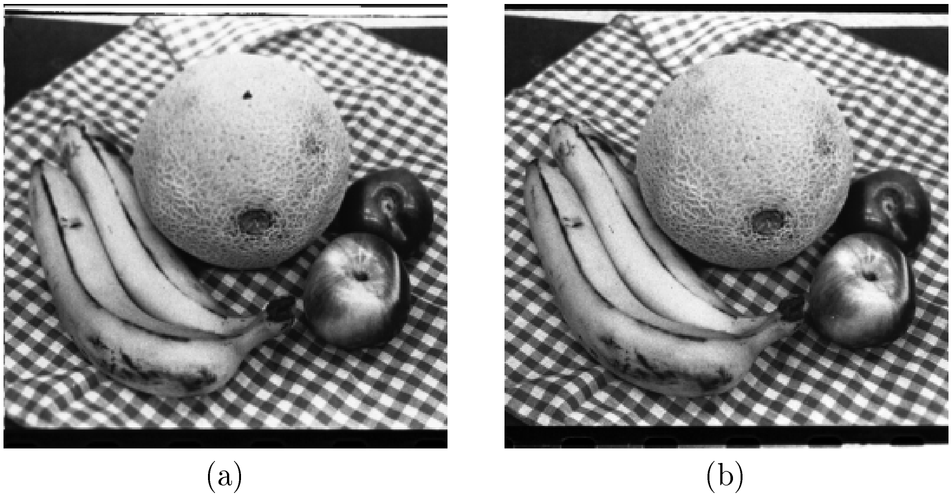

(a) (b)

Figure B.1: Test stereo images *Fruit*. (a) left image (b) right image

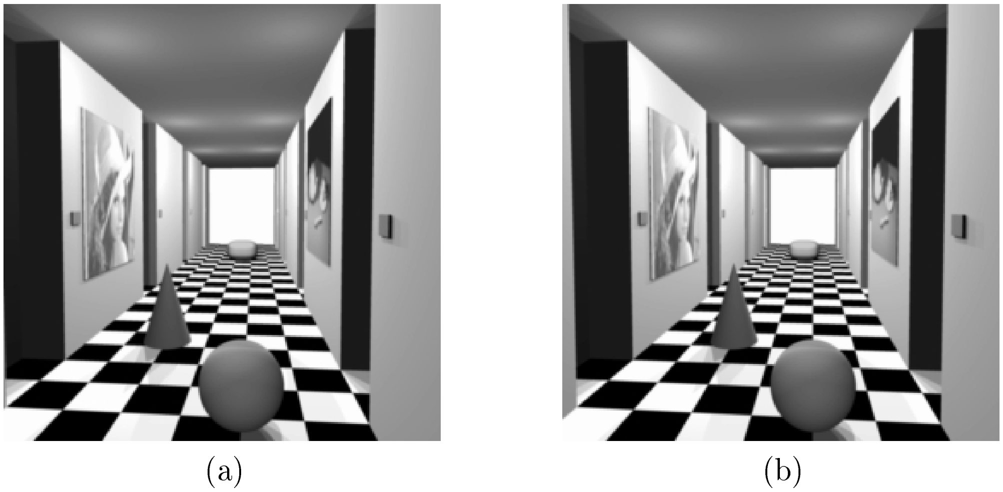

Figure B.2: Test stereo images *Room*. (a) left image (b) right image

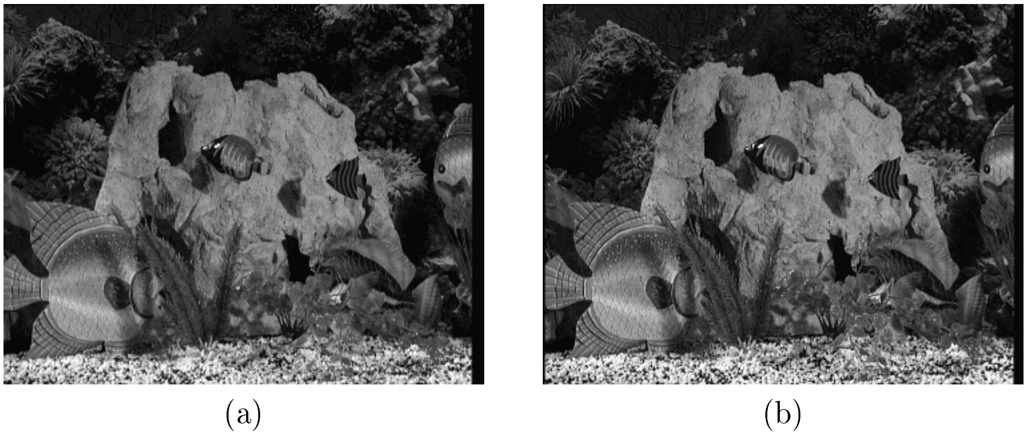

Figure B.3: Test stereo images *Aqua*. (a) left image (b) right image.

Reference List

[1] J. Hsu, C.F. Babbs, D.M. Chelberg, Z. Pizlo, and E.J. Delp, "Design of studies to test the effectiveness of stereo imaging/ truth or dare: Is stereo viewing really better?," in *Proc. SPIE Stereoscopic Displays and Applications V*, Feb. 1994, vol. 2177A, pp. 211–222.

[2] T. Motoki, H. Isono, and I. Yuyama, "Present status of three-dimensional television research," *Proceedings of the IEEE*, vol. 83, no. 7, pp. 1009–1021, July 1995.

[3] M. Waldowski, "A new segmentation algorithm for videophone applications based on stereo image pair," *IEEE Trans. on Comm.*, vol. 39, no. 12, pp. 1856–1868, Dec. 1991.

[4] T. Aach and A. Kaup, "Disparity-based segmentation of stereoscopic foreground/background image sequences," *IEEE Trans. on Comm.*, vol. 42, no. 2, pp. 673–679, Feb. 1994.

[5] E. Izquierdo, "Stereo matching for enhanced telepresence in three-dimensional videocommunications," *IEEE Trans. on CSVT*, vol. 7, no. 4, pp. 629–643, Aug. 1997.

[6] D.P. Miller, "Evaluation of vision systems for teleoperated land vehicles," *IEEE Control Systems Magazine*, pp. 37–41, June 1988.

[7] D. R. Shres, F.F. Holly, and P.G. Harnder, "High ratio bandwidth reduction of video imaging for teleoperation," *SPIE Image and Video Processing*, vol. 1903, pp. 236–245, Nov. 1993.

[8] M.W. Siegel, P. Gunatilake, S. Sethuraman, and A.G. Jordan, "Compression of stereo image pairs and streams," in *Proc. SPIE SDVRS*, Feb. 1994, vol. 2177, pp. 258–268.

[9] M. Stark, "Low cost universal stereoscopic virtual reality interfaces," in *Proc. SPIE Stereoscopic Displays and Applications*, 1993, vol. 1915.

[10] B.G. Haskell, A. Puri, and A.N. Netravali, *Digital Video: Introduction to MPEG-2*, The MIT Press, 1986.

[11] A. Puri, R. V. Kollarits, and B. G. Haskell, “Basics of stereoscopic video, new compression results with MPEG-2 and a proposal for MPEG-4,” *J. on Signal Processing: Image Comm.*, vol. 10, pp. 201–234, 1997.

[12] M. E. Lukacs, “Predictive coding of multi-viewpoint image sets,” in *Proc. ICASSP*, Oct. 1986, pp. 521–524.

[13] M. G. Perkins, “Data compression of stereopairs,” *IEEE Trans. on Comm.*, vol. 40, pp. 684–696, Apr. 1992.

[14] B. Julesz, *Foundations of Cyclopeon Perception*, The University of Chicago Press, 1971.

[15] I. Dinstein, M.G. Kim, A. Henik, and J. Tzelgov, “Compression of stereo images using subsampling transform coding,” *Optical Engineering*, vol. 30, no. 9, pp. 1359–1364, Sept. 1991.

[16] V.S. Nalwa, *A Guided Tour of Computer Vision*, Addson-Wesley, 1993.

[17] B.K.P. Horn, *Robot Vision*, The MIT Press, 1986.

[18] R.E.H. Franich, *Disparity Estimation in Stereo Digital Images*, Ph.D. thesis, TUDelft, 1996.

[19] U.R. Dohnd and J.K. Aggarwal, “Structure from stereo: A review,” *IEEE Trans. on SMC*, vol. 19, no. 6, pp. 1489–1510, June 1989.

[20] D. Marr and T. Poggio, “Cooperative computation of stereo disparity,” *Science*, vol. 194, pp. 283–287, 1976.

[21] B. Lucas and T. Kanade, “An iterative image registration technique with an application to stereo vision,” in *Proc. of the 7th Int. J. Conf on AI*, 1981, pp. 674–679.

[22] D. Marr and T. Poggio, “A computational theory of human stereo vision,” *Proc. of Roy. Soc. Lond.*, vol. B.204, pp. 301–328, 1979.

[23] T. Poggio, V. Torre, and C. Koch, “Computational vision and regularization theory,” *Nature*, vol. 317, pp. 314–319, 1985.

[24] P. Anandan, “A computational framework and an algorithm for the measurement of visual motion,” *Int. J. of Computer Vision*, vol. 2, pp. 283–310, 1989.

[25] J. Marroquin, S. Mitter, and T. Poggio, “Probabilistic solutions of ill-posed problems in computational vision,” *J. of the Am. Stat. Soc.*, vol. 82, pp. 76–89, 1987.

[26] A. Yuille, "Energy functions for early vision and analog networks," *Bio. Cyb.*, vol. 61, pp. 115–123, 1989.

[27] H. Jeong, W. Woo, C. Kim, and J. Kim, "A unification theory for early vision," in *Proc. First Korea-Japan Joint Conf. on the Computer*, Oct. 1991, pp. 298–309.

[28] J. Kim and H. Jeong, "Parallel relaxation algorithm for disparity compensation," *IEE Electronics Letters*, vol. 33, no. 6, pp. 1367–1368, July 1997.

[29] H.H. Baker and T.O. Binford, "Depth from edge and intensity-based stereo," in *Proc. ICAI*, 1981, pp. 631–636.

[30] D. Marr, *Vision*, San Francisco: Freeman, 1982.

[31] W.E.L. Grimson, "Computational experiments with a feature-based stereo algorithm," *IEEE Trans. on PAMI*, vol. 7, no. 1, pp. 17–34, Jan. 1985.

[32] W. Hoff and N. Ahuja, "Surfaces from stereo: Integrating feature matching, disparity estimation and contour detection," *IEEE Trans. on PAMI*, vol. 11, no. 2, pp. 121–136, Feb. 1989.

[33] J. Weng, N. Ahuja, and T.S. Huang, "Matching two perspective views," *IEEE Trans. on PAMI*, vol. 14, no. 8, pp. 806–825, Aug. 1992.

[34] D. Terzopoulos, "The computation of visible surface representation," *IEEE Trans. on PAMI*, vol. 10, no. 4, pp. 417–438, July 1988.

[35] T.D. Sanger, "Stereo disparity computation using gabor filter," *Bio. Cyb.*, vol. 59, pp. 405–418, 1988.

[36] D.J. Fleet, A.D. Jepson, and M.R.M. Jenkin, "Phase-based disparity estimation," *CVGIP: Image Understanding*, vol. 53, no. 2, pp. 198–210, Mar. 1991.

[37] P. Gunatilake, A.G. Jordan, and M.W. Siegel, "Compression of stereo video streams," in *SMPTE Proc. International Workshop on HDTV*, Oct. 1993.

[38] I. Dinstein, G. Guy, and J. Rabany, "On the compression of stereo images: Preliminary results," *Signal Processing*, vol. 17, no. 4, pp. 373–381, Aug. 1989.

[39] W. Woo and A. Ortega, "Blockwise dependent bit allocation for stereo image coding," *IEEE Trans. on CSVT*, submitted, Apr. 1998, revised Oct. 1998.

[40] H. Aydinoglu, F. Kossentini, Q. Jiang, and M. H. Hayes, "Region based stereo image coding," in *Proc. IEEE ICIP*, Washington, Oct. 1995, pp. 57–60.

[41] H. Aydinoglu and M. H. Hayes, "Stereo image coding: A projection approach," *IEEE Trans. on IP*, pp. 506–516, Apr. 1998.

[42] H. Aydinoglu and M. H. Hayes, "Performance analysis of stereo image coding algorithms," in *Proc. IEEE ICASSP*, 1996, pp. 2191–2195.

[43] M.B. Slima, J. Konrad, and A. Barwicz, "Improvement of stereo disparity estimation through balanced filtering: The sliding-block approach," *IEEE Trans. on CSVT*, vol. 7, no. 6, pp. 913–920, Dec. 1997.

[44] D. Tzovaras and M.G. Strintzis, "Motion and disparity field estimation using Rate-Distortion optimization," *IEEE Trans. on CSVT*, vol. 8, no. 2, pp. 171–180, Apr. 1998.

[45] W. Woo and A. Ortega, "Modified overlapped block matching for stereo image coding," in *Proc. SPIE EI-VCIP*, Jan. 1999, vol. 3653.

[46] M. Accame, F. G. De Natal, and D. D. Giusto, "Hierarchical block matching for disparity estimation in stereo sequence," in *Proc. IEEE ICIP*, May 1993, pp. 200–207.

[47] D. Tzovaras, S. Vachtsevanos, and M.G. Strintzis, "Optimization of quadtree segmentation and hybrid two-dimensional and three-dimensional motion estimation in a rate-distortion framework," *IEEE J. on SAC*, vol. 15, no. 9, pp. 1726–1738, Dec. 1997.

[48] G. J. Sullivan and R. L. Baker, "Efficient quadtree of images and video," *IEEE Trans. on IP*, vol. 3, no. 3, pp. 327–331, May 1994.

[49] S. Sethuraman, M.W. Siegel, and A.G. Jordan, "A multiresolution framework for stereoscopic image sequence compression," in *Proc. IEEE ICIP*, Oct. 1994, vol. 2, pp. 361–365.

[50] S. Sethuraman, M.W. Siegel, and A.G. Jordan, "A multiresolution region based segmentation scheme for stereoscopic image sequence compression," in *Proc. SPIE EI-Digital Video Compression: Algorithms and Technologies*, Feb. 1995, vol. 2419, pp. 265–274.

[51] S. Sethuraman, M.W. Siegel, and A.G. Jordan, "Segmentation based coding of stereoscopic image sequences," in *Proc. SPIE EI-Digital Video Compression: Algorithms and Technologies*, Jan. 1996, vol. 2668, pp. 420–429.

[52] M.W. Siegel, S. Sethuraman andJ. S. McVeigh, and A.G. Jordan, "Compression and interpolation of 3d-stereoscopic and multi-view video," in *Proc. SPIE SDVRS*, Feb. 1997, vol. 3012, pp. 227–238.

[53] W. Woo and A. Ortega, "Stereo image compression based on the disparity field segmentation," in *Proc. SPIE EI-VCIP*, Feb. 1997, vol. 3024, pp. 391–402.

[54] M. Kunt, A. Ikonomopoulos, and M. Kocher, "Second-generation image coding techniques," *Proc. of the IEEE*, vol. 73, no. 4, pp. 549–574, Apr. 1985.

[55] F. Marques, M. Pardas, and P. Salembier, *Coding-Oriented Segmentation of Video Sequences*, In Video Coding: The second Generation Approach, 1996.

[56] D. Tzovaras, N. Grammalidis, and M.G. Strintzis, "Object-based coding of stereo image sequences using joint 3D motion/disparity compensation," *IEEE Trans. on CSVT*, vol. 7, no. 2, pp. 312–327, Apr. 1997.

[57] S. Malassiotis and M.G. Strinzis, "Object-based coding of stereo image sequences using 3-D model," *IEEE Trans. on CSVT*, vol. 7, no. 6, pp. 892–905, Dec. 1997.

[58] M.S. Moellenhoff and M.W. Maier, "Transform coding of stereo image residuals," *IEEE Trans. on IP*, vol. 7, no. 6, pp. 804–812, June 1998.

[59] W. Woo and A. Ortega, "Dependent quantization for stereo image coding," in *Proc. SPIE EI-VCIP*, Jan. 1998, vol. 3309, pp. 902–913.

[60] N. Grammalidis and M.G. Strintzis, "Disparity and occlusion estimation in multiocular systems and their coding for the communication of multiview image sequences," *IEEE Trans. on CSVT*, vol. 8, no. 3, June 1998.

[61] J.L. Mannos and D.J. Sakrison, "The effects of a visual fidelity criterion on the encoding of images," *IEEE Trans. Info. Theory*, vol. 20, pp. 525–536, 1974.

[62] N.B. Nill, "A visual model weighted cosine transform for image compression and quality assessment," *IEEE Trans. on Comm.*, vol. 33, no. 6, pp. 551–557, June 1985.

[63] A.B. Watson and M.P. Eckert, "Motion-contrast sensitivity: Visibility of motion gradients of various spatial frequencies," *J. of the Opt. Soc. of America A*, pp. 496–505, 1994.

[64] S. Pei and C. Lei, "Vary low bit-rate coding algorithm for stereo video with spatiotemporal HVS model and binary correlation disparity estimator," *IEEE Trans. on JSAC*, vol. 16, pp. 98–107, Jan. 1998.

[65] R.M. Gray and D.L. Neuhoff, "Quantization," *IEEE Trans. on Info. Theory*, vol. 44, no. 6, Oct. 1998.

[66] C. Chen and K. Pang, "The optimal transform of motion-compensated frame difference images in a hybrid coder," *IEEE Trans. on CAS-II*, vol. 40, no. 6, pp. 393–397, June 1993.

[67] D.J. Connor and J.O. Limb, "Properties of frame-difference signals generated by moving images," *IEEE Trans. on Comm.*, vol. COM-22, no. 10, pp. 1564–1575, Oct. 1974.

[68] R.C. Reininger and J. Gibson, "Distribution of the two-dimensional DCT coefficients for images," *IEEE Trans. on Comm.*, vol. 31, no. 6, pp. 835–839, June 1983.

[69] B. Girod, "The efficiency of motion compensating prediction for hybrid coding of video sequence," *IEEE J. on S. Areas in Comm.*, vol. 5, no. 7, pp. 1140–1154, Aug. 1987.

[70] P. Gerken and H. Schiller, "A low bit-rate image sequence coder combining a progressive dpcm on interleaved rasters with a hybrid DCT technique," *IEEE J. on S. Areas in Comm.*, vol. 5, no. 7, pp. 1079–1089, Aug. 1987.

[71] A. Puri and R. Aravind, "Motion-compensated video coding with adaptive perceptual quantization," *IEEE Trans. on CSVT*, vol. 1, no. 4, pp. 351–361, Dec. 1991.

[72] C. Chu and K. Aggarawal, "The integration of image segmentation maps using region and edge information," *IEEE Trans. on PAMI*, vol. 15, no. 12, pp. 1241–1252, Dec. 1993.

[73] C.A. Gonzales and E. Viscito, "Motion video adaptive quantization in the transform domain," *IEEE Trans. on CSVT*, vol. 1, no. 4, pp. 374–378, Dec. 1991.

[74] C. Stiller and D. Lappe, "Laplacian pyramid coding of prediction error images," in *Proc. SPIE VCIP*, 1991.

[75] J.M. Shapiro, "Embedded image coding using zerotrees of wavelet coefficients," *IEEE Trans. On signal Processing*, vol. 41, no. 12, pp. 3445–3462, Dec. 1993.

[76] F. Muller and K. Illgner, "Embedded pyramid coding of displaced frame difference," in *Proc. IEEE ICIP*, 1995.

[77] H. Samet and M. Tamminen, "Computing geometric properties of images represented by linear quadtrees," *IEEE Trans. on PAMI*, vol. 7, no. 2, pp. 229–240, Mar. 1985.

[78] L.E. Davission, "Rate-Distortion theory and application," *Proceeding of the IEEE*, vol. 7, no. 60, pp. 800–808, July 1972.

[79] T.M. Cover and J.A. Thomas, *Elements of Information Theory*, Wiley-Interscience, 1991.

[80] K. Ramchandran, A. Ortega, and M. Vetterli, "Bit allocation for dependent quantization with applications to multiresolution and MPEG video coders," *IEEE Trans. on IP*, vol. 3, no. 5, pp. 533–545, Sept. 1994.

[81] A. Ortega, *Optimization Techniques for Adaptive Quantization of Image and Video Under Delay Constraints*, Ph.D. dissertation, Dept. of EE, Columbia Univ., 1994.

[82] Y. Shoham and A. Gersho, "Efficient bit allocation for an arbitrary set of quantizers," *IEEE Trans. on ASSP*, vol. 36, pp. 1445–1453, Sept. 1988.

[83] S. Geman and D. Geman, "Stochastic relaxation, Gibbs distributions and the bayesian restoration of images," *IEEE Trans. on PAMI*, pp. 721–741, Nov. 1984.

[84] J.E. Besag, "Spatial interaction and the statistical analysis of lattice systems," *J. Royal Statistical. Soc.*, vol. B36, pp. 192–236, 1974.

[85] N. M. Nasrabadi, S. P. Clifford, and Y. Liu, "Integration of stereo vision and optical flow by using an energy minimizing approach," *Optical Society of America*, vol. 6, pp. 900–907, June 1989.

[86] W. Woo and A. Ortega, "Stereo image compression based on the disparity compensation using the MRF model," in *Proc. SPIE VCIP*, Mar. 1996, vol. 2727, pp. 28–41.

[87] W.C. Chung, F. Kossentini, and M.J.T. Smith, "Rate-Distortion constrained statistical motion estimation for video coding," in *Proc. IEEE ICIP*, Oct. 1995, pp. 184–187.

[88] J. Ribas-Corbera and D. Neuhoff, "Optimal bit allocations for lossless video coders: Motion vectors vs. difference frames," in *Proc. IEEE ICIP*, Oct. 1995, pp. 180–183.

[89] G. M. Schuster and A. K. Katsaggelos, "A theory for the optimal bit allocation between displacement vector field and displaced frame difference," *IEEE Jr. on Sel. Areas in Comm.*, vol. 15, no. 9, pp. 13–26, Dec. 1997.

[90] M.C. Chen and A.N. Willson Jr., "Rate-Distortion optimal motion estimation algorithm for motion-compensated transform video coding," *IEEE Trans. On CSVT*, vol. 8, no. 2, pp. 147–158, Apr. 1998.

[91] L.J. Lin and A. Ortega, "Bit-rate control using piecewise approximated Rate-Distortion characteristics," *IEEE Trans. on CSVT*, vol. 8, no. 4, pp. 486–499, Aug. 1998.

[92] T. Wiegand, M. Lightstone, D. Mukherjee, T.G. Campbell, and S.K. Mitra, "Rate-distortion optimized mode selection for very low bit-rate video coding and the emerging H.263 standard," *IEEE Trans. on CSVT*, vol. 6, no. 2, pp. 182–190, Apr. 1996.

[93] H. Everett, "Generalized Lagrange multiplier method for solving problems of optimum allocation of resources," *Operational Res.*, vol. 11, pp. 399–417, 1963.

[94] G.L. Nemhauser and L.A. Wolsey, *Integer and Combinatorial Optimization*, Wiley, 1988.

[95] G.D. Forney, "The Viterbi algorithm," *The Proc. IEEE*, vol. 61, pp. 268–278, Mar. 1973.

[96] W. Pennebaker and J. Mitchell, *JPEG Still Image Compression Standard*, Van Nostrand Rheinhold, 1994.

[97] B.L. Tseng and D. Anastassiou, "Multi-viewpoint video coding with mpeg-2 compatibility," *IEEE Trans. on CSVT*, vol. 6, no. 4, pp. 414–419, Aug. 1996.

[98] K. Illgner and F. Muller, "Motion estimation using overlapped block motion compensation and Gibbs-modeled vector fields," in *Proc. IEEE IMDSP*, Mar. 1996, pp. 126–127.

[99] H. Watanabe and S. Singhal, "Windowed motion compensation," in *Proc. SPIE VCIP*, Nov. 1991, vol. 1605, pp. 582–589.

[100] M. Orchard and G. Sullivan, "Overlapped block motion compensation: An estimation-theoretic approach," *IEEE Trans. on IP*, vol. 5, no. 3, pp. 693–699, 1994.

[101] H. Dankworth and W. Niehsen, "Analytical overlapped block motion compensation," in *Proc. NORSIG97*, 1997, pp. 75–80.

[102] R. Rajagopalan, E. Feig, and M.T. Orchard, "Motion optimization of ordered blocks for overlapped block motion compensation," *IEEE Trans. on CSVT*, vol. 8, no. 2, pp. 119–123, Apr. 1998.

[103] S. Nogaki and M. Ohta, "An overlapped block motion compensation for high quality motion picture coding," in *Proc. IEEE ISCAS*, 1992.

[104] J.K.Su and R.M. Mersereau, "Non-iterative Rate-constrained motion estimation for OBMC," in *Proc. IEEE ICIP*, 1997, pp. 33–36.

[105] T. Kuo and C. Kuo, "Complexity reduction for overlapped block motion compensation," in *Proc. SPIE EI-VCIP*, Feb. 1997, vol. 3024, pp. 303–314.

[106] T. Kuo and C. Kuo, "A hybrid BMC/OBMC motion compensation scheme," in *Proc. IEEE ICIP*, Oct. 1997, vol. 2, pp. 795–798.

[107] B. Tao and M.T. Orchard, "Joint application of overlapped block motion compensation and loop fieltering for low bit-rate video coding," in *Proc. IEEE ICIP*, 1997.

[108] B. Girod, "Motion-compensating prediction with fractional-pel accuracy," *IEEE Trans. on Comm.*, vol. 41, no. 4, pp. 604–611, Apr. 1993.

[109] K. Illgner and F. Muller, "Analytical analysis of subpel motion compensation," in *Proc. PCS*, 1997, pp. 135–140.

[110] W. Woo and A. Ortega, "Block-based disparity estimation and compensation for stereo image coding," *IEEE Trans. on CSVT*, In preparation, 1999.

[111] A. Puri, H.M. Hang, and D.L. Schilling, "Interframe coding with variable block-size motion compensation," in *GLOBECOM*, Nov. 1987, pp. 65–69.

[112] M. T. Orchard, "Predictive motion-field segmentation for image sequence coding," *IEEE Trans. on SP*, vol. 41, no. 12, pp. 3416–3424, Dec. 1993.

[113] J. Kim and S. Lee, "Hierachical variable block size motion estimation technique for motion sequence coding," *SPIE Optical Engineering*, vol. 33, no. 8, pp. 2553–2561, Aug. 1994.

[114] G. Hunter and K. Steiglitz, "Operations on images using quad trees," *IEEE Trans. on PAMI*, vol. 1, no. 2, pp. 145–153, Apr. 1979.

[115] P.A. Chou, T. Lookabaugh, and R.M. Gray, "Optimal pruning with applications to tree-structured source coding and modeling," *IEEE Trans. on Inform. Theory*, vol. 35, pp. 299–315, Mar. 1989.

[116] F. Moscheni, F. Dufaux, and H. Nicolas, "Entropy criterion for optimal bit allocation between motion and prediction error information," in *Proc. SPIE VCIP*, Nov. 1993, pp. 235–242.

[117] J. Lee, "Optimal quadtree for variable block size motion estimation," in *Proc. IEEE ICIP*, Oct. 1995, vol. 3, pp. 480–483.

[118] Y. Yang and S. Hemami, "Rate-constrained motion estimation and perceptual coding," in *Proc. IEEE ICIP*, 1997, pp. 81–84.

[119] H. Bi and W. Chan, "Rate-Distortion optimization of hierarchical displacement fields," *IEEE Trans. on CSVT*, vol. 8, no. 1, pp. 18–24, Feb. 1998.

[120] J. Hartung, A. Jacquin, J. Pawlyk, J. Rosenberg, H. Okada, and P.E. Crouch, "Object-oriented h.263 compatible video coding platform for conferencing applications," *IEEE Trans. on JSAC*, vol. 16, no. 1, pp. 42–55, Jan. 1998.

[121] A. Ortega, K. Ramchandran, and M. Vetterli, "Optimal trellis-based buffered compression and fast approximation," *IEEE Trans. on IP*, vol. 3, no. 1, pp. 26–40, Jan. 1994.

[122] K. Kim, M.W. Siegel, and J. Son, "Synthesis of a high resolution 3d-stereoscopic image from a high resolution monoscopic image and a low resolution depth map," in *Proc. SPIE Stereoscopic Displays and Virtual Reality Systems V*, Jan. 1998, vol. 3095, pp. 76–86.

[123] B.L. Tseng and D. Anastassiou, "A theoretical study on an accurate reconstruction of multiview images based on the viterbi algorithm," in *Proc. IEEE ICIP*, 1995.

[124] T. Kaneko and M. Okudaira, "Encoding of arbitrary curves based on the chain code representation," *IEEE Trans. on Comm.*, vol. 33, no. 7, pp. 697–707, July 1985.

[125] A.K. Jain, *Fundamentals of Digital Image Processing*, Prentice-Hall, 1989.

[126] C. Lu and J.G. Dunham, "Highly efficient coding scheme for contour lines based on chain code representations," *IEEE Trans. on Comm.*, vol. 39, no. 10, pp. 1511–1514, Oct. 1991.

[127] G. M. Schuster and A. K. Katsaggelos, "An efficient boundary encoding scheme which is optimal in the rate distortion sense," in *Proc. IEEE ICIP*, Sept. 1996, pp. 77–80.

[128] G. M. Schuster and A. K. Katsaggelos, "An optimal polygonal boundary encoding scheme in the rate distortion sense," *IEEE Trans. on IP*, vol. 7, no. 1, pp. 13–26, Jan. 1998.